AD_____
(Leave blank)

Award Number: W81XWH-10-1-0491

TITLE: *M Current-Based Therapies for Nerve Agent Seizures*

PRINCIPAL INVESTIGATOR: Jaideep Kapur, MD PhD

CONTRACTING ORGANIZATION:
University of Virginia,

Charlottesville, VA 22904-4195

REPORT DATE: July 2012

TYPE OF REPORT: Revised Annual

PREPARED FOR: U.S. Army Medical Research and Materiel Command
Fort Detrick, Maryland 21702-5012

DISTRIBUTION STATEMENT: (Check one)

X Approved for public release; distribution unlimited

☐ Distribution limited to U.S. Government agencies only; report contains proprietary information

The views, opinions and/or findings contained in this report are those of the author(s) and should not be construed as an official Department of the Army position, policy or decision unless so designated by other documentation.

REPORT DOCUMENTATION PAGE

Form Approved
OMB No. 0704-0188

Public reporting burden for this collection of information is estimated to average 1 hour per response, including the time for reviewing instructions, searching existing data sources, gathering and maintaining the data needed, and completing and reviewing this collection of information. Send comments regarding this burden estimate or any other aspect of this collection of information, including suggestions for reducing this burden to Department of Defense, Washington Headquarters Services, Directorate for Information Operations and Reports (0704-0188), 1215 Jefferson Davis Highway, Suite 1204, Arlington, VA 22202-4302. Respondents should be aware that notwithstanding any other provision of law, no person shall be subject to any penalty for failing to comply with a collection of information if it does not display a currently valid OMB control number. **PLEASE DO NOT RETURN YOUR FORM TO THE ABOVE ADDRESS.**

1. REPORT DATE	2. REPORT TYPE	3. DATES COVERED
July 2012	Revised Annual	1 July 2011- 30 June 2012

4. TITLE AND SUBTITLE
M current Based Therapies for Nerve agent Seizures

5a. CONTRACT NUMBER

5b. GRANT NUMBER
W81XWH-10-1-0491

5c. PROGRAM ELEMENT NUMBER

6. AUTHOR(S)
Jaideep Kapur, Jian Li Sun, Terry Zhang, Marko Todorovic

E-Mail: jk8t@virginia.edu

5d. PROJECT NUMBER

5e. TASK NUMBER

5f. WORK UNIT NUMBER

7. PERFORMING ORGANIZATION NAME(S) AND ADDRESS(ES)

University of Virginia
Charlottesville, VA 22908

8. PERFORMING ORGANIZATION REPORT NUMBER

9. SPONSORING / MONITORING AGENCY NAME(S) AND ADDRESS(ES)
U.S. Army Medical Research and Materiel Command
Fort Detrick, Maryland 21702-5012

10. SPONSOR/MONITOR'S ACRONYM(S)

11. SPONSOR/MONITOR'S REPORT NUMBER(S)

12. DISTRIBUTION / AVAILABILITY STATEMENT
Approved for Public Release; Distribution Unlimited

13. SUPPLEMENTARY NOTES

14. ABSTRACT- This is a proposal to develop novel, mechanism-based therapies for the treatment of organophosphate (OP) nerve agent-induced seizures. We proposed to study the effects of organophosphates anmuscarinic agonists on glutamatergic transmission, and on intrinsic excitability of principal hippocampal neurons ttest the hypothesis that cholinergic stimulation enhances excitatory synaptic transmission and increases and excitability (Aims 1 & 2). We have completed experiments 1.1-1.4 and 2.1-2.2 as proposed for years 1 &2 of this study and experimental results supported the hypothesis. A manuscript describing these results is now publishedonline: M-type potassium channels modulate Schaffer-collateral CA glutamatergic synaptic transmission. J Physiol. 2012 doi: 10.1113/jphysiol.2012.235820. Third goal was to test whether drugs that open M channels wouterminate status epilepticus induced by an organophosphate and cholinergic agonist (Li/Pilocarpine). Two modelof organophasphate-induced seizures were characterized and published: Characterization of status epilepticus induced by two organophosphates in rats. Epilepsy Res. http://dx.doi.org/10.1016/j.eplepsyres.2012.04.014. Experiments reveal M channel opener flupirtine terminates refractory status epilepticus in two models.
.

15. SUBJECT TERMS- Seizures, status epilepticus Cholinergic, M Current, Synaptoic transmission.

16. SECURITY CLASSIFICATION OF:			17. LIMITATION OF ABSTRACT	18. NUMBER OF PAGES	19a. NAME OF RESPONSIBLE PERSON
a. REPORT	b. ABSTRACT	c. THIS PAGE			USAMRMC
U	U	U	UU		19b. TELEPHONE NUMBER *(include area code)*

Table of Contents

Page

Introduction:

This is a proposal to develop novel, mechanism-based therapies for the treatment of organophosphate (OP) nerve agent-induced seizures. The primary goal of this proposal is to test two interrelated **hypotheses**: 1) Cholinergic nerve agents cause neuronal hyper-excitability by inhibiting M/KCNQ2/3 potassium channels. 2) Cholinergic seizures can be blocked by drugs that can open potassium channels mediating M currents. These hypotheses will be tested by accomplishing three aims. **Aim 1)** To test whether modulation of M channel modulators (antagonists and openers) glutamatergic transmission on CA1 pyramidal neurons and dentate granule cells. **Aim 2)** To characterize the effects of M current enhancers on excitabtility and bursting of CA1 pyramidal neurons. **Aim 3)** To test anticonvulsant action of three M-Channel openers in cholinergic overstimulation-induced status epilepticus.

Body:

We proposed to study the effects of organophosphates and muscarinic agonists on glutamatergic transmission, and on intrinsic excitability of principal hippocampal neurons to test the hypothesis that cholinergic stimulation enhances excitatory synaptic transmission and increases and excitability (Aims 1 & 2). We have completed experiments 1.1-1.4 and 2.1-2.2 as proposed for years 1 &2 of this study and experimental results supported the hypothesis.

Materials and methods

Slice preparation

All studies were performed according to protocols that were approved by the University of Virginia Animal Use and Care Committee, and the US Army Medical Research and Material Command Animal Care and Use Review Office (ACURO). Adult male (175-250 g) Sprague-Dawley rats were anesthetized with isoflurane prior to decapitation, which was followed by quick removal of the brain. The removed brains were then sectioned to 300 μm slices using a Leica VT 1200 slicer (Leica Microsystems, Wetzlar, Germany) in ice-cold oxygenated slicing solution. The solution contained the following (in mM): 120 sucrose, 65.5 NaCl, 2 KCl, 1.1 KH2PO4, 25 NaHCO3, 10 D-glucose, 1 CaCl2, and 5 MgSO4. The slices were then incubated for at least one hour at 32 °C in oxygenated ACSF that contained (in mM): 127 NaCl, 2 KCl, 1.1 KH2PO4, 25.7 NaHCO3, 10 D-glucose, 2 CaCl2, and 1.5 MgSO4; the osmolarity in the chamber was 290–300 mOsm. After incubation, the slices were transferred to the recording chamber on the stage of an Olympus Optical BX51 microscope (Olympus, Tokyo). Unless otherwise stated, all chemicals were obtained from Sigma (St. Louis, MO).

Whole-cell recording

Whole-cell patch-clamp recordings were performed under infrared differential interference contrast microscopy (Olympus); a 40× water-immersion objective was used to visually identify CA1 and CA3 pyramidal neurons. The slices were continuously perfused with ACSF solution that was saturated with 95% O2 and 5% CO2 at room temperature. Patch electrodes (final resistances, 3–5 MΩ) were pulled from borosilicate glass (Sutter Instruments, Novato, CA) on a horizontal Flaming-Brown microelectrode puller (Model P-97, Sutter Instruments). For voltage-clamp recordings, the electrode tips were filled with a filtered internal recording solution that consisted of the following components (in mM): 117.5 CsMeSO4, 10 HEPES, 0.3 EGTA, 15.5 CsCl, and 1.0 MgCl2; the pH was 7.3 (with CsOH), and the osmolarity was 310 mOsm. The electrode shank contained (in mM) 4 ATP Mg2+ salt, 0.3 GTP Na+ salt, and 5 QX-314. For current-clamp recording, the pipette solution contained the following (in mM): 135 K-gluconate, 2.5 NaCl, 10 HEPES, 0.5 EGTA, 4.0 MgATP, 0.4 NaGTP, 0.1 CaCl2; the pH was 7.3, and the osmolarity was 310 mOsm.

Neurons were voltage clamped at -60 mV using a PC-505B amplifier (Warner Instruments, Hamden, CT). Electrode capacitance was electronically compensated. Access resistance was continuously monitored, and if the series resistance increased by 20% at any time, the recording was terminated. Currents were filtered at 2 kHz, digitized using a Digidata 1322 digitizer (Molecular Devices, Sunnyvale, CA), and acquired using Clampex 10.2 software (Molecular Devices).

Spontaneous excitatory postsynaptic currents (sEPSCs) were recorded from CA1 pyramidal neurons after blocking the GABAA receptors with the antagonist picrotoxin (50 μM). In preliminary experiments, a combination of 6-cyano-7-nitroquinoxalene-2,3-dione (CNQX) and 2-amino-5-phosphonovaleric acid (APV) blocked all EPSCs. Miniature EPSCs (mEPSCs) were recorded by blocking action potentials with 1 μM TTX (Alomone labs, Jerusalem, Israel). All drugs were bath-applied via a peristaltic pump.

Data analysis

The offline digitized data were analyzed with MiniAnalysis (Synaptosoft, Decatur, GA) and Clampfit 10.2 (Molecular Devices). To detect sEPSCs and mEPSCs, a detection threshold was set at three times the root mean square (RMS) of the baseline noise. After detection, the frequency and peak amplitude of EPSCs from individual neurons were analyzed. Each detected event from the 20- to 30-min recording session was visually inspected to remove false detections. The Kolmogorov-Smirnov (K-S) test was used to compare amplitudes and inter-event intervals for continuously recorded EPSCs. The input resistance of CA3 neuron under current-clamp recording was analyzed by comparing the slope of current-voltage relationship and measured directly by Clampfit 10.2 at the peak of membrane potentials. The event frequency and amplitudedrug effects were compared using a paired Student's t-test with a significance level of $p < 0.05$. Data values were expressed as means ± SEM unless otherwise noted.

Results

An M1 muscarinic agonist increases mEPSC frequency in CA1 neurons

Previous studies suggested that muscarinic receptor activation increased presynaptic glutamate release from perforant path to dentate granule cells (Kozhemyakin et al., 2010). In the present study, we investigated the effect of the M1 muscarinic receptor agonist McN-A-343 on glutamate release recorded from Schaffer collateral-CA1 synapses. Application of McN-A-343 (10 μM) increased the frequency of mEPSCs that were recorded from CA1 pyramidal neurons by 69.89 ± 8.28 % (0.12 ± 0.03 Hz vs. 0.21 ± 0.05 Hz; $n = 7$, $p < 0.01$), but it did not change their amplitudes (16.51 ± 1.14 pA vs. 16.79 ± 1.47 pA; $n = 7$, $p = 0.38$, Fig. 1A,B). McN-A-343 caused a significant leftward shift in the cumulative distribution of the inter-event intervals but had no effect on the cumulative distribution of the amplitudes of the mEPSCs (K-S test, Fig. 1C,D). This suggested that the activation of M1 receptors increased action potential-independent glutamate release from the presynaptic terminals of Schaffer collateral-CA1 synapses.

M-channels regulate presynaptic glutamate release in CA1 neurons

Cholinergic M1 receptor activation inhibits M-channels (Bernheim et al., 1992; Brown & Adams, 1980; Marrion et al., 1989), so we tested whether M-channels regulate glutamate release in these synapses. Blocking M-channels increased the frequency of sEPSCs. After

recording sEPSCs for 10 min, M-channel blocker XE991 (10 μM) was applied for 10 min, and it increased the frequency of sEPSCs by 147.56 ¬± 18.21 % (0.11¬± 0.03 Hz vs. 0.30 ¬± 0.01 Hz, n = 7, p < 0.01) but did not affect their amplitudes (16.91± 0.92 pA vs. 16.65 ¬± 0.80 pA, n = 7, p = 0.50). Blocking M-channels caused a significant leftward shift in the cumulative distribution of sEPSCs inter-event intervals but had no effect on the cumulative distribution of their amplitudes (K-S test, data not shown). These data suggested that M-channels modulate action potential-dependent glutamate release from Schaffer collateral CA1 pyramidal neuron synapses.

To study whether the effect of XE991 on release was action potential-independent, its effect on mEPSCs was studied. XE991 (10 μM) increased the frequency of mEPSCs by 82.21 ± 7.36 % (0.13 ± 0.02 Hz vs. 0.22 ± 0.03 Hz, n = 8, p < 0.01) but had no effect on their amplitudes (17.70 ± 1.26 pA vs. 18.10 ± 1.27 pA, n = 8, p = 0.30, Fig. 2A). XE991 also caused a significant leftward shift in the cumulative distribution of the mEPSC inter-event intervals (Fig. 2B) but had no effect on the cumulative distribution of their amplitudes (Fig. 2C). The frequency of mEPSCs kept increasing after 10 min of XE991 application. The slices were perfused with ACSF to washout the drug effect. The mEPSC frequency remained elevated for 50 min of washing and returned to baseline at 90 min (data not shown).

The effect of XE991 on mEPSC frequency was confirmed by applying linopirdine (10 μM), which also blocks M-channels. Linopirdine increased the frequency of mEPSCs by 68.22 ± 6.05 % (0.12 ± 0.01 Hz vs. 0.21 ± 0.03 Hz, n = 6, p < 0.01) but had no effect on their amplitudes (15.35 ± 1.13 pA vs. 15.78 ± 0.94 pA, n = 6, p = 0.23). It also caused a significant leftward shift in the cumulative distribution of the mEPSC inter-event intervals (Fig. 3A). These results suggested that the inhibition of M-channel current enhances the frequency of mEPSCs.

Flupirtine (20 μM), an M-channel opener, decreased mEPSC frequency by 25.50 ± 8.04 % compared to baseline (0.41 ± 0.08 Hz vs. 0.27 ± 0.04 Hz, n = 8, p < 0.01). Flupirtine caused a significant rightward shift in the cumulative distribution of the inter-event intervals of mEPSCs (Fig. 3B). These data suggested that M-channels are capable of modulating neurotransmitter release independent from action potentials.

To confirm that the effect M1 agonist was mediated by M channels, we incubated the slice with XE991 for 25 min. After 5 min baseline recording in XE991-containing medium, McN-A-343 was applied, and its effect was blocked. Overall, McN-A-343 did not change the frequency of mEPSCs (baseline 0.53 ± 0.07 Hz, McN-A-343 0.56 ± 0.08 Hz; n = 7, p = 0.38). In 2 cells, there was a modest (< 10 %) increase in frequency but the cumulative frequency plot of inter-event intervals from these cells was not shifted (Fig 3C). This result suggested blocking M-channels prevented McN-A-343 enhancement of mEPSC frequency.

Calcium influx through voltage-gated calcium channels underlies the effect of XE991 on mEPSC frequency

Calcium plays a critical role in neurotransmitter release. The increase in mEPSC frequency caused by the application of XE991 could be due to Ca2+ release from intracellular stores or the entry of extracellular Ca2+. First, we tested whether release from intracellular stores plays a role in the effect of XE991. Release from intracellular calcium stores was blocked by incubating the slice with 2.5 μM thapsigargin for 20 min. The effect of M channel blocker XE991 (10 μM) was not affected. XE991 increased the frequency of mEPSCs by 83.88 ± 17.22 % (Fig 4A), which is comparable to the effect of XE991 without thapsigargin incubation (82.21 ± 7.36 %, n = 8, p < 0.01); it significantly left shifted the cumulative distribution of inter-event

intervals (n = 9, $p < 0.01$, Fig 4B). This result suggested that intracellular store release does not contribute to the enhancement of M channel inhibition on mEPSCs frequency.

Therefore, we tested whether the effect of XE991 on the frequency of mEPSCs was dependent on extracellular Ca2+ by recording mEPSCs in a calcium-free medium. The effect of XE991 on mEPSCs was eliminated in ACSF that lacked calcium. Application of XE991 neither changed the frequency of mEPSCs (0.13 ± 0.02 Hz vs. 0.12 ± 0.01 Hz, n = 8, p = 0.30, Fig. 4C) nor shifted the cumulative distribution of the inter-event intervals of mEPSCs (Fig. 4D). These data suggested that the effect of XE991 on spontaneous glutamate release was dependent on the influx of Ca2+.

We also studied the effect of McN-A-343 in a calcium-free medium. The McN-A-343 enhancement of mEPSCs was blocked in calcium-free medium (baseline, 0.40 ± 0.08 Hz, McN-A-343, 0.41 ± 0.07 Hz, n = 7, p = 0.36). There was no significant shift on the cumulative distribution of inter-event intervals of mEPSCs (data not shown). This suggested that the effect of M1 receptor activation on the frequency of mEPSC is largely mediated by increasing calcium influx from extracellular space.

To test whether Ca2+ enters Schaffer collateral terminals by activation of presynaptic voltage-gated calcium channels due to M-channel inhibition, we studied the effect of P/Q- and N-type calcium channel blockers on the XE991-mediated enhancement of mEPSC frequency. These two channels are expressed in the presynaptic terminals of Schaffer-collaterals (Qian & Noebels, 2000; Wheeler et al., 1994). Slices were incubated with either ω-agatoxin TK (200 nM) or ω-conotoxin GVIA (1 μM) (Peptides International, Louisville, KY) for 15 min prior data collection. In the presence of ω-agatoxin TK, which blocks P/Q-type calcium channels, the XE991-mediated enhancement of mEPSC frequency was prevented in approximately half of the cells that were studied. In 5 out of 9 neurons, the application of XE991 did not increase the frequency of mEPSCs (0.23 ± 0.08 Hz vs. 0.20 ± 0.06 Hz, p = 0.46, Fig. 5A,C). In the other 4 CA1 pyramidal neurons, XE991 still significantly increased the frequency of mEPSCs (0.16 ± 0.03 Hz vs. 0.31 ± 0.07 Hz, $p < 0.05$, Fig. 5B,D). Blocking N-type channels with ω-conotoxin GVIA also prevented the effect of XE991 on the frequency of mEPSCs in half of the CA1 pyramidal neurons from which recordings were made. In 4 of 8 neurons, the effect of XE991 was eliminated (0.33 ± 0.05 Hz vs. 0.34 ± 0.04 Hz, p = 0.47, Fig. 6A,C). In the other 4 neurons, XE991 significantly increased the frequency of mEPSCs (0.24 ± 0.04 Hz vs. 0.43 ± 0.07 Hz, $p < 0.05$, Fig. 6B,D).

Next, we applied the blockers of two channels simultaneously. Slices were incubated in ω-agatoxin TK and ω-conotoxin GVIA for 25-40 min, and after 5 min baseline recording, XE991 was applied. The mean frequency was not significantly increased (baseline, 0.78 ± 0.08 Hz, XE991, 0.82 ± 0.09 Hz; n = 8, p = 0.08 , Fig 7A), and there was no significant shift of cumulative distribution of inter-event intervals for each cell and pooled data (Fig 7B). This result suggested the enhancement of the frequency of mEPSCs by XE991 was mediated by calcium influx though P/Q- and N-type calcium channels.

McN-A-343 and XE991 depolarize and increase action potential firing in CA3 neurons

The aforementioned data suggested that inhibition of M-channels resulted in the depolarization of presynaptic terminals of the CA3 pyramidal neuron, which then activated P/Q- or N-type calcium channels, thereby causing calcium influx and ultimately leading to increased glutamate release. We tested the effect of M-channels on the membrane properties of CA3 pyramidal neurons. To study the effects of McN-A-343 and XE991 on CA3 pyramidal neurons,

current-clamp recordings of the membrane potentials were obtained from neurons in slices from juvenile rats (24-30 28 days old). McN-A-343 significantly depolarized CA3 neurons and increased the frequency of action potential firing (0.17 ± 0.08 Hz vs. 2.16 ± 0.72 Hz, n = 6, $p < 0.01$) of CA3 pyramidal neurons (Fig. 8A,C). To measure the membrane potential more accurately, action potentials were blocked by TTX (1 μM). Application of McN-A-343 depolarized CA3 pyramidal neuron membrane potentials from -61.39 ± 1.49 mV to -49.00 ± 1.78 mV (n = 7, $p < 0.01$, Fig. 8B,D).

XE991 had similar effect to that of McN-A-343. It increased the action potential firing frequency (0.42 ± 0.17 Hz vs. 0.79 ± 0.20 Hz, n = 9, $p < 0.01$, Fig. 9A,D) and depolarized CA3 pyramidal neurons (-61.32 ± 2.45 mV vs. -52.62 ± 2.43 mV, n = 10, $p < 0.05$, Fig. 9B,E). Furthermore, and consistent with these findings, the M-channel opener flupirtine (20 μM) hyperpolarized CA3 neurons (-58.02 ± 1.61, vs. -62.97 ± 1.36, n = 7, $p < 0.01$) (Fig. 9C,F).

To test whether the inhibition of M-channels increases membrane input resistance in CA3 pyramidal neurons, current-voltage (I-V) relationships were studied. Current was injected from -40 pA to15 pA in 5 pA steps. Exposure to McN-A-343 shifted the I-V curve to a more negative voltage membrane potentials with negative current injectingions steps. The slope of the I-V curve increased from 1.40 to 1.97, which suggested an increase in input resistance due to the presence of McN-A-343 (Fig. 10A, n = 6). McN-A-343 increased the input resistance from 156.43 ± 17.51 to 228.07 ± 17.16 (? megaohm)(n = 6, $p < 0.01$). Exposure to XE991 had an effect on membrane input resistance that was similar to that of exposure to McN-A-343 in CA3 pyramidal neurons. The slope of the I-V curve increased from 1.22 to 1.75, suggesting increased input resistance in the presence of XE991 (Fig. 10B, n = 7). XE991 increased the input resistance from 129.75 ± 8.63 to 194.53 ± 17.92 (n = 7, $p < 0.01$). These results suggested that the M1 agonist McN-A-343 and the M-channel blocker XE991 close M-type potassium channels in CA3 pyramidal neurons.

Discussion

The present study found that M1 muscarinic activation potentiated glutamate release and that inhibiting M-channels had a similar effect. The application of M-channel blockers increased the frequency of sEPSCs and mEPSCs but had no effect on their amplitudes; the application of an M1 muscarinic receptor agonist had a similar effect to that of the M-channel blockers. The effect of XE991 was dependent on Ca2+ influx through P/Q- and N-type calcium channels. Both the blocking of M-channels and the activation of M1 receptors depolarized CA3 pyramidal neurons. These results suggest that M1 receptor activation inhibits M-type potassium channels and depolarizes CA3 neurons. This causes an influx of Ca2+ through presynaptic voltage-dependent calcium channels and increase spontaneous glutamate release to CA1 neurons. This study demonstrates that M-channels modulate action-potential-independent neurotransmitter release from presynaptic terminals in Schaffer collateral-CA1 pyramidal neuron synapses. These actions occur in addition to the effects on cell soma and axon initial segment, resulting from increased membrane resistance..

M1 receptor agonists and M-channel blockers increase presynaptic glutamate release

In the present study, McN-A-343, a selective agonist for M1receptors, significantly increased the frequency of mEPSCs but had no effect on their amplitudes, which suggests that M1 receptor activation increases presynaptic action potential-independent glutamate release from the Schaffer collaterals. These results are consistent with results from other studies about muscarinic potentiation of glutamatergic transmission in the hippocampus.

M1 is the predominant muscarinic receptor in the hippocampus (accounting for approximately 60% of all muscarinic receptors in the hippocampus), whereas M2 and M4 are less abundant (approximately 20%) (Volpicelli & Levey, 2004). The muscarinic agonist carbachol has been associated with increases in presynaptic glutamate release in cultured rat hippocampal neurons and dentate granule cells in slices (Bouron & Reuter, 1997; Kozhemyakin et al., 2010). An M1 agonist has been shown to cause the potentiation of N-methyl-D-aspartate (NMDA) receptor currents in CA1 hippocampal pyramidal neurons (Marino et al., 1998). The activation of muscarinic receptors induces a long-lasting synaptic enhancement at Schaffer collaterals both in vivo and in vitro via an increase in the postsynaptic release of calcium stored in the endoplasmic reticulum (Fernández de Sevilla et al., 2008). A recent study that combined calcium imaging with two-photon laser glutamate uncaging suggests that M1 receptor activation increases glutamate synaptic potentials and Ca2+ transients in CA1 pyramidal neurons (Giessel & Sabatini, 2010).

Muscarinic M1 (or at some sites M3 or possibly M5) receptor activation inhibits the M-channel (Brown & Passmore, 2009), which was first named in the 1980s (Brown & Adams, 1980; Constanti & Brown, 1981). Immunochemical studies suggest that M-channels are highly expressed in the axon initial segments of neurons (Chung et al., 2006; Pan et al., 2006; Rasmussen et al., 2007). Thus, M-channels are very important for tuning the firing rates and excitability of various neurons (Gu et al., 2005; Shah et al., 2008; Shen et al., 2005; Yue & Yaari, 2004). Interestingly, M-channel activity also affects the release of neurotransmitters from superior cervical ganglion (SCG) neurons and hippocampal synaptosomes (Hernandez et al., 2008; Martire et al., 2004).

Our findings in the current study suggest that M-channels modulate action-potential-independent neurotransmitter release from the presynaptic terminals of the Schaffer collaterals. M-channels are active at the resting membrane potential (Constanti & Brown, 1981) and are expressed in presynaptic terminals (Chung et al., 2006; Cooper et al., 2001; Garcia-Pino et al., 2010). The presynaptic potentiation effect of the M-channel blocker XE991 was reversed over a long period of time. This might be due to its binding kinetics. The dissociation of linopirdine, an analogue of XE991, is slow and begins after 60 min (Wolff et al., 2005).

M1 receptor agonist and M-channel blocker depolarize CA3 neurons

An M1 agonist and an M-channel blocker depolarized CA3 pyramidal neurons. This finding is consistent with the location and function of the receptor in these neurons. The M1 receptor is the most commonly expressed muscarinic receptor in the hippocampus in both the pyramidal neuron layer and the stratum radiatum of the CA3 and CA1 regions (Tayebati et al., 2002). A comparable slow, muscarinic receptor-dependent depolarization can be evoked in pyramidal neurons by the direct electrical stimulation of cholinergic afferents in the hippocampus (Cole & Nicoll, 1983; Madison et al., 1987; Segal, 1988; Morton & Davies, 1997; Pitler & Alger, 1990) or medial septal nucleus in a septo-hippocampal slice (Cobb & Davies, 2005). The medial septal nucleus provides the major source of cholinergic innervations to the hippocampus (Dutar et al., 1995) and presents a direct synaptic input to both principal neurons and interneurons (Frotscher & Léránth, 1985; Léránth & Frotscher, 1987).

Muscarinic acetylcholine receptors modulate several ionic conductances in addition to the M-current, including IAHP (the Ca2+-activated K+ current that is responsible for slowing action potential discharges) and Ileak (the background leak current) (Halliwell, 1990). Activation of mAChRs also potentiates two mixed cation currents (Ih, the hyperpolarization-activated cation current; and Icat, the Ca2+-dependent non-specific cation current) (Colino & Halliwell,

1993; Halliwell, 1990) and the N-methyl-D-aspartate (NMDA) receptor (Markram & Segal, 1990). This may explain why, in our study, the M1 agonist McN-A-343 had a stronger depolarization effect than the M-channel blocker XE991 in CA3 pyramidal neurons.

Muscarinic receptor and intracellular calcium level

Current study suggested that M1 receptor activation depolarizes presynaptic membrane and activates voltage-gated calcium channel to increase intracellular calcium level and neurotransmitter release by inhibition of M-channles. Previous studies suggested that muscarinic stimulation inhibits voltage-gated calcium channels (Qian & Saggau, 1997;Toselli et al., 1989). However these studies did not classify the subtype of muscarnic receptor that mediates this effect. It was reported that the inhibitory effect of muscarinic receptor activation on calcium channels was mediated by M4 subtype in rat sympathetic neurons (Bernheim et al., 1992) and by M2 subtype in rat magocellular cholinergic basal forebrain neurons (Allen & Brown, 1993). There is no report to suggest that M1 subtype muscarinic receptor inhibits calcium channels.

Muscarinic receptors activate inositol 1,4,5-trisphosphate (IP3) receptor to trigger calcium release from endoplasmic reticulum (ER) stores in CA1 pyramidal neurons, and appears to be action potential independent (Power & Sah, 2002). Other study suggested this effect is mediated by M1 receptor (Fernández de Sevilla et al., 2008). Role of these stores in enhancing synaptic release remains uncertain. Although spontaneous transmitter release (in the absence of action potentials) is largely mediated by calcium release from internal stores (Emptage et al., 2001), our study suggest the modulation of spontaneous transmitter release could be mediated by calcium influx though voltage-gated calcium channels.

Overall, this study demonstrated that M1 muscarinic receptor activation inhibits M-type potassium channels, thereby increasing excitatory glutamate neurotransmitter release from the presynaptic terminals of CA3 neurons by increasing the rate of calcium influx through voltage-dependent calcium channels. This effect of M1 receptor activation could contribute to the generation of seizures.

Third goal was to test whether drugs that open M channels would terminate status epilepticus induced by an organophosphate and cholinergic agonist (Li/Pilocarpine). Two models of organophosphate-induced seizures were characterized and published in the Journal Epilepsy Research. A copy of the paper is attached (appendix). The abstract follows.

Materials and Methods
Surgery
All procedures on animals were performed according to a protocol approved by the institutional Animal Care and Use Committee. Adult male Sprague-Dawley rats (Taconic) weighing 175-300g were housed with food and water ad libitum. The animals were anesthetized with ketamine (50 mg/kg) and xylazine (10 mg/kg) for implantation. For animals undergoing intrahippocampal infusion, a bipolar electrode was implanted in the left ventral hippocampus (AP -5.3, ML -4.9, DV -5.0 to dura; incisor bar -3.3). A guide cannula (Plastics One, Roanoke, VA) was implanted into the right ventral hippocampus (AP -5.8, ML +4.6, DV -2.5 from dura; incisor bar -3.3), alongside a second bipolar electrode. A teflon coated 0.01 inch diameter stainless-steel wire positioned near the frontal sinus served as a ground electrode. For animals undergoing peripheral injection studies, three supra-dural cortical electrodes were placed over the cortex. In both procedures, the electrodes were inserted into a strip connector and then secured to the skull with dental acrylic as previously described (Lothman et al., 1988).

Intrahippocampal Infusion

Following a 1 week recovery, animals were connected via a cable to a data acquisition system (Stellate systems). Paraoxon was suspended in 4% hydroxypropyl-B-cyclodextrin (Sigma, St. Louis, MO). An injection needle connected to a 0.1 mL Hamilton syringe and driven by an infusion pump (KD scientific, Portland, OR) was back filled with paraoxon and inserted such that it extended 3 mm below the end of the cannula guide. Paraoxon was then infused at a rate of either 0.5 □L/min or 1 □l/min for a total volume of 20 □L. EEG and video monitoring began 10 minutes prior to paraoxon infusion and continued for 24 hours after infusion completion.

EEG recordings were subsequently reviewed for the presence of seizures as well as SE. Seizures were characterized by the appearance of high frequency (>2 Hz), rhythmic spike wave discharges with amplitudes at least three times that of the baseline EEG. Animals were considered to have SE if there was continuous epileptiform activity for 30 min, during which spike frequencies were more than 2 Hz, and spike amplitude was at least 3 times the background . Behavioral seizures were scored according to the Racine scale (Racine, 1972).

Peripheral injection

EEG recording was initiated prior to administration of 2 mg/kg atropine (Sigma, St. Louis, MO) and 50 mg/kg 2 pralidoxime (2-PAM) iodide (Sigma, St. Louis, MO) intraperitoneally. After 30 minutes, DFP (Sigma, St. Louis, MO) or paraoxon (Chem Service, West Chester, PA) was injected subcutaneously (SC). In some experiments animals were given 10 mg/kg diazepam 10 minutes or 30 minutes after onset of continuous SE activity. A non-diazepam injected group served as controls. 2-PAM and atropine were both dissolved in solution within one hour of injection. DFP and paraoxon were both mixed into cold saline immediately prior to injection. Animals were monitored via EEG and video for 24 hours following organophosphate injection. Epileptiform activity was monitored and defined as follows. Seizures were defined as the appearance of high frequency (>2 Hz), rhythmic spike wave discharges with amplitudes at least 3 times that of the baseline EEG. The criterion for the onset of SE was the occurrence of continuous seizure activity for 10 minutes, during which spike frequencies do not drop below 2 Hz. The end of SE was characterized by non-uniform spike frequencies that remained lower than 1 Hz. EEG data was polled every 10 minutes after the onset of SE to determine SE termination during a 5 hour interval after SE began.

Immunohistochemistry for Fluorojade and NeuN

The procedures of tissue preparation were described in detail previously (Sun et al., 2004;Sun et al., 2007). Briefly, animals were anesthetized with an overdose of pentobarbitone sodium and perfused through the ascending aorta with 50-100 ml 0.9% NaCl followed by 350-450 ml 4% paraformaldehyde in 0.1 M phosphate buffer (PB, pH 7.4). Brains were removed and post-fixed in the same fixative for 2 hours at 4oC. Brains were frozen by immersion in -70oC isopentane. Coronal sections from the anterior block were cut at 40 μm to collect dorsal sections.

In order to stain for NeuN and Fluoro-Jade B, immunohistochemical technique was modified as described previously (Jakab and Bowyer, 2002;Sun et al., 2007). Sections were incubated for 48 hours at 4°C in the anti-NeuN primary antibody mouse anti-NeuN, (diluted at 1:200,Millipore) followed by incubation with a secondary antibody conjugated to Alexa Fluor 594 (5□g/ml; molecular probes) for 60 minutes at room temperature. Sections were wet-mounted on glass slides, air-dried at 50°C for 15 minutes, and stained with Fluoro-Jade B. The slides were immersed in distilled water for 1 minute and oxidized in a 0.006% solution of KMnO4 for 5 minutes. After rinsing in distilled water twice for 30 seconds, sections were stained for 10 minutes in a 0.0003% solution of Fluoro-Jade B in 0.1% acetic acid. Finally, sections were rinsed in distilled water, air-dried, and cleared with xylene.

Results

Seizures and SE caused by paraoxon infusion

Infusion of 100 nmol paraoxon into the hippocampus caused electrographic seizures in 2/9 (22.2%) animals tested. None of the animals had seizures lasting beyond the end of infusion and 2 animals displayed intermittent seizures during paraoxon infusion which were not self-sustaining. No change in baseline EEG, and no behavioral seizures occurred in the remaining 7 animals (figure 11 A).

Infusion of 200 nmol paraoxon into the hippocampus caused electrographic seizures in 43/52 (82.7%) animals tested. In 32 animals seizures lasted beyond the end of infusion (61.5%) and 11 animals displayed intermittent seizures during paraoxon infusion which were not self-sustaining, and did not continue through the end of infusion (figure 11B). There was no change in baseline EEG in remaining 9 animals. These animals did not display behavioral characteristics indicative of seizure activity.

Among animals with seizures lasting beyond paraoxon infusion, two distinct types of electrographic seizure activity occurred: intermittent and continuous seizures. Intermittent seizures, which occurred in 18 animals, frequently appeared first in the paraoxon infusion site in the right hippocampus, and then spread to the contra-lateral (left) hippocampus(Figure 11C). Seizures consisted of rhythmic high frequency spike wave discharges that evolved in frequency and amplitude. There were brief periods of suppression of activity between seizures.

Continuous seizures occurred in 14 animals following paraoxon infusion, and these consisted of sustained bilateral discharges of repetitive spike patterns evolving over time (Fig. 11D). Continuous electrographic seizures started at approximately 15 minutes post infusion, and persisted for 4-18 hours. These prolonged self-sustaining seizures constituted SE. Paraoxon-induced SE was further confirmed upon observation of behavioral seizures. Animals experiencing SE exhibited freezing, staring, blinking, and hyper-exploratory movement, as well as wet-dog shaking movements for 4-18 hours.

Infusion of 300 nmol paraoxon into the hippocampus caused electrographic seizures in 10/11 (90.9%) of animals tested. The seizures in all of these animals continued beyond the end of infusion in form of SE with behavioral seizures ranging from 2-5 on the Racine scale. The majority of animals in SE (7) died of respiratory arrest, several of these exhibited symptoms of peripheral cholinergic stimulation, including muscle contractions and fasciculations. The remaining 3 animals survived, exhibiting seizures that lasted long beyond the end of infusion. Only 1 animal receiving paraoxon 300 nM infusion displayed neither behavioral characteristics indicative of seizure activity, nor EEG seizure activity (9.0%).

The location of the cannula was confirmed by sectioning the hippocampus. In many animals, the cannula and electrode tracts were localized by sectioning the brain in the plane of the electrode. In other animals, immunohistochemistry for neuronal stain Neun and staining for neuro-degeneration dye fluorojade J, was performed 3 days after SE caused by infusion of paraoxon. The site of infusion was at the ventricular border the CA3 layer of the hippocampus, (figure 2 A). Fluorojade positive neurons were present in CA1and CA3 regions and of the hippocampus and the subiculum (figure 2 B,C). Occasional Fluorojade positive cells were present in the hilus.

Peripheral injection of Paraoxon

Preliminary experiments were performed to optimize the model. Paraoxon (0.35 mg/kg) administered by the intra-peritoneal route caused widespread muscle contractions, fasciculations, rare tonic convulsions, respiratory arrest and death in all four animals tested. Pretreatment of animals with scopolamine (4 mg/kg) protected against peripheral and systemic effects of paraoxon (n = 4 animals). Subsequently oxime reactivator 2-PAM and muscarinic antagonist atropine was combined with peripheral paraoxon administration. In preliminary

experiments we tested other doses of these agents and confirmed that most optimal doses were used.

Paraoxon (1 mg/kg) was administered SC to 23 animals 30 minutes after pre-treatment with 2 mg/kg atropine and 50 mg/kg 2-PAM and prolonged seizures were observed. SE occurred in 17 of the 23 animals (74%) with animals displaying a combination of chewing, head-bobbing, single and bilateral limb clonus and rearing, leading to constant full body tremors. In 3 animals there was no effect from the OP injection and 3 animals died from respiratory arrest without any seizures.

In these animals electrographic seizures either started as continuous long lasting seizures or evolved from discrete seizures to continuous seizures (Figure 13, panel control). The mean time for the onset of first electrographic seizure in animals treated with paraoxon was 6m 4s ± 42s. The first seizure was also the onset or continuous EEG activity in 29% (5/17) of the animals studied. In 7 of the 18 animals, a discrete electrographic seizure lasting 30-60 seconds was the first electrographic seizure, followed by a prolonged period of suppression. This was followed by the onset of continuous electrographic seizure activity. The remaining 35% (6/17) progressed from discrete seizure continuous EEG with a period of brief suppression (10-30 seconds) between 30-60 second seizure bursts. The mean time for onset of continuous electrographic seizure activity after paraoxon injection was 10m 3s ± 1m. At the onset of continuous EEG seizure activity, electrographic spiking occurred at a rate of 2-4 Hz, and frequency increased to 4-8 Hz within 10 minutes of onset.

One group of animals (n=6) was left untreated after the onset of continuous seizures. One animal died 2h 45m after the onset of continuous seizures. The mean SE duration was 10h 15m ± 1h 42m in the remaining five animals, ranging from 7-17 hours. The SE ended with the frequency of epileptiform activity falling below 1 Hz in all 5 of the animals within 18 hours of onset.

A group of animals (n =6) in paraoxon induced SE was treated with 10 mg/kg diazepam ten minutes after the onset of continuous seizure activity (Figure 13, middle panel). Diazepam terminated continuous seizures at this time point (Figure 14, middle panel). In two of these animals, SE was terminated within the first 10 minutes of treatment (figure 14). In these animals, spike frequency dropped from 4-6 Hz to 0 and baseline EEG was restored. Seizures did not recur. In two animals SE ended 90 -150 minutes after onset (figure 14). The spike frequency gradually dropped from 4-6 Hz with poly-spikes to single spikes with a frequency of less than 1 Hz (figure 3). All animals were seizure free by seven hours. There was no mortality within 24 hours.

Animals (n =5) treated with 10 mg/kg of diazepam 30 minutes after continuous EEG activity also responded to treatment, with (60%) becoming seizure free within 10 minutes of treatment (figure 3 right panel). Only one of the five animals was still having seizures 70 minutes after continuous seizures began, and continuous seizures lasted for 12 hours (figure 14). No animal in this group died during the 24 hour period.

DFP

Preliminary experiments were performed to optimize DFP model of SE. Rats that were pretreated with 1 mg/kg atropine 30 minutes and then given 1.25 mg/kg DFP SC (n=4) all died from respiratory arrest, whereas 50% of rats pretreated with 1 mg/kg atropine and 25 mg/kg 2-PAM (n=4) survived and exhibited prolonged seizure activity. Higher DFP dose of 1.5 mg/kg combined with a pretreatment of larger doses of atropine (2 mg/kg) and 2-PAM (50 mg/kg) caused death in 2 animals. These observations and previously published data suggested that 1.25 mg/kg DFP SC in cold saline with a pretreatment of 2 mg/kg atropine and 50 mg/kg 2-PAM were likely to produce SE in animals.

This combination was used to study DFP induced SE, and it caused continuous seizure activity and SE in 15 out of 19 (79%) of the animals studied, with the remainder dying of respiratory

arrest. Animals in SE group exhibited a combination of chewing, head-bobbing, single and bi-limb clonus and rearing, leading to constant full body tremors and SE. The mean time to first EEG seizure in this group was 21m 43s ± 3m 25s. In 7 of 15 animals, the first electrographic seizure was also the onset of continuous seizure activity. In 7 other animals, seizure progression went from periods of discrete seizures, separated by normal EEG followed by seizures lasting 10 to 30 seconds with periods of suppression, after which seizures merged into continuous epileptiform activity. In one animal, a brief discrete seizure was followed by continuous seizure activity. Continuous epileptiform activity started at a frequency of 2 Hz and accelerated to 4-6 Hz within ten minutes. The latency to the development of continuous electrographic activity was 24m 41s ± 3m 48s after DFP injection.
In 5 animals left untreated after the DFP induced SE, 3 survived to 5 hours after continuous seizure onset and the remaining died. Seizures stopped in one animal 4.5 hours after the onset of continuous seizure activity, while the other two displayed electrographic seizures which lasted for more than 8 hours.
DFP induced seizures were much more resistant to diazepam treatment when given at 30 minutes than when treated at 10 minutes (Figures 15,16). Three out of the five rats (60%) given diazepam after 10 minutes after continuous EEG activity demonstrated rapid drop in spike wave discharge frequency and amplitude with return of baseline EEG; the remaining two out of five animals (40%) continued to have seizures for more than 5 hours. No animal in this group died within the 24 hour after SE onset.
Diazepam given 30 minutes after the start of continuous EEG activity did not stop SE within 60 and 120 minutes after onset of SE in any of the 5 animals tested (Figures 15, 16). First termination of SE in these animals first occurred 2.5 hours after treatment injection, with 60% (3/5) of rats coming out of SE within the first 5 hours of diazepam injection (Figure 6). In addition, while treatment at 30 minutes did eventually terminate SE, this termination was marked by appearance arrhythmic spikes and the baseline EEG was not restored in any animal.

We have characterized SE induced by two different organophosphates, intrahippocampal infusion of paraoxon and peripheral injection of DFP or paraoxon following treatment of 2-PAM and atropine. Peripheral injection of OP agents has a higher incidence of producing self-sustaining seizures, while intrahippocampal infusion has the benefit of not requiring pretreatment with 2-PAM and atropine.
Treatment of status epilepticus (Experiment 3.1, 3.2): We tested whether the action of M-Channel opener flupirtine in cholinergic over-stimulation-induced status epilepticus. Last year we reported that flupirtine alone is ineffective in terminating Lithium/Pilocarpine induced status epilepticus. However, a combination of flupirtine and diazepam terminated status epilepticus.

We then tested the efficacy of flupirtine in terminating DFP induced status epilepticus. DFP-induced status epilepticus is of importance because it is induced by an organophosphate, which is a choline-esterase inhibitor. Flupirtine alone was effective in 80% of animals, in 2 hours (figure 17 red line). However, a combination of flupirtine and diazepam were effective in rapidly terminating refractory status epilepticus. Status epilepticus was terminated in all animals within 30 minutes (figure 17 blue line,). The results are displayed in figure in the appendix. We are preparing a manuscript to report these results.

We have also tested the efficacy of retigabine (Potiga), which is another M channel opener in lithium pilocarpine model. We tested doses 1, 2, 4, 35 and 75 mg/ Kg alone and they were ineffective in terminating status epilepticus. The drug was not effective either when combined with 10 mg/Kg diazepam.

Finally in a related project we found that AMPA type glutamate receptor are modified during status epilepticus. This work was published in Annals of Neurology and supported by NIH grants.

Key Research Accomplishments:

- We demonstrated that muscarinic stimulation causes enhanced synaptic transmission at Schaffer collateral CA1 pyramidal neuron synapses in the hippocampus.
- We developed two models of organophosphate induced seizures and status epilepticus.
- We tested potassium channel opener flupirtine in an organophosphate model and found it to be effective in terminating status epilepticus when combined with diazepam.

REPORTABLE OUTCOMES

1) Sun J, Kapur J. M-type potassium channels modulate Schaffer-collateral CA1 glutamatergic synaptic transmission. J Physiol. 2012 Jul 9. [Epub ahead of print] PubMed PMID: 22674722. doi: 10.1113/jphysiol.2012.235820

2) Todorovic MS, Cowan ML, Balint CA, Sun C, Kapur J. Characterization of status epilepticus induced by two organophosphates in rats. Epilepsy Res. 2012 May 9. [Epub ahead of print] PubMed PMID: 22578704. http://dx.doi.org/10.1016/j.eplepsyres.2012.04.014

Conclusions:

These studies demonstrate that muscarinic stimulation of hippocampal neurons increases their excitability and enhances neurotransmitter release at Schaffer collateral-CA1 synapses. This enhancement occurs by inhibition of M-type (KCNQ2/3) potassium channels. Drugs that open M –type potassium channels can counter the effect of muscarinic stimulation in hippocampal slices. Drugs that open M type channels were effective in terminating organophosphate-induced status epilepticus.

Future plans: As proposed in the original application aims 1 &2, we will extend these studies to perforant path-dentate granule cell synapse in the hippocampus. We will also test whether another M channel opener terminates status epilepticus.

References

Allen, T. G. & Brown, D. A. (1993). M2 muscarinic receptor-mediated inhibition of the Ca2+ current in rat magnocellular cholinergic basal forebrain neurones. J Physiol 466, 173-189.

Bernheim, L., Mathie, A., & Hille, B. (1992). Characterization of muscarinic receptor subtypes inhibiting Ca2+ current and M-current in rat sympathetic neurons. Proc Natl Acad Sci U S A 89, 9544-9548.

Biervert, C., Schroeder, B.C., Kubisch, C., Berkovic, S. F., Propping, P., Jentsch, T. J., & Steinlein, O. K. (1998). A potassium channel mutation in neonatal human epilepsy. Science 279, 403-406.

Bouron, A. & Reuter, H. (1997). Muscarinic stimulation of synaptic activity by protein kinase C is inhibited by adenosine in cultured hippocampal neurons. Proc Natl Acad Sci U S A 94, 12224-12229.

Brown, D. A. & Adams, P. R. (1980). Muscarinic suppression of a novel voltage-sensitive K+ current in a vertebrate neurone. Nature 283, 673-676.

Brown, D. A. & Passmore, G. M. (2009). Neural KCNQ (Kv7) channels. Br J Pharmacol 156, 1185-1195.

Chu-Shore, C. J. & Thiele, E. A. (2010). New drugs for pediatric epilepsy. Semin Pediatr Neurol 17, 214-223.

Chung, H. J., Jan, Y. N., & Jan, L. Y. (2006). Polarized axonal surface expression of neuronal KCNQ channels is mediated by multiple signals in the KCNQ2 and KCNQ3 C-terminal domains. Proc Natl Acad Sci U S A 103, 8870-8875.

Cobb, S. R. & Davies, C. H. (2005). Cholinergic modulation of hippocampal cells and circuits. J Physiol 562, 81-88.

Cole, A. E. & Nicoll, R. A. (1983). Acetylcholine mediates a slow synaptic potential in hippocampal pyramidal cells. Science 221, 1299-1301.

Colino, A. & Halliwell, J. V. (1993). Carbachol potentiates Q current and activates a calcium-dependent non-specific conductance in rat hippocampus in vitro. Eur J neurosci 5, 1198-1209.

Constanti, A. & Brown, D. A. (1981). M-currents in voltage-clamped mammalian sympathetic neurones. Neurosci Lett 24, 289-294.

Cooper, E. C., Harrington, E., Jan, Y. N., & Jan, L. Y. (2001). M-channel KCNQ2 subunits are localized to key sites for control of neuronal network oscillations and synchronization in mouse brain. J Neurosci 21, 9529-9540.

Delmas, P. & Brown, D. A. (2005). Pathways modulating neural KCNQ/M (Kv7) potassium channels. Nat Rev Neurosci 6, 850-862.

Devaux, J. J., Kleopa, K. A., Cooper, E. C., & Scherer, S. S. (2004). KCNQ2 is a nodal K+ channel. J Neurosci 24, 1236-1244.

Dutar, P., Bassant, M. H., Senut, M. C., & Lamour, Y. (1995). The septohippocampal pathway: structure and function of a central cholinergic system. Physiol Rev 75, 393-427.

Emptage, N. J., Reid, C. A., & Fine, A. (2001). Calcium stores in hippocampal synaptic boutons mediate short-term plasticity, store-operated Ca2+ entry, and spontaneous transmitter release. Neuron 29, 197-208.

Fernandez de Sevilla, D., Núñez, A., Borde, M., Malinow, R., & Buño W. (2008). Cholinergic-mediated IP3-receptor activation induces long-lasting synaptic enhancement in CA1 pyramidal neurons. J Neurosci 28, 1469-1478.

Frotscher, M. & Léránth, C. (1985). Cholinergic innervation of the rat hippocampus as revealed by choline acetyltransferase immunocytochemistry: a combined light and electron microscopic study. J Comp Neurol 239, 237-246.

Garcia-Pino, E., Caminos, E., & Juiz, J. M. (2010). KCNQ5 reaches synaptic endings in the auditory brainstem at hearing onset and targeting maintenance is activity-dependent. J Comp Neurol 518, 1301-1314.

Geiger, J., Weber, Y. G., Landwehrmeyer, B., Sommer, C., & Lerche, H. (2006). Immunohistochemical analysis of KCNQ3 potassium channels in mouse brain. Neurosci Lett 400, 101-104.

Giessel, A. J. & Sabatini, B. L. (2010). M1 muscarinic receptors boost synaptic potentials and calcium influx in dendritic spines by inhibiting postsynaptic SK channels. Neuron 68, 936-947.

Gu, N., Vervaeke, K., Hu, H., & Storm, J. F. (2005). Kv7/KCNQ/M and HCN/h, but not KCa2/SK channels, contribute to the somatic medium after-hyperpolarization and excitability control in CA1 hippocampal pyramidal cells. J. Physiol 566, 689-715.

Halliwell, J. V. (1990). Physiological mechanisms of cholinergic action in the hippocampus. Prog Brain Res 84, 255-272.

Hamilton, S. E., Loose, M. D., Qi, M., Levey, A. I., Hille, B., McKnight, G. S., Idzerda, R. L., & Nathanson, N. M. (1997). Disruption of the M1 receptor gene ablates muscarinic receptor-dependent M-current regulation and seizure activity in mice. Proc.Natl.Acad.Sci.U.S.A 94, 13311-13316.

Hernandez, C. C., Zaika, O., Tolstykh, G. P., & Shapiro, M. S. (2008). Regulation of neural KCNQ channels: signalling pathways, structural motifs and functional implications. J Physiol 586, 1811-1821.

Higley, M. J., Soler-Llavina, G. J., & Sabatini, B. L. (2009). Cholinergic modulation of multivesicular release regulates striatal synaptic potency and integration. Nat Neurosci 12, 1121-1128.

Jentsch, T. J. (2000). Neuronal KCNQ potassium channels:physislogy and role in disease. Nat Rev Neurosci 1, 21-30.

Kanaumi, T., Takashima, S., Iwasaki, H., Itoh, M., Mitsudome, A., & Hirose, S. (2008). Developmental changes in KCNQ2 and KCNQ3 expression in human brain: possible contribution to the age-dependent etiology of benign familial neonatal convulsions. Brain Dev 30, 362-369.

Kozhemyakin, M., Rajasekaran, K., & Kapur, J. (2010). Central cholinesterase inhibition enhances glutamatergic synaptic transmission. J Neurophysiol 103, 1748-1757.

Langmead, C. J., Watson, J., & Reavill, C. (2008). Muscarinic acetylcholine receptors as CNS drug targets. Pharmacol Ther 117, 232-243.

Léránth, C. & Frotscher, M. (1987). Cholinergic innervation of hippocampal GAD- and somatostatin-immunoreactive commissural neurons. J Comp Neurol 261, 33-47.

Madison, D. V., Lancaster, B., & Nicoll, R. A. (1987). Voltage clamp analysis of cholinergic action in the hippocampus. J Neurosci 7, 733-741.

Marino, M. J., Rouse, S. T., Levey, A. I., Potter, L. T., & Conn, P. J. (1998). Activation of the genetically defined M1 muscarinic receptor potentiates N-methyl-d-aspartate (NMDA) receptor currents in hippocampal pyramidal cells. Proc.Natl.Acad.Sci.U.S.A 95, 11465-11470.

Markram, H., & Segal, M. (1990). Acetylcholine potentiates responses to N-methyl-d-aspartate in the rat hippocampus. Neurosci Lett 113, 62-65.

Marrion, N. V., Smart, T. G., Marsh, S. J., & Brown, D. A. (1989). Muscarinic suppression of the M-Current in the rat sympathetic-ganglion is mediated by receptors of the M1-subtype. Br J Pharmacol 98, 557-573.

Martire, M., Castaldo, P., D'Amico, M., Preziosi, P., Annunziato, L., & Taglialatela, M. (2004). M- channels containing KCNQ2 subunits modulate norepinephrine, aspartate, and GABA release from hippocampal nerve terminals. J Neurosci 24, 592-597.

Morton, R. A. & Davies, C. H. (1997). Regulation of muscarinic acetylcholine receptor-mediated synaptic responses by adenosine receptors in the rat hippocampus. J Physiol 502, 75-90.

Pan, Z., Kao, T., Horvath, Z., Lemos, J., Sul, J. Y., Cranstoun, S. D., Bennett, V., Scherer, S. S., & Cooper, E. C. (2006). A common ankyrin-G-based mechanism retains KCNQ and NaV channels at electrically active domains of the axon. J Neurosci 26, 2599-2613.

Peretz, A., Sheinin, A., Yue, C., Degani-Katzav, N., Gibor, G., Nachman, R., Gopin, A., Tam, E., Shabat, D., Yaari, Y., & Attali, B. (2007). Pre- and postsynaptic activation of M-channels by a novel opener dampens neuronal firing and transmitter release. J Neurophysiol 97, 283-295.

Pitler, T. A. & Alger, B. E. (1990). Activation of the pharmacologically defined M3 muscarinic receptor depolarizes hippocampal pyramidal cells. Brain Res 534, 257-262.

Power, J. M. & Sah, P. (2002). Nuclear calcium signaling evoked by cholinergic stimulation in hippocampal CA1 pyramidal neurons. J Neurosci 22, 3454-3462.

Qian, J. & Noebels, J. L. (2000). Presynaptic Ca2+ influx at a mouse central synapse with Ca2+ channel subunit mutations. J Neurosci 20, 163-170.

Qian, J. & Saggau, P. (1997). Presynaptic inhibition of synaptic transmission in the rat hippocampus by activation of muscarinic receptors: involvement of presynaptic calcium influx. Br J Pharmacol 122, 511-519.

Raol, Y. H., Lapides, D. A., Keating, J. G., Brooks-Kayal, A. R., & Cooper, E. C. (2009). A KCNQ channel opener for experimental neonatal seizures and status epilepticus. Ann Neurol 65, 326-336.

Rasmussen, H. B., Frøkjær-Jensen, C., Jensen, C. S., Jensen, H. S., Jørgensen, N. K., Misonou, H., Trimmer, J. S., Olesen, S.P., & Schmitt, N. (2007). Requirement of subunit co-assembly and ankyrin-G for M-channel localization at the axon initial segment. J Cell Sci 120, 953-963.

Safiulina, V. F., Zacchi, P., Taglialatela, M., Yaari, Y., & Cherubini, E. (2008). Low expression of Kv7/M channels facilitates intrinsic and network bursting in the developing rat hippocampus. J Physiol 586, 5437-5453.

Segal, M. (1988). Synaptic activation of a cholinergic receptor in rat hippocampus. Brain Res 452, 79-86.

Selyanko, A. A., Delmas, P., Hadley, J. K., Tatulian, L., Wood, I. C., Mistry, M., London, B., & Brown, D. A. (2002). Dominant-negative subunits reveal potassium channel families that contribute to M-like potassium currents. J. Neurosci 22, RC212.

Shah, M. M., Migliore, M., Valencia, I., Cooper, E. C., & Brown, D. A. (2008). Functional significance of axonal Kv7 channels in hippocampal pyramidal neurons. Proc Natl Acad Sci U S A 105, 7869-7874.

Shah, M. M., Mistry, M., Marsh, S. J., Brown, D. A., & Delmas, P. (2002). Molecular correlates of the M-current in cultured rat hippocampal neurons. J Physiol 544, 29-37.

Shen, W., Hamilton, S. E., Nathanson, N. M., & Surmeier, D. J. (2005). Cholinergic suppression of KCNQ channel currents enhances excitability of striatal medium spiny neurons. J Neurosci 25, 7449-7458.

Sim, J. A. & Griffith, W. H. (1996). Muscarinic Inhibition of glutamatergic transmission onto rat magnocellular basal forebrain neurons in a thin-slice preparation. Eur J Neurosci 8, 880-891.

Smolders, I., Khan, G. M., Manil, J., Ebinger, G., & Michotte, Y. (1997). NMDA receptor-mediated pilocarpine-induced seizures: characterization in freely moving rats by microdialysis. Br J Pharmacol 121, 1171-1179.

Stephen, L. J. & Brodie, M. I. (2011). Pharmacotherapy of epilepsy newly approved and developmental agents. CNS Drugs 25, 89-107.

Tayebati, S. K., Amenta, F., El-Assouad, D., & Zaccheo, D. (2002). Muscarinic cholinergic receptor subtypes in the hippocampus of aged rats. Mech of Ageing Dev 123, 521-528.

Toselli, M., Lang, J., Costa, T., & Lux, H. D. (1989). Direct modulation of voltage-dependent calcium channels by muscarinic activation of a pertussis toxin-sensitive G-protein in hippocampal neurons. Pflugers Arch 415, 255-261.

Vervaeke, K., Gu, N., Agdestein, C., Hu, H., & Storm, J. F. (2006). Kv7/KCNQ/M-channels in rat glutamatergic hippocampal axons and their role in regulation of excitability and transmitter release. J Physiol 576, 235-256.

Vogt, K. E. & Regehr, W. G. (2001). Cholinergic modulation of excitatory synaptic transmission in the CA3 area of the hippocampus. J.Neurosci 21, 75-83.

Volpicelli, L. A. & Levey, A. I. (2004). Muscarinic acetylcholine receptor subtypes in cerebral cortex and hippocampus. Prog Brain Res 145, 59-66

Wang, H. S., Pan, Z., Shi, W., Brown, B. S., Wymore, R. S., Cohen, I. S., Dixon, J. E., & McKinnon, D. (1998). KCNQ2 and KCNQ3 potassium channel subunits: molecular correlates of the M-channel. Science 282, 1890-1893.

Weber, Y. G., Geiger, J., Kämpchen, K., Landwehrmeyer, B., Sommer, C., & Lerche, H. (2006). Immunohistochemical analysis of KCNQ2 potassium channels in adult and developing mouse brain. Brain Res 1077, 1-6.

Wheeler, D. B., Randall, A., & Tsien, R. W. (1994). Roles of N-type and Q-type Ca2+ channels in supporting hippocampal synaptic transmission. Science 264, 107-111.

Wolff, C., Gillard, M., Fuks, B., & Chatelain, P. (2005). [3H]linopirdine binding to rat brain membranes is not relevant for M-channel interaction. Eur J Pharmacol 518, 10-17.

Wu, Y. J. & Dworetzky, S. I. (2005). Recent developments on KCNQ potassium channel openers. Curr Med Chem 12, 453-460.

Yajeya, J., De La Fuente, A., Criado, J. M., Bajo, V., Sánchez-Riolobos, A., & Heredia, M. (2000). Muscarinic agonist carbachol depresses excitatory synaptic transmission in the rat basolateral amygdala in vitro. Synapse 38, 151-160.

Yue, C. & Yaari, Y. (2004). KCNQ/M Channels control spike afterdepolarization and burst generation in hippocampal neurons. J Neurosci 24, 4614-4624.

Zhang, H. M., Chen, S. R., & Pan, H. L. (2007). Regulation of glutamate release from primary afferents and interneurons in the spinal cord by muscarinic receptor subtypes. J. Neurophysiol. 97, 102-109.

Appendices

Figure 1-17 & PDF reprints of two publications

Figure1. M1 muscarinic agonist increased the frequency of mEPSCs recorded from CA1 pyramidal neurons. A, Representative traces of mEPSCs recorded from CA1 pyramidal neurons before (left) and after (right) the application of 10 μM McN-A-343. B, Representative averaged traces of mEPSCs before (black) and during (grey) the application of McN-A-343 along with the overlay of the two traces. C and D, Cumulative probability plots of mEPSC frequency (C) and amplitude (D) obtained by pooling data from 7 neurons before (solid lines) and after (dotted lines) application of McN-A-343.

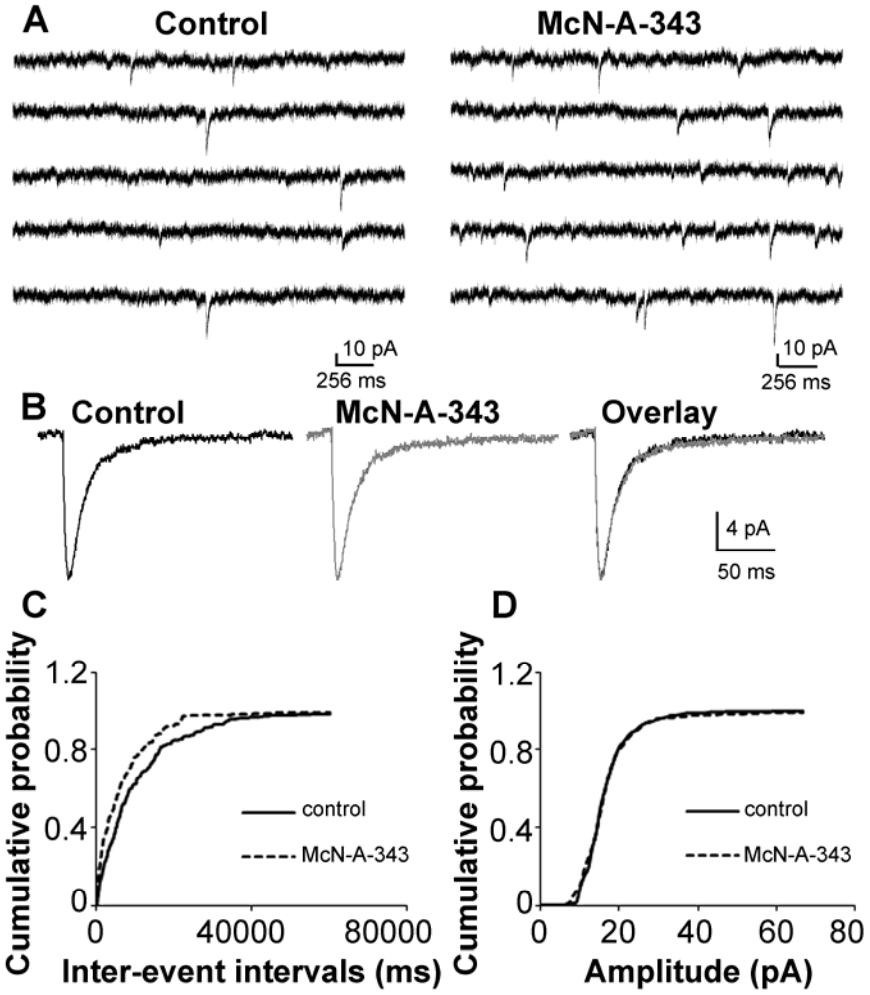

Figure 2. M-channel blocker XE991 increased mEPSC frequency in CA1 neurons. A, Representative mEPSC recordings obtained from a CA1 pyramidal neuron before (left) and after (right) the application of 10 μM XE991. B and C, Cumulative probability plots of mEPSC frequency (C) and amplitude (D) obtained by pooling data from 8 neurons before (solid lines) and after (dotted lines) the application of XE991.

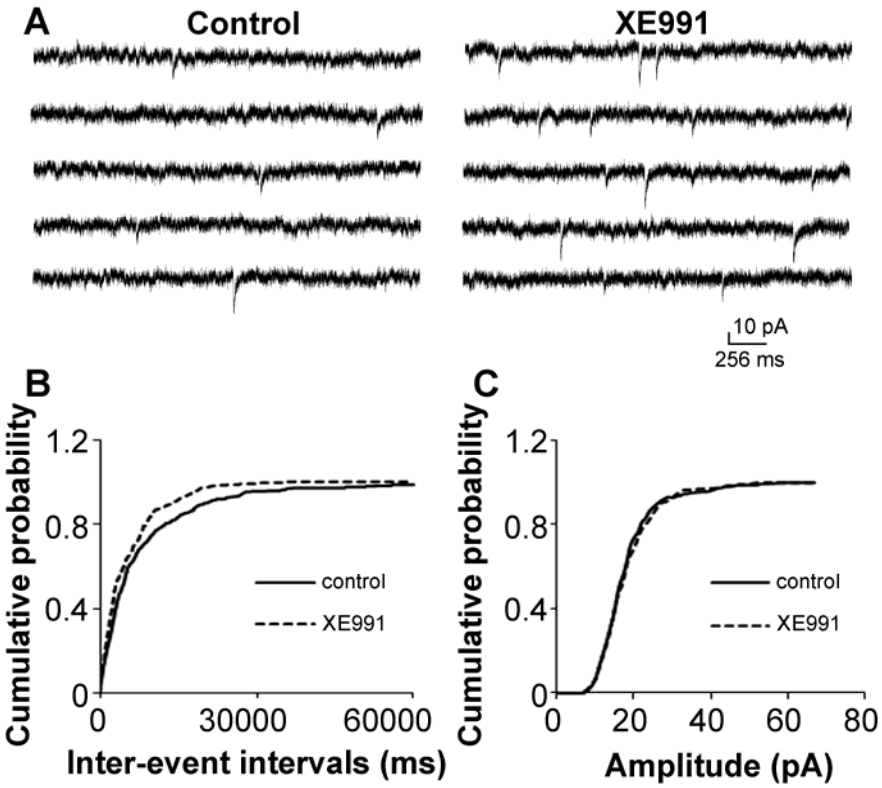

Figure 3. The effect of linopirdine and flupirtine, and the occlusion of XE991 to the effect of McN-A-343 on mEPSC in CA1 neurons. A, and B, Cumulative probability plots of mEPSC frequency by pooling data from neurons before (solid lines) and after (dotted lines) the application of linopirdine (A), flupirtine (B). C, Cumulative probability plot of mEPSC frequency by pooling data from neurons before (solid lines) and after (dotted lines) the application of McN-A-343 after 25 min incubation in XE991.

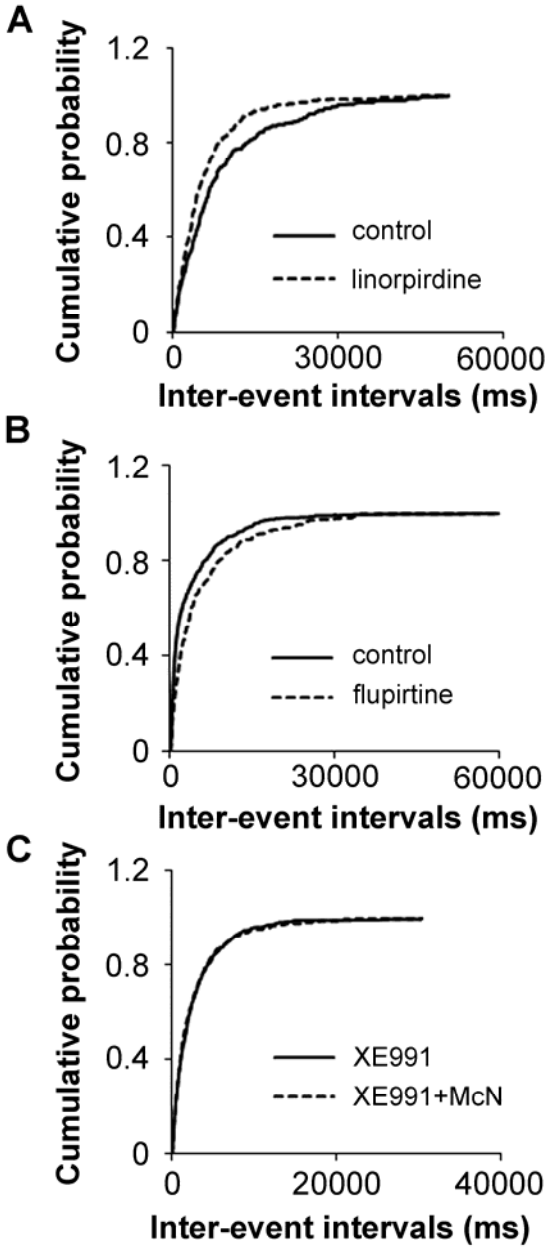

Figure 4. The effect of XE991 on mEPSC frequency was eliminated in calcium-free ACSF. A and C, Representative mEPSC recordings obtained from a CA1 pyramidal neuron before (top) and after (bottom) the application of 10 μM XE991 after 20 min incubation in thapsigargin (2.5 μM) (A) or in calcium-free ACSF (C). B and D, Cumulative probability plots of the frequency of mEPSCs obtained by pooling data from 8 neurons before (solid lines) and after (dotted lines) the application of XE991 in thapsigargin incubation (B) or in calcium-free ACSF (D).

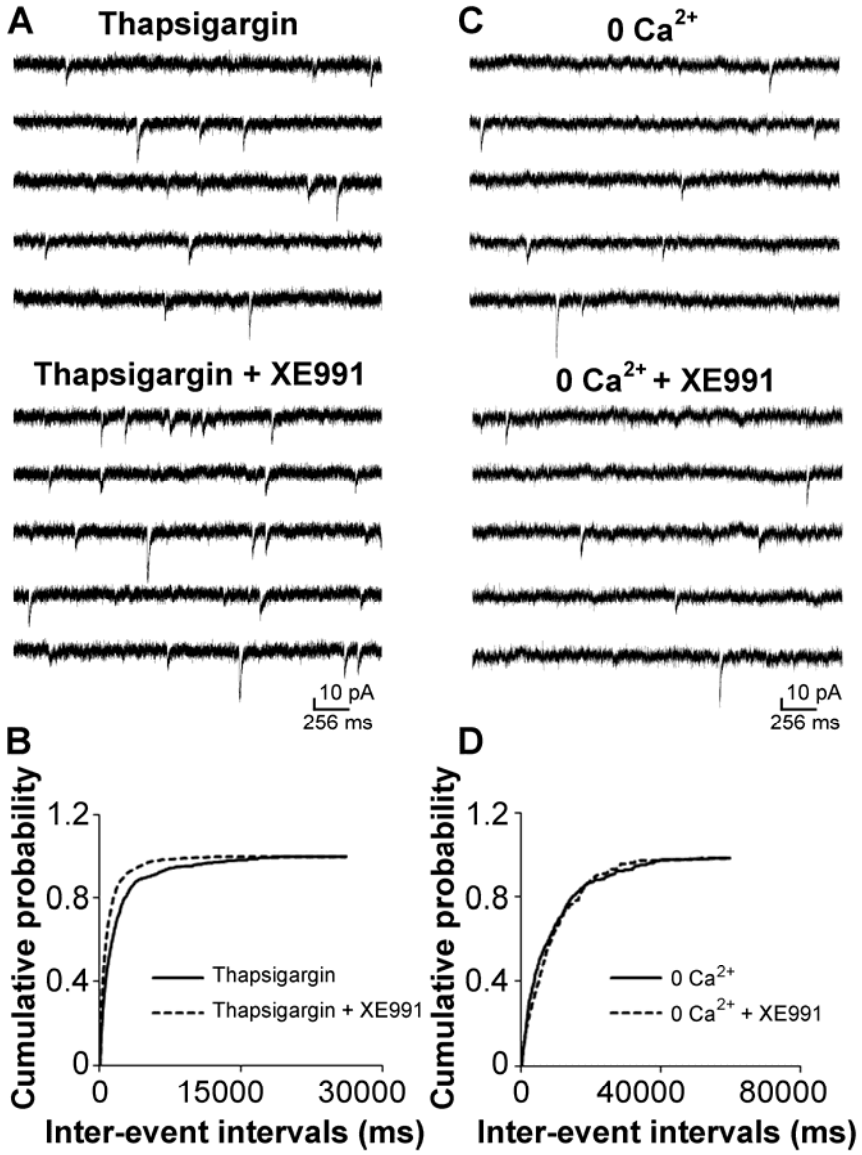

Figure 5. P/Q-type calcium channel blocker on the effect of XE991 on mEPSC frequency. A and B, Representative mEPSC recordings obtained from a CA1 pyramidal neuron in which the blocking of P/Q-type of calcium channels by 200 nM ω-agatoxin TK did (A) or did not (B) prevent the effect of 10 μM XE991. The left panels include data from recordings in the presence of ω-agatoxin TK before the application of XE991, and the right panels include data from recordings after the application of XE991. C and D, Cumulative probability plots of mEPSC frequency obtained by pooling data from CA1 pyramidal neurons before (solid lines) and after (dotted lines) the application of XE991 in the presence of ω-agatoxin TK that did (C) or did not prevent (D) the effect of XE991.

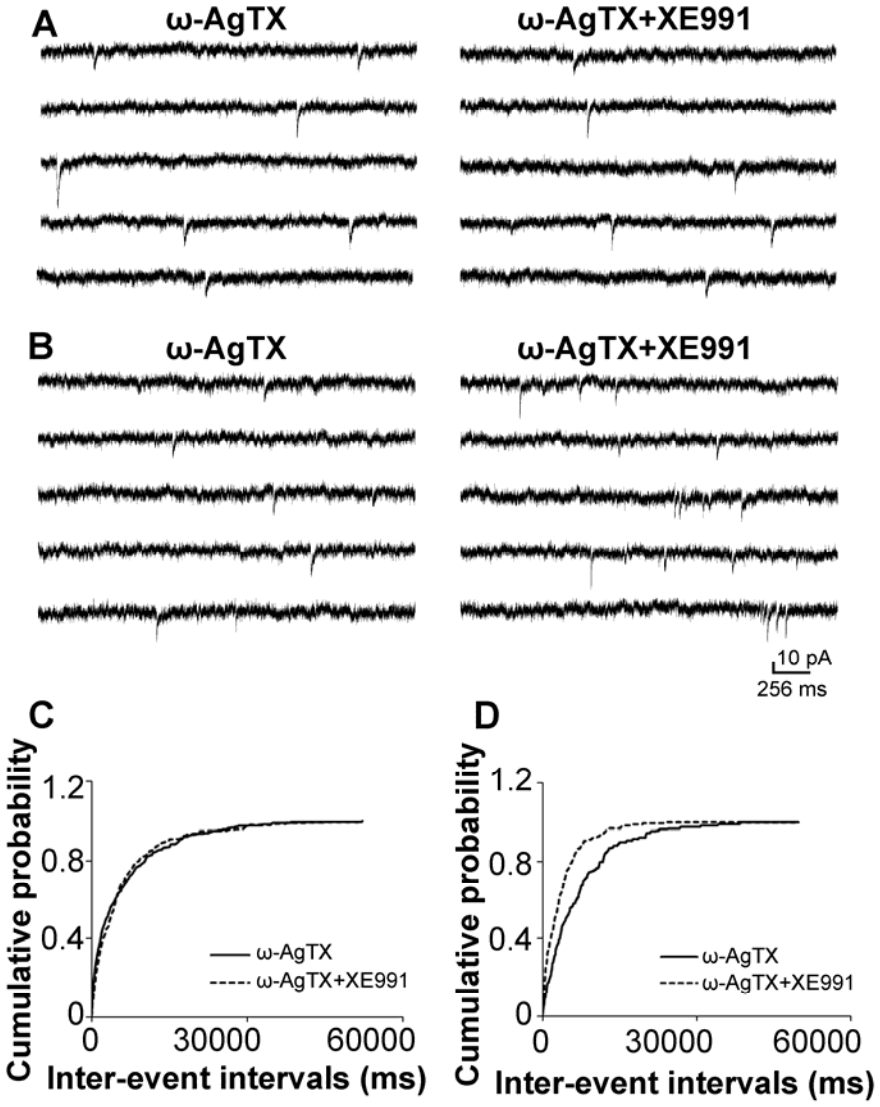

Figure 6. N-type calcium channel blocker on the effect of XE991 on mEPSC frequency.

A and B, Representative mEPSC recordings obtained from a CA1 pyramidal neuron in which the blocking of N-type calcium channels by ω-conotoxin GVIA (1 μM) did (A) or did not (B) prevent the effects of 10 μM XE991. Data in the left panels are from recordings in the presence of ω-conotoxin GVIA before the application of XE991, and data in the right panels are from recordings after the application of XE991. C and D, Cumulative probability plots of mEPSC frequency obtained by pooling data from CA1 pyramidal neurons before (solid lines) and after (dotted lines) the application of XE991 in the presence of ω-conotoxin GVIA that did (C) or did not (D) prevent the effect of XE991.

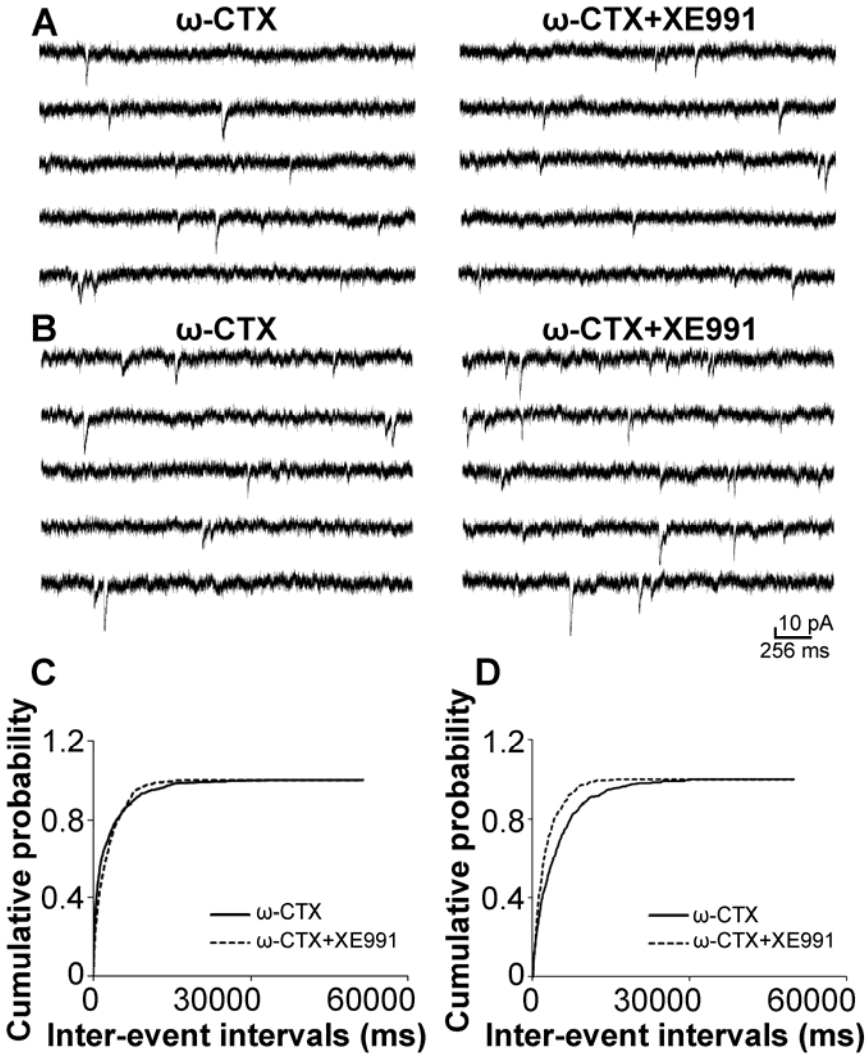

Figure 7 Combination of P/Q- and N-type calcium channel blockers on the effect of XE991 on mEPSC frequency.

A, Representative mEPSC recordings obtained from a CA1 pyramidal neuron in the presence of both ω-agatoxin TK and ω-conotoxin GVIA before the application of XE991(top), and after the application of XE991 (bottom). B, Cumulative probability plots of mEPSC frequency obtained by pooling data from CA1 pyramidal neurons before (solid lines) and after (dotted lines) the application of XE991 in the presence of ω-agatoxin TK and ω-conotoxin GVIA.

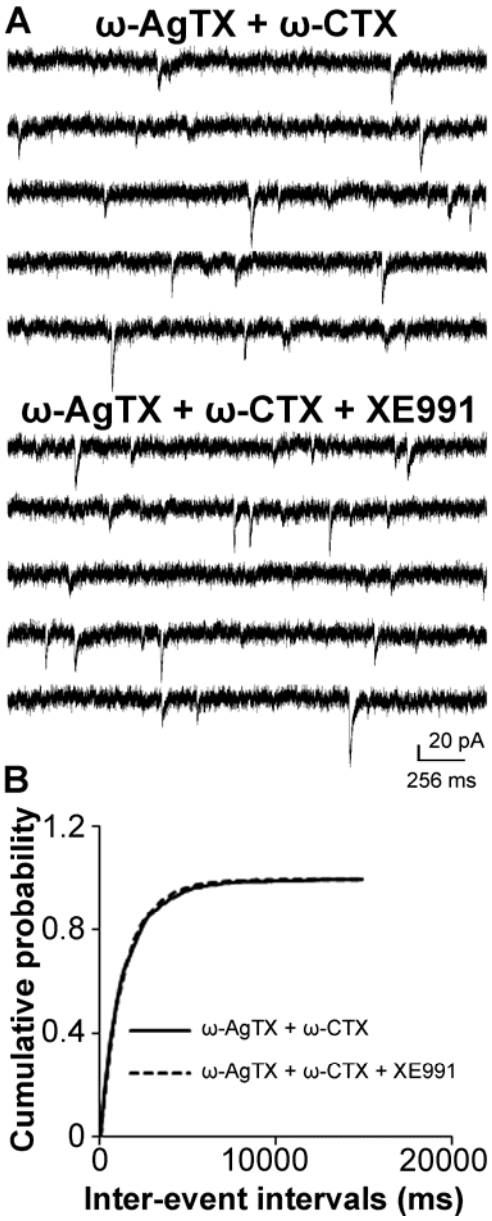

Figure 8. M1 agonist McN-A-343 depolarized and increased action potential firing in CA3 pyramidal neurons. A, Representative traces of the membrane potential of a CA3 pyramidal neuron before, during, and after a wash of McN-A-343. Note the profound depolarization and the repetitive action potentials. B. A representative trace of the depolarizing effect of McN-A-343 on the membrane potential of a CA3 pyramidal neuron with action potentials blocked by TTX (1 μM). C and D, Quantification of the effect of McN-A-343 on the firing frequency (C) and membrane potential (D) of CA3 pyramidal neurons (means ± SEM).

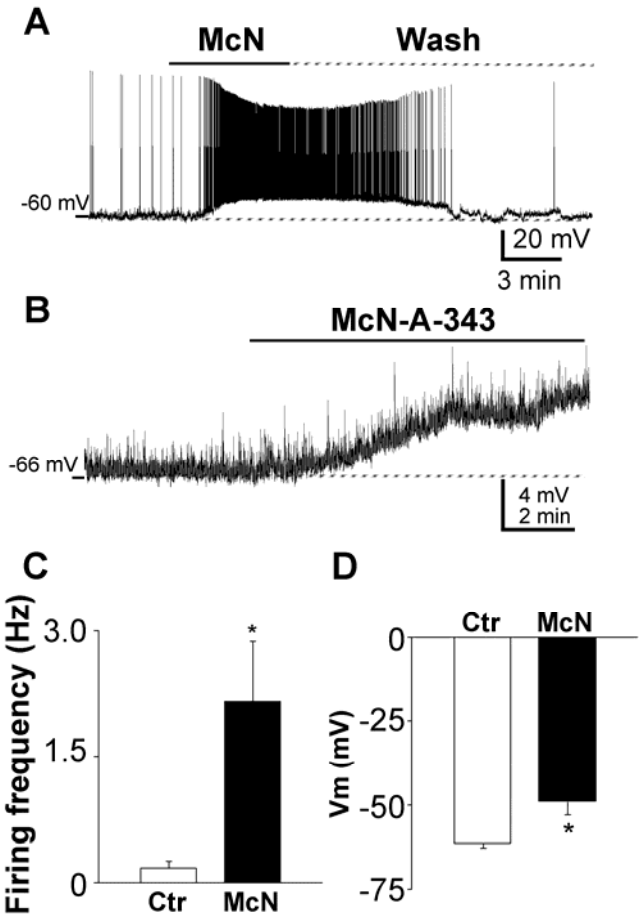

Figure 9. M-channel blocker and opener on membrane potential and action potential firing in CA3 pyramidal neurons. A, Representative effect of XE991 on the membrane potential of CA3 pyramidal neurons. B and C, Representative recordings of the effects of XE991 (B) and flupirtine (C) on the membrane potential of CA3 pyramidal neurons in the presence of TTX (1 μM). D, Quantification of the effect of XE991 on the firing frequency of CA3 pyramidal neurons (means ± SEM). E and F, Quantification of the effect of XE991 (E) and flupirtine (F) on the membrane potential of CA3 pyramidal neurons (means ± SEM).

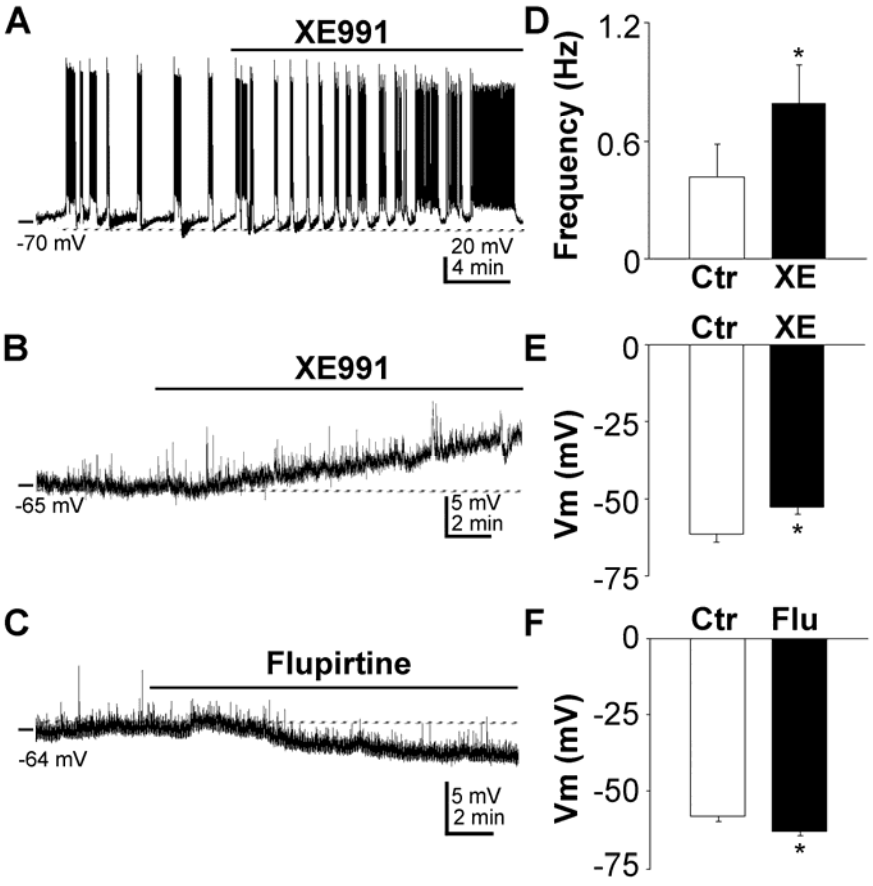

Figure 10. McN-A-343 and XE991 increased input resistance in CA3 neurons. A, (top) Representative recordings of current injections from -40 pA (in 5 pA steps) before (left) and after (right) the application McN-A-343, (bottom) I-V relationship before (open circles) and after (filled circle) the application of McN-A-343 in CA3 neurons (n = 6). B, (top) Representative recordings of current injections from -40 pA (in 5 pA steps) before (left) and after (right) the application of XE991, (bottom) I-V relationship before (open circles) and after (filled circles) the application of XE991 in CA3 neurons (n = 7).

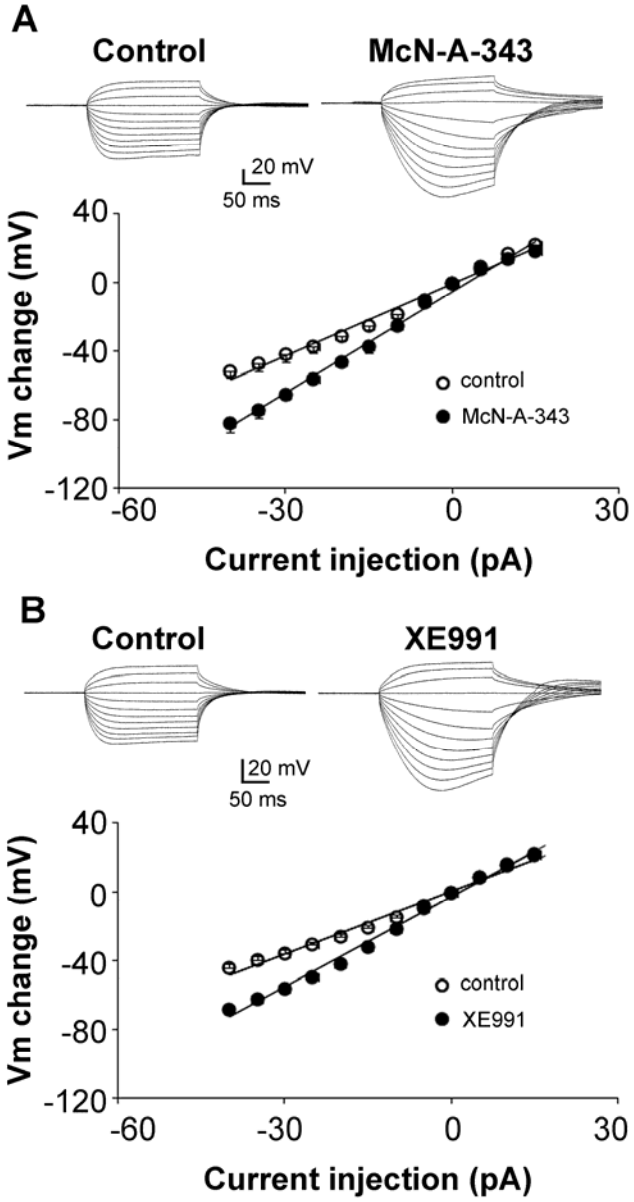

Figure 11) Seizures caused by intra-hippocampal infusion of the organophosphate paraoxon. A) displays % fraction of animals having seizures in response to 100 nmols (n= 9), 200 nmols (n= 52) and 300 nmols (n = 11)of intra-hippocampal paraoxon. B) A pie chart of four responses to 200 nmols paraoxon infused in the hippocampus: no seizures, seizures during infusion, intermittent post infusion seizures and continuous post infusion seizures. C) Displays EEG recordings from right (R) and left (L) hippocampus showing intermittent seizures following infusion of 200 nmol paraoxon solution into the right hippocampus. A seizure begins in the right hippocampus, spreads to the left hippocampus and ends several second later (middle two traces), and soon thereafter another seizure begins and spreads to the left hippocampus. D) Displays a continuous electrographic seizures occurring in right and left hippocampi, note faster time base. The seizure consists of continuous spike-wave discharges.

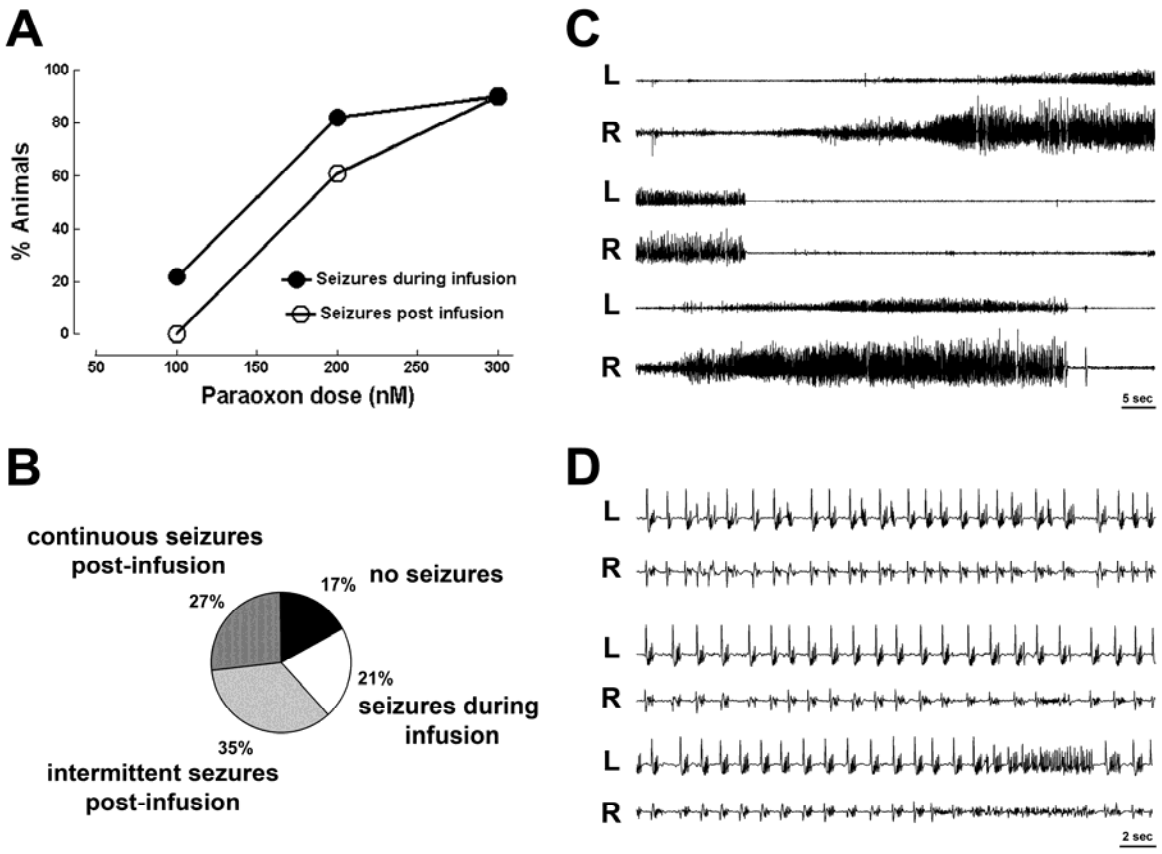

Figure 12) Images of hippocampal sections from animals that had prolonged seizures following intra-hippocampal paraoxon administration, which were stained for neuronal injury stain FluoroJade B (green) and neuronal marker NeuN (red). A) A low magnification image of the hippocampus showing drug infusion site close to the CA3 region of the hippocampus. B) A section of the hippocampus displaying green fluorojade positive CA3, CA1 pyramidal neurons and neurons in the subiculum. C) A higher magnification image of Fluorojade positive neurons in the CA3 region of the hippocampus.

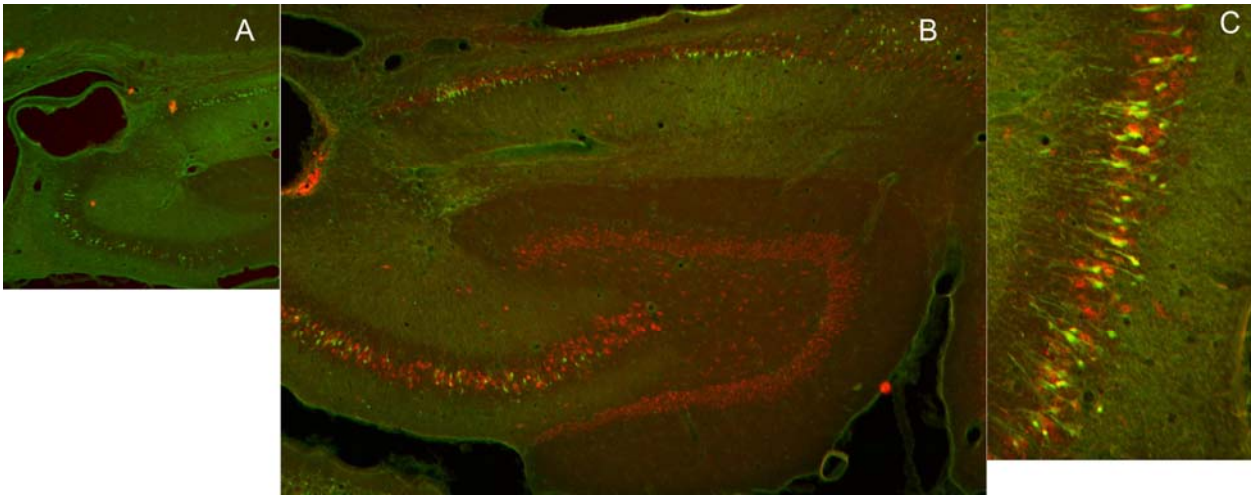

Figure 13) EEG recordings from hippocampi of animals given paraoxon subcutaneously after injection of atropine and 2-PAM. Left panel shows samples of recording from an animal in SE. Note continuous electrographic seizures for 4 hours with evolving morphology and frequency. Middle panel (10 minute treatment) shows EEG from an animal treated with diazepam 10 minutes after the onset of continuous electrographic seizures. Seizures were terminated promptly and animals stayed seizure free. Right panel (30 minute treatment) shows onset of continuous seizures and their termination when diazepam was administered 30 minutes after the onset of continuous electrographic seizures.

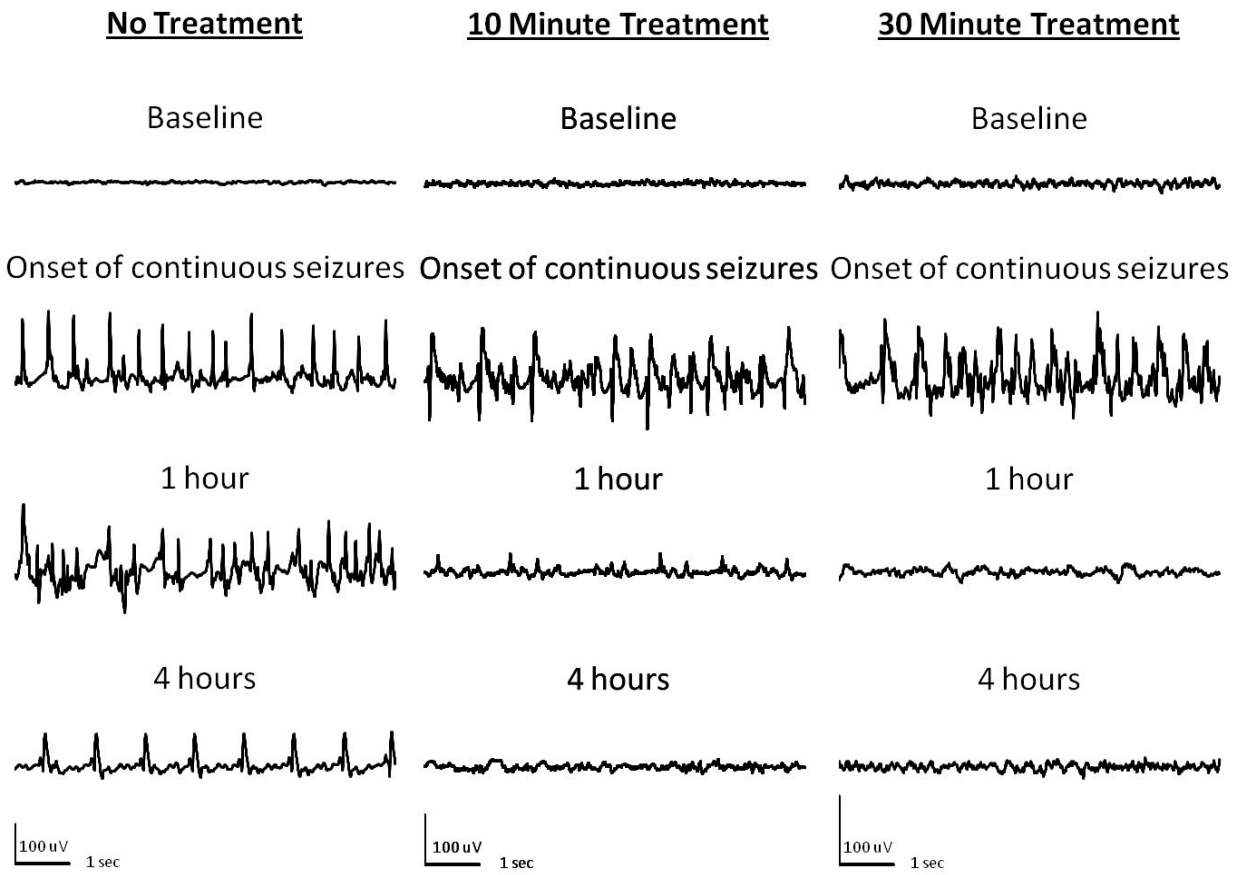

Figure 14) Time-course of SE induced by peripheral paraoxon injection in three groups: no further treatment, diazepam given 10 minutes after the onset of continuous seizures (Blue line) or 30 minutes after the onset of continuous seizures (Red line). In this study, 23 animals were studied, 17 developed continuous seizures, 6 were left untreated (control), 6 received diazepam 10 minutes after the onset of continuous seizures, and 5 received diazepam 30 minutes after the onset of continuous electrographic seizures. Diazepam effectively terminated SE in similar proportion of animals regardless of time of treatment (inset bar charts).

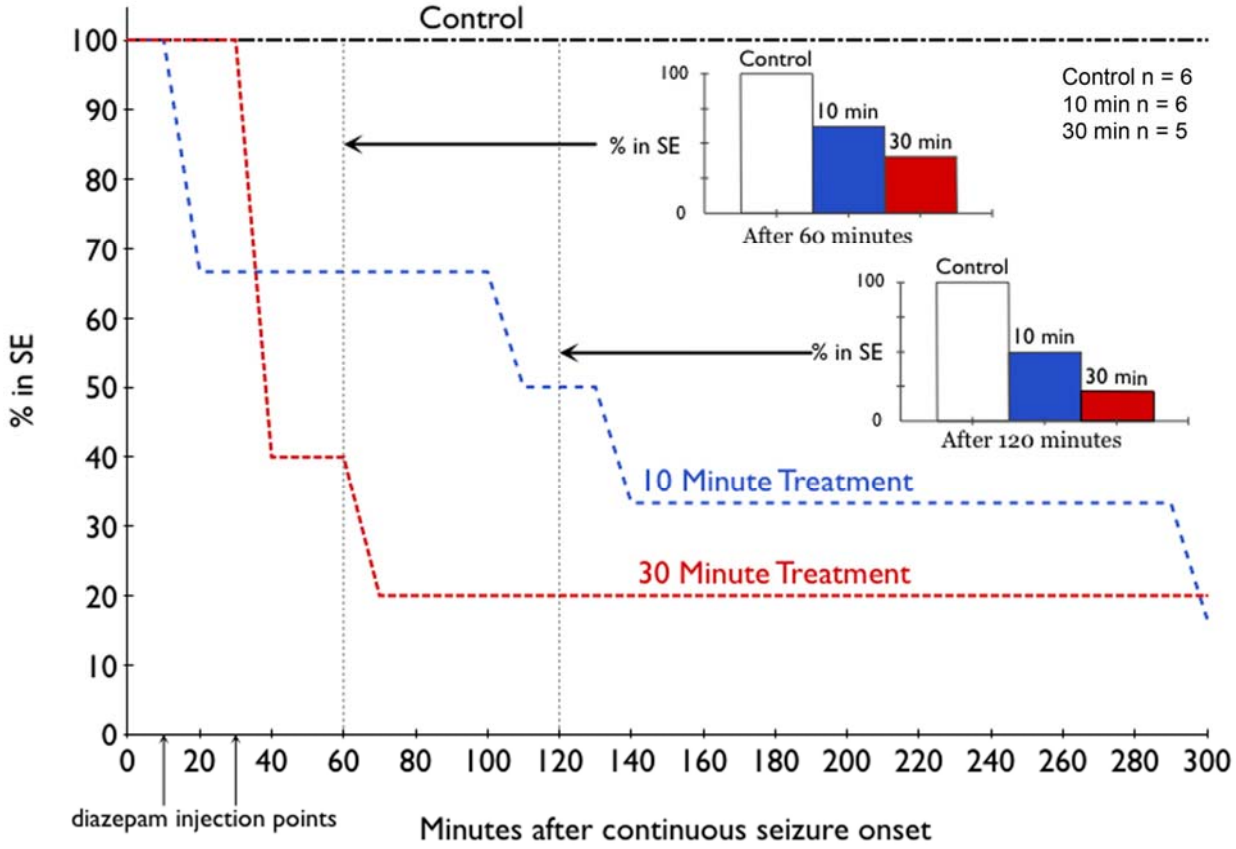

Figure 15) SE induced by peripheral injection of DFP and response to diazepam treatment. Samples of recording from an animal in SE show continuous electrographic seizures for 4 hours. Recordings an animal treated with diazepam 10 minutes after the onset of continuous electrographic seizures (Middle panel, 10 minute treatment) demonstrate prompt termination of SE.. When diazepam was administered 30 minutes after the onset of continuous electrographic seizures (Right panel 30 minute treatment) SE continued with only a mild suppression of amplitude of spikes but continued high frequency spike-wave discharges (1 hour) and complex poly-spike-wave rhythmic discharges (4 hour).

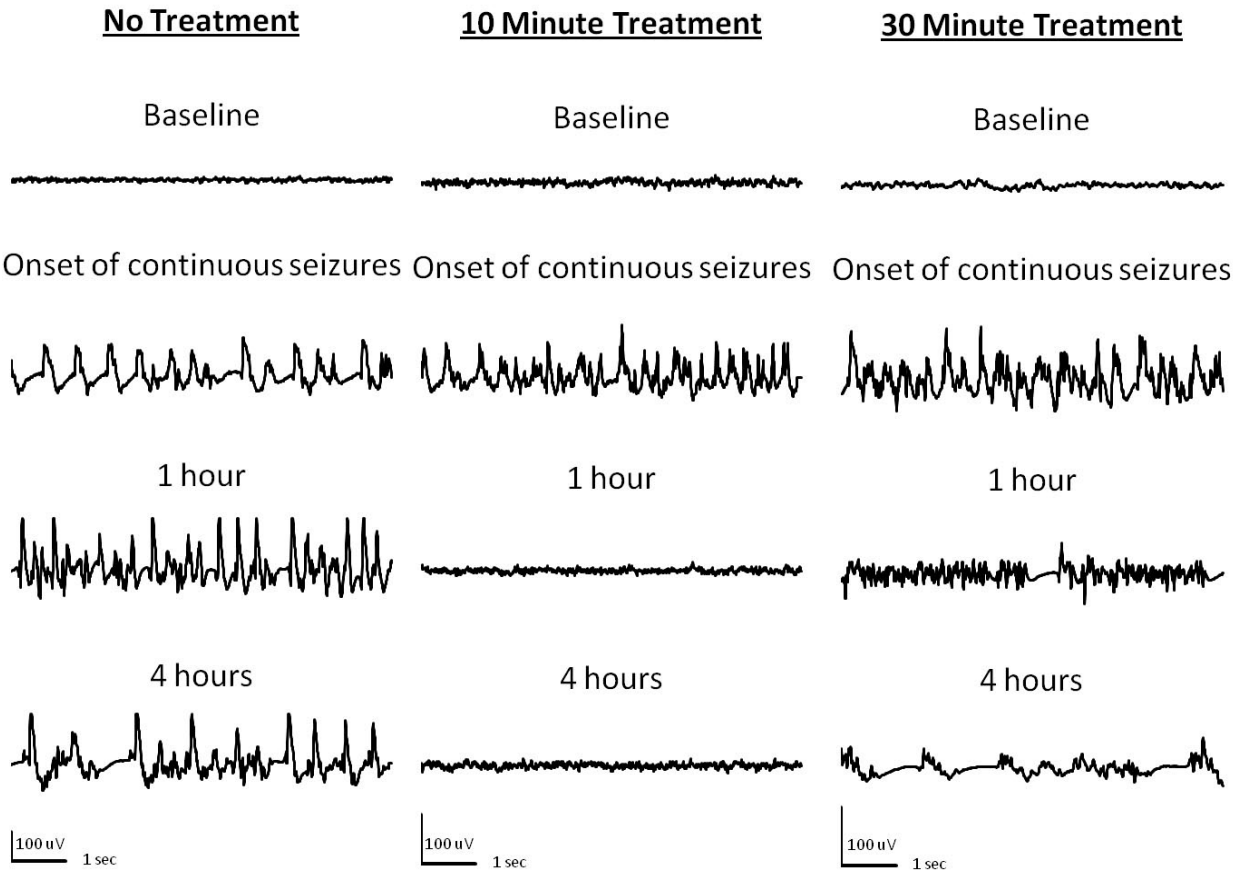

Figure 16) Time-course of SE induced by peripheral DFP injection in three groups: no further treatment, diazepam given 10 minutes after the onset of continuous seizures (Blue line) or 30 minutes after the onset of continuous seizures (Red line). Continuous seizures developed in 15 of 19 animals treated with DFP, and 5 were left untreated (control), 5 each were treated diazepam 10 or 30 minutes after the onset of continuous electrographic seizures. Diazepam effectively terminated SE in animals treated 10 minutes after the onset of continuous electrographic seizure but not in animals treated 30 minutes (inset bar charts).

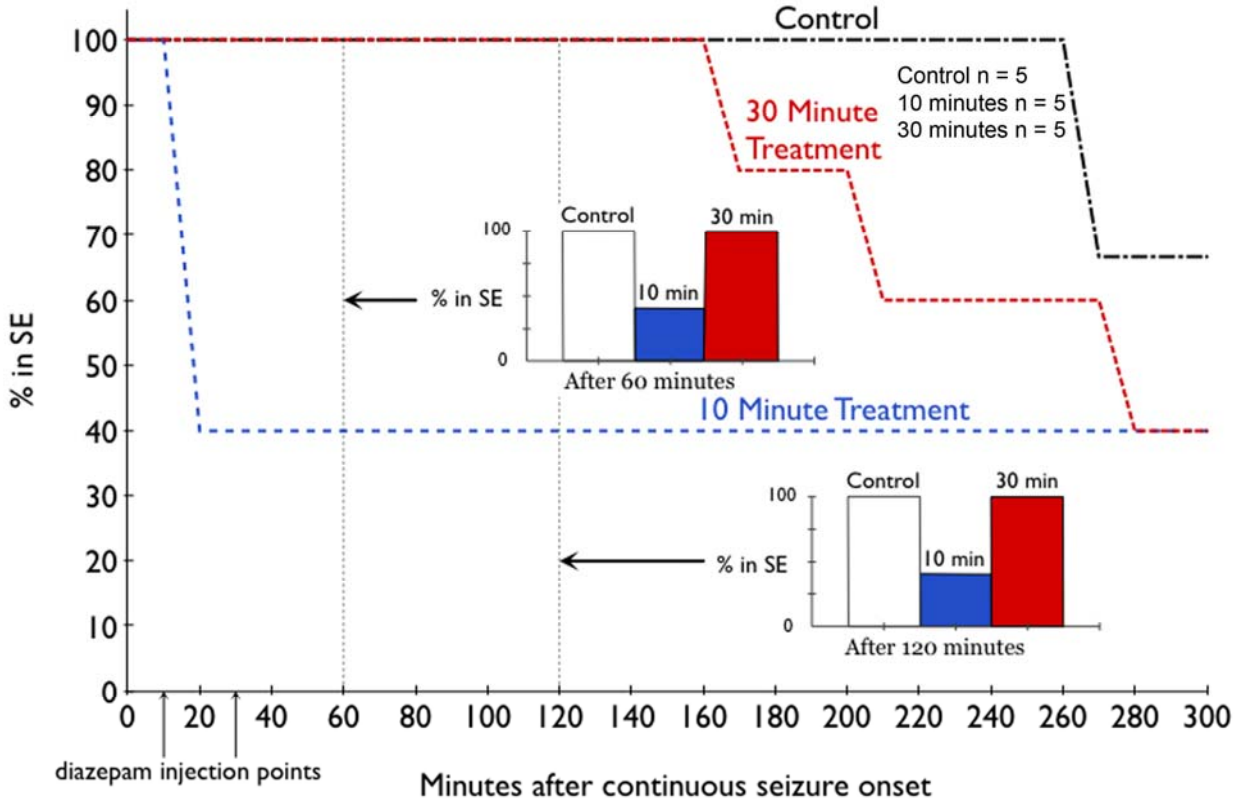

Figure 17. This demonstrates the Time-course of termination of status epilepticus (SE) following treatment with saline (controls), flupirtine 50 mg/Kg alone (red line) and flupirtine 50 mg/Kg combined with diazepam. Note that M channel opener flupirtine is more effective when combined with diazepam.

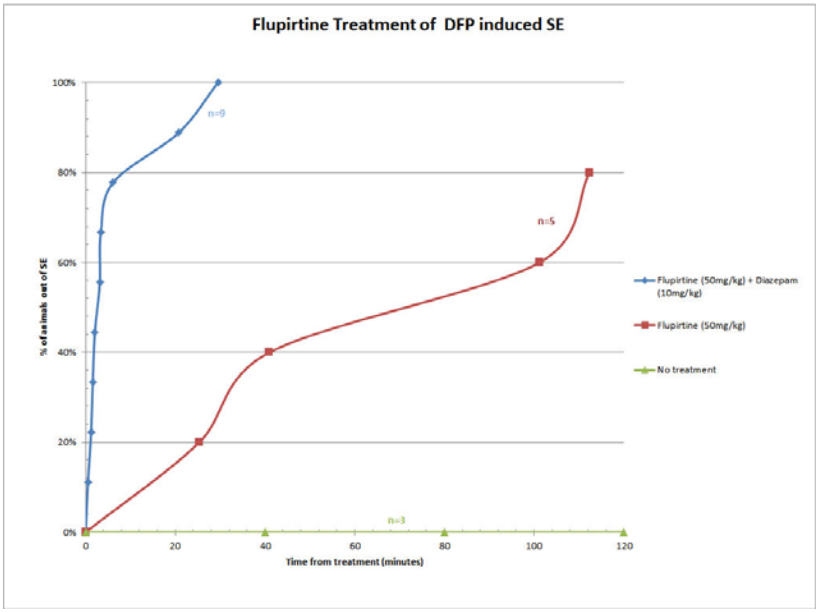

J Physiol 00.0 (2012) pp 1–12

The Journal of Physiology

M-type potassium channels modulate Schaffer collateral–CA1 glutamatergic synaptic transmission

Jianli Sun and Jaideep Kapur

Department of Neurology, University of Virginia, Health Sciences Center, Charlottesville, VA 22908-0394 USA

Key points

- M-type potassium channels play a key role in modulating neuronal excitability. However, the effects of M-channel activation on synaptic transmission are poorly understood.
- This study found that an M1 receptor agonist and M-channel blockers increased action potential-independent glutamate release at Schaffer collateral–CA1 pyramidal neuron synapses in acute hippocampus slices.
- This enhancement was dependent on Ca^{2+} influx from extracellular space but not intracellular calcium stores.
- Inhibition of M-channels results in the depolarization of CA3 pyramidal neurons and activated presynaptic voltage-gated P/Q- and N-type calcium channels, which in turn causes Ca^{2+} influx and increased glutamate release.
- Thus, M1 muscarinic agonists modulate action potential-independent glutamatergic synaptic transmission in the hippocampus by inhibition of presynaptic M-channels.

Abstract Previous studies have suggested that muscarinic receptor activation modulates glutamatergic transmission. M-type potassium channels mediate the effects of muscarinic activation in the hippocampus, and it has been proposed that they modulate glutamatergic synaptic transmission. We tested whether M1 muscarinic receptor activation enhances glutamatergic synaptic transmission via the inhibition of the M-type potassium channels that are present in Schaffer collateral axons and terminals. Miniature excitatory postsynaptic currents (mEPSCs) were recorded from CA1 pyramidal neurons. The M1 receptor agonist, NcN-A-343, increased the frequency of mEPSCs, but did not alter their amplitude. The M-channel blocker XE991 and its analogue linopirdine also increased the frequency of mEPSCs. Flupirtine, which opens M-channels, had the opposite effect. XE991 did not enhance mEPSCs frequency in a calcium-free external medium. Blocking P/Q- and N-type calcium channels abolished the effect of XE991 on mEPSCs. These data suggested that the inhibition of M-channels increases presynaptic calcium-dependent glutamate release in CA1 pyramidal neurons. The effects of these agents on the membrane potentials of presynaptic CA3 pyramidal neurons were studied using current clamp recordings; activation of M1 receptors and blocking M-channels depolarized neurons and increased burst firing. The input resistance of CA3 neurons was increased by the application of McN-A-343 and XE991; these effects were consistent with the closure of M-channels. Muscarinic activation inhibits M-channels in CA3 pyramidal neurons and its efferents – Schaffer collateral, which causes the depolarization, activates voltage-gated calcium channels, and ultimately elevates

© 2012 The Authors. The Journal of Physiology © 2012 The Physiological Society

DOI: 10.1113/jphysiol.2012.235820

Downloaded from J Physiol (jp.physoc.org) at UNIV OF VIRGINIA on July 30, 2012

the intracellular calcium concentration to increase the release of glutamate on CA1 pyramidal neurons.

(Resubmitted 1 May 2012; accepted after revision 1 June 2012; first published online 6 June 2012)

Corresponding author J. Kapur: Department of Neurology, Box 800394, University of Virginia-HSC, Charlottesville, VA 22908, USA. Email: jk8t@virginia.edu

Abbreviations M1, muscarinic type 1; mEPSCs, miniature excitatory postsynaptic currents; CNQX, 6-cyano-7-nitroquinoxalene-2,3-dione; K-S, Kolmogorov–Smirnov; NcN-A-343, (4-hydroxy-2-butynyl)-1-trimethylammonium-3-chlorocarbanilate chloride; sEPSC, spontaneous excitatory postsynaptic current; XE-991,10,10-bis(4-pyridinylmethyl)-9(10*H*)-anthracenone.

Introduction

Muscarinic acetylcholine receptors (mAChRs) are seven-transmembrane-domain G protein-coupled receptors (GPCRs) that are widely expressed throughout the central nervous system. The M1 subtype is the predominant mAChR in the cortex, hippocampus, striatum and thalamus (Langmead *et al.* 2008). Muscarinic receptor activation has distinct effects on glutamatergic transmission in different neurons. It inhibits glutamatergic transmission in magnocellular neurons of the basal forebrain (Sim & Griffith, 1996), along with neurons in the basolateral amygdala (Yajeya *et al.* 2000), striatum (Higley *et al.* 2009) and spinal cord (Zhang *et al.* 2007). In the CA3 region of the hippocampus, muscarinic activation inhibits associational-commissural synaptic transmission via presynaptic calcium channel inhibition; however, it enhances mossy fibre–CA3 pyramidal neuron synaptic transmission (Vogt & Regehr, 2001). The activation of muscarinic receptors induces a long-lasting synaptic enhancement at Schaffer collateral–CA1 pyramidal neuron synapses by increasing the release of calcium from postsynaptic endoplasmic reticulum stores both *in vivo* and *in vitro* (Fernández de Sevilla *et al.* 2008). Muscarinic activation also enhances glutamatergic transmission in dentate granule cells (Kozhemyakin *et al.* 2010). M1 muscarinic receptor activation also inhibits M-type potassium channels (Brown & Adams, 1980; Marrion *et al.* 1989; Bernheim *et al.* 1992). M-type potassium channels belong to the Kv7 (KCNQ) K^+ channel family (Wang *et al.* 1998; Selyanko *et al.* 2002). M-channels activate at a subthreshold membrane potential and do not inactivate, so they generate a steady voltage-dependent outward current near the resting membrane potential (Constanti & Brown, 1981; Delmas & Brown, 2005). Mutations of the KCNQ2 and KCNQ3 genes cause benign familial neonatal convulsions (BFNC) (Biervert *et al.* 1998; Jentsch, 2000). The expression of KCNQ channels increases during early development in rodent hippocampus (Shah *et al.* 2002; Geiger *et al.* 2006; Weber *et al.* 2006; Safiulina *et al.* 2008), but the expression of KCNQ2 and KCNQ3 has different developmental pattern in human brain (Kanaumi *et al.* 2008). It has been suggested that the highest density of KCNQ2 and KCNQ3 immunoreactivity in the CA1 region is in the axon initial segments, where action potentials are generated and the Kv7 channels co-localize with Na^+ channels via binding to ankyrin G. This localization allows M-channels to powerfully limit neuronal excitability (Devaux *et al.* 2004; Chung *et al.* 2006; Pan *et al.* 2006) and therefore function as a 'brake' on repetitive firing and play a key role in regulating the excitability of various central and peripheral neurons (Yue & Yaari, 2004; Gu *et al.* 2005; Shen *et al.* 2005; Brown & Randall, 2009). Other studies have suggested that M-channels are expressed in presynaptic terminals (Cooper *et al.* 2001; Chung *et al.* 2006; Garcia-Pino *et al.* 2010). Physiological studies have suggested that M-channels regulate the release of neurotransmitters. Drugs that block or open M-channels can regulate presynaptic fibre volley and the evoked EPSPs recorded from CA1 pyramidal neurons (Vervaeke *et al.* 2006). M-channel blocking by XE991 increases the release of noradrenaline, and retigabine, an M-channel opener, decreases noradrenaline release in cultured sympathetic neurons (Hernandez *et al.* 2008). These drugs also regulate neurotransmitter release from hippocampal synaptosomes (Martire *et al.* 2004) and cultured hippocampal neurons (Peretz *et al.* 2007). However, the mechanism by which M-channels regulate neurotransmitter release remains unclear. The current study demonstrates that both M1 muscarinic activation and M-channel inhibition enhance action-potential-independent glutamate release in Schaffer collateral–CA1 pyramidal neuron synapses. This action appears to be dependent on the depolarization of CA3 pyramidal neurons and the activation of voltage-gated calcium channels.

Methods

Slice preparation

All studies were performed according to protocols that were approved by the University of Virginia Animal Use and Care Committee, and the US Army Medical Research and Material Command Animal Care and Use Review Office (ACURO). Adult male (175–250 g) Sprague–Dawley rats were anaesthetized with isoflurane

© 2012 The Authors. The Journal of Physiology © 2012 The Physiological Society

Downloaded from J Physiol (jp.physoc.org) at UNIV OF VIRGINIA on July 30, 2012

prior to decapitation, which was followed by quick removal of the brain. The removed brains were then sectioned to 300 μm slices using a Leica VT 1200 slicer (Leica Microsystems, Wetzlar, Germany) in ice-cold oxygenated slicing solution. The solution contained the following (in mM): 120 sucrose, 65.5 NaCl, 2 KCl, 1.1 KH_2PO_4, 25 $NaHCO_3$, 10 D-glucose, 1 $CaCl_2$, and 5 $MgSO_4$. The slices were then incubated for at least 1 h at 32°C in oxygenated ACSF that contained (in mM): 127 NaCl, 2 KCl, 1.1 KH_2PO_4, 25.7 $NaHCO_3$, 10 D-glucose, 2 $CaCl_2$, and 1.5 $MgSO_4$; the osmolarity in the chamber was 290–300 mosmol l^{-1}. After incubation, the slices were transferred to the recording chamber on the stage of an Olympus Optical BX51 microscope (Olympus, Tokyo, Japan). Unless otherwise stated, all chemicals were obtained from Sigma-Aldrich (St Louis, MO, USA).

Whole-cell recording

Whole-cell patch-clamp recordings were performed under infrared differential interference contrast microscopy (Olympus); a 40× water-immersion objective was used to visually identify CA1 and CA3 pyramidal neurons. The slices were continuously perfused with ACSF solution that was saturated with 95% O_2 and 5% CO_2 at room temperature. Patch electrodes (final resistances, 3–5 MΩ) were pulled from borosilicate glass (Sutter Instruments, Novato, CA, USA) on a horizontal Flaming-Brown micro-electrode puller (Model P-97, Sutter Instruments). For voltage-clamp recordings, the electrode tips were filled with a filtered internal recording solution that consisted of the following components (in mM): 117.5 $CsMeSO_4$, 10 Hepes, 0.3 EGTA, 15.5 CsCl, and 1.0 $MgCl_2$; the pH was 7.3 (with CsOH), and the osmolarity was 310 mosmol l^{-1}. The electrode shank contained (in mM) 4 Mg-ATP salt, 0.3 Na-GTP salt, and 5 QX-314. For current-clamp recording, the pipette solution contained the following (in mM): 135 potassium gluconate, 2.5 NaCl, 10 Hepes, 0.5 EGTA, 4.0 Mg-ATP, 0.4 Na-GTP, 0.1 $CaCl_2$; the pH was 7.3, and the osmolarity was 310 mosmol l^{-1}. Neurons were voltage clamped at −60 mV using a PC-505B amplifier (Warner Instruments, Hamden, CT, USA). Electrode capacitance was electronically compensated. Access resistance was continuously monitored, and if the series resistance increased by 20% at any time, the recording was terminated. Currents were filtered at 2 kHz, digitized using a Digidata 1322 digitizer (Molecular Devices, Sunnyvale, CA, USA), and acquired using Clampex 10.2 software (Molecular Devices). Spontaneous excitatory postsynaptic currents (sEPSCs) were recorded from CA1 pyramidal neurons after blocking the $GABA_A$ receptors with the antagonist picrotoxin (50 μM). In preliminary experiments, a combination of 6-cyano-7-nitroquinoxalene-2,3-dione (CNQX) and 2-amino-5-phosphonovaleric acid (APV) blocked all EPSCs. Miniature EPSCs (mEPSCs) were recorded by blocking action potentials with 1 μM TTX (Alomone labs, Jerusalem, Israel). All drugs were bath-applied via a peristaltic pump.

Data analysis

The offline digitized data were analysed with Mini-Analysis (Synaptosoft, Decatur, GA, USA) and Clampfit 10.2 (Molecular Devices). To detect sEPSCs and mEPSCs, a detection threshold was set at three times the root mean square (RMS) of the baseline noise. After detection, the frequency and peak amplitude of EPSCs from individual neurons were analysed. Each detected event from the 20–30 min recording session was visually inspected to remove false detections. The Kolmogorov–Smirnov (K-S) test was used to compare amplitudes and inter-event intervals for continuously recorded EPSCs. The input resistance of CA3 neuron under current-clamp recording was analysed by comparing the slope of current–voltage relationship and measured directly by Clampfit 10.2 at the peak of membrane potentials. The drug effects were compared using a paired Student's t test with a significance level of $P < 0.05$. Data are expressed as means ± SEM unless otherwise noted.

Results

An M1 muscarinic agonist increases mEPSC frequency in CA1 neurons

Previous studies suggested that muscarinic receptor activation increased presynaptic glutamate release from perforant path to dentate granule cells (Kozhemyakin *et al.* 2010). In the present study, we investigated the effect of the M1 muscarinic receptor agonist McN-A-343 on glutamate release recorded from Schaffer collateral–CA1 synapses. Application of McN-A-343 (10 μM) increased the frequency of mEPSCs that were recorded from CA1 pyramidal neurons by 69.89 ± 8.28% (0.12 ± 0.03 Hz *vs.* 0.21 ± 0.05 Hz; $n = 7$, $P < 0.01$), but it did not change their amplitudes (16.51 ± 1.14 pA *vs.* 16.79 ± 1.47 pA; $n = 7$, $P = 0.38$, Fig. 1*A* and *B*). McN-A-343 caused a significant leftward shift in the cumulative distribution of the inter-event intervals but had no effect on the cumulative distribution of the amplitudes of the mEPSCs (K-S test, Fig. 1*C* and *D*). This suggested that the activation of M1 receptors increased action potential-independent glutamate release from the presynaptic terminals of Schaffer collateral–CA1 synapses.

© 2012 The Authors. The Journal of Physiology © 2012 The Physiological Society

Downloaded from J Physiol (jp.physoc.org) at UNIV OF VIRGINIA on July 30, 2012

M-channels regulate presynaptic glutamate release in CA1 neurons

Cholinergic M1 receptor activation inhibits M-channels (Brown & Adams, 1980; Marrion *et al.* 1989; Bernheim *et al.* 1992), so we tested whether M-channels regulate glutamate release in these synapses. Blocking M-channels increased the frequency of sEPSCs. After recording sEPSCs for 10 min, M-channel blocker XE991 (10 μM) was applied for 10 min, and it increased the frequency of sEPSCs by $147.56 \pm 18.21\%$ (0.11 ± 0.03 Hz *vs.* 0.30 ± 0.01 Hz, $n = 7$, $P < 0.01$), but did not affect their amplitudes (16.91 ± 0.92 pA *vs.* 16.65 ± 0.80 pA, $n = 7$, $P = 0.50$). Blocking M-channels caused a significant leftward shift in the cumulative distribution of sEPSC inter-event intervals but had no effect on the cumulative distribution of their amplitudes (K-S test, data not shown). These data suggested that M-channels modulate action potential-dependent glutamate release from Schaffer collateral–CA1 pyramidal neuron synapses. To study whether the effect of XE991 on release was action potential independent, its effect on mEPSCs was studied. XE991 (10 μM) increased the frequency of mEPSCs by $82.21 \pm 7.36\%$ (0.13 ± 0.02 Hz *vs.* 0.22 ± 0.03 Hz, $n = 8$, $P < 0.01$), but had no effect on their amplitudes (17.70 ± 1.26 pA *vs.* 18.10 ± 1.27 pA, $n = 8$, $P = 0.30$, Fig. 2*A*). XE991 also caused a significant leftward shift in the cumulative distribution of the mEPSC inter-event intervals (Fig. 2*B*), but had no effect on the cumulative distribution of their amplitudes (Fig. 2*C*). The frequency of mEPSCs kept increasing after 10 min of XE991 application. The slices were perfused with ACSF to wash out the drug effect. The mEPSC frequency remained elevated for 50 min of washing and returned to baseline at 90 min (data not shown). The effect of XE991 on mEPSC frequency was confirmed by applying linopirdine (10 μM), which also blocks M-channels. Linopirdine increased the frequency of mEPSCs by $68.22 \pm 6.05\%$ (0.12 ± 0.01 Hz *vs.* 0.21 ± 0.03 Hz, $n = 6$, $P < 0.01$) but had no effect on their amplitudes (15.35 ± 1.13 pA *vs.* 15.78 ± 0.94 pA, $n = 6$, $P = 0.23$). It also caused a significant leftward shift in the cumulative distribution of the mEPSC inter-event intervals (Fig. 3*A*). These results suggested that the inhibition of M-channel current enhances the frequency of mEPSCs. Flupirtine (20 μM), an M-channel opener, decreased mEPSC frequency by $25.50 \pm 8.04\%$ compared to baseline (0.41 ± 0.08 Hz *vs.* 0.27 ± 0.04 Hz, $n = 8$, $P < 0.01$). Flupirtine caused a significant rightward shift in the cumulative distribution of the inter-event intervals of mEPSCs (Fig. 3*B*). These data suggested that M-channels are capable of modulating neurotransmitter

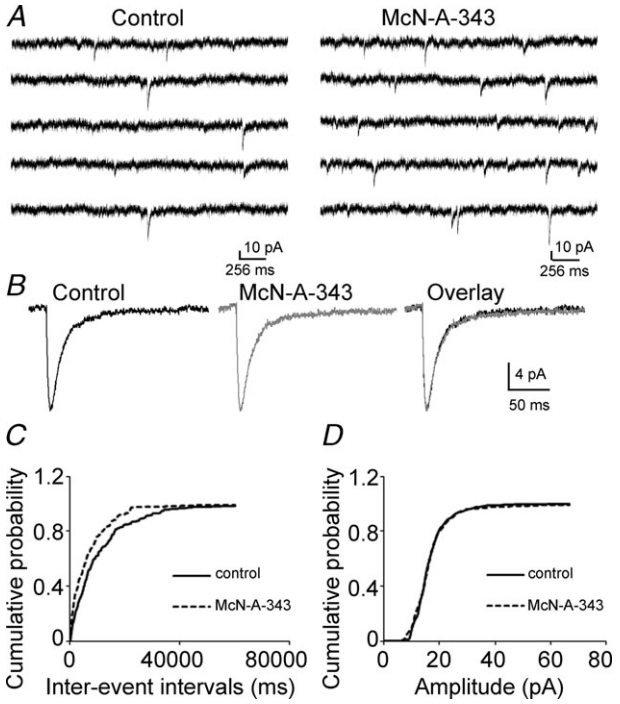

Figure 1. M1 muscarinic agonist increased the frequency of mEPSCs recorded from CA1 pyramidal neurons
A, representative traces of mEPSCs recorded from CA1 pyramidal neurons before (left) and after (right) the application of 10 μM McN-A-343. *B*, representative averaged traces of mEPSCs before (black) and during (grey) the application of McN-A-343 along with the overlay of the two traces. *C* and *D*, cumulative probability plots of mEPSC frequency (*C*) and amplitude (*D*) obtained by pooling data from 7 neurons before (continuous lines) and after (dashed lines) application of McN-A-343.

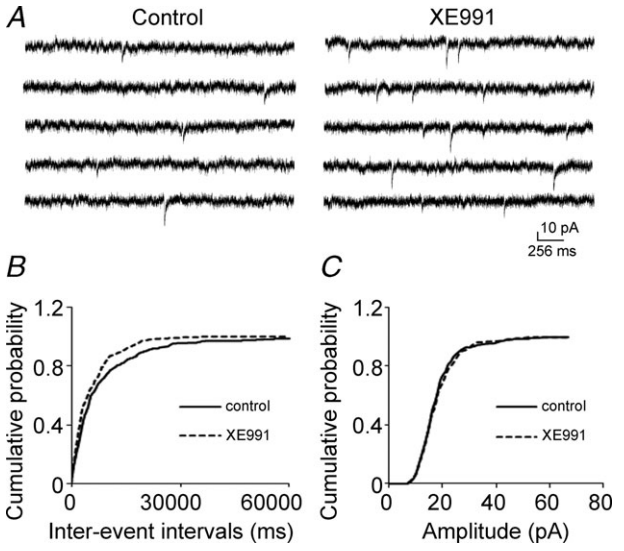

Figure 2. M-channel blocker XE991 increased mEPSC frequency in CA1 neurons
A, representative mEPSC recordings obtained from a CA1 pyramidal neuron before (left) and after (right) the application of 10 μM XE991. *B* and *C*, cumulative probability plots of mEPSC frequency (*C*) and amplitude (*D*) obtained by pooling data from 8 neurons before (continuous lines) and after (dashed lines) the application of XE991.

© 2012 The Authors. The Journal of Physiology © 2012 The Physiological Society

Downloaded from J Physiol (jp.physoc.org) at UNIV OF VIRGINIA on July 30, 2012

release independent from action potentials. To confirm that the effect of M1 agonist was mediated by M-channels, we incubated the slice with XE991 for 25 min. After 5 min baseline recording in XE991-containing medium, McN-A-343 was applied, and its effect was blocked. Overall, McN-A-343 did not change the frequency of mEPSCs (baseline 0.53 ± 0.07 Hz, McN-A-343 0.56 ± 0.08 Hz; $n = 7$, $P = 0.38$). In two cells, there was a modest (<10%) increase in frequency but the cumulative frequency plot of inter-event intervals from these cells was not shifted (Fig. 3*C*). This result suggested blocking M-channels prevented McN-A-343 enhancement of mEPSC frequency.

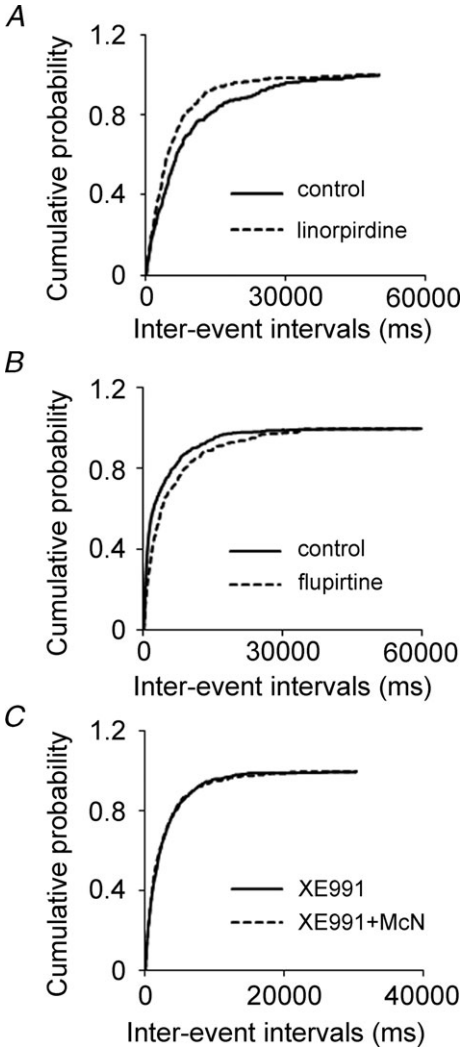

Figure 3. The effect of linopirdine and flupirtine, and the occlusion of XE991 to the effect of McN-A-343 on mEPSC in CA1 neurons
A, and *B*, cumulative probability plots of mEPSC frequency by pooling data from neurons before (continuous lines) and after (dotted lines) the application of linopirdine (*A*), flupirtine (*B*). *C*, cumulative probability plot of mEPSC frequency by pooling data from neurons before (continuous lines) and after (dashed lines) the application of McN-A-343 after 25 min incubation in XE991.

Calcium influx through voltage-gated calcium channels underlies the effect of XE991 on mEPSC frequency

Calcium plays a critical role in neurotransmitter release. The increase in mEPSC frequency caused by the application of XE991 could be due to Ca^{2+} release from intracellular stores or the entry of extracellular Ca^{2+}. First, we tested whether release from intracellular stores plays a role in the effect of XE991. Release from intracellular calcium stores was blocked by incubating the slice with 2.5 μM thapsigargin for 20 min. The effect of M-channel blocker XE991 (10 μM) was not affected. XE991 increased the frequency of mEPSCs by $83.88 \pm 17.22\%$ (Fig. 4*A*), which is comparable to the effect of XE991 without thapsigargin incubation ($82.21 \pm 7.36\%$, $n = 8$, $P < 0.01$); it significantly left shifted the cumulative distribution of inter-event intervals ($n = 9$, $P < 0.01$, Fig. 4*B*). This result suggested that intracellular store release does not

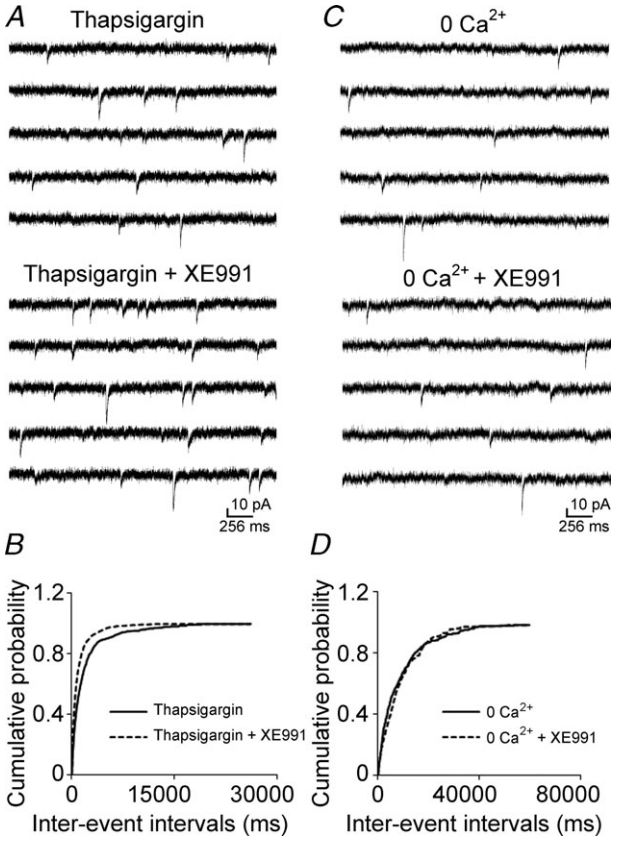

Figure 4. The effect of XE991 on mEPSC frequency was eliminated in calcium-free ACSF
A and *C*, representative mEPSC recordings obtained from a CA1 pyramidal neuron before (top) and after (bottom) the application of 10 μM XE991 after 20 min incubation in thapsigargin (2.5 μM) (*A*) or in calcium-free ACSF (*C*). *B* and *D*, cumulative probability plots of the frequency of mEPSCs obtained by pooling data from 8 neurons before (continuous lines) and after (dashed lines) the application of XE991 in thapsigargin incubation (*B*) or in calcium-free ACSF (*D*).

© 2012 The Authors. The Journal of Physiology © 2012 The Physiological Society

Downloaded from J Physiol (jp.physoc.org) at UNIV OF VIRGINIA on July 30, 2012

contribute to the enhancement of M-channel inhibition on mEPSCs frequency.

Therefore, we tested whether the effect of XE991 on the frequency of mEPSCs was dependent on extracellular Ca^{2+} by recording mEPSCs in a calcium-free medium. The effect of XE991 on mEPSCs was eliminated in ACSF that lacked calcium. Application of XE991 neither changed the frequency of mEPSCs (0.13 ± 0.02 Hz *vs.* 0.12 ± 0.01 Hz, $n = 8$, $P = 0.30$, Fig. 4*C*) nor shifted the cumulative distribution of the inter-event intervals of mEPSCs (Fig. 4*D*). These data suggested that the effect of XE991 on spontaneous glutamate release was dependent on the influx of Ca^{2+}.

We also studied the effect of McN-A-343 in a calcium-free medium. The McN-A-343 enhancement of mEPSCs was blocked in calcium-free medium (baseline, 0.40 ± 0.08 Hz, McN-A-343, 0.41 ± 0.07 Hz, $n = 7$, $P = 0.36$). There was no significant shift on the cumulative distribution of inter-event intervals of mEPSCs (data not shown). This suggested that the effect of M1 receptor activation on the frequency of mEPSC is largely mediated by increasing calcium influx from extracellular space. To test whether Ca^{2+} enters Schaffer collateral terminals by activation of presynaptic voltage-gated calcium channels due to M-channel inhibition, we studied the effect of P/Q- and N-type calcium channel blockers on the XE991-mediated enhancement of mEPSC frequency. These two channels are expressed in the presynaptic terminals of Schaffer collaterals (Wheeler *et al.* 1994; Qian & Noebels, 2000). Slices were incubated with either ω-agatoxin TK (200 nM) or ω-conotoxin GVIA (1 μM) (Peptides International, Louisville, KY, USA) for 15 min prior to data collection. In the presence of ω-agatoxin TK, which blocks P/Q-type calcium channels, the XE991-mediated enhancement of mEPSC frequency was prevented in approximately half of the cells that were studied. In 5 out of 9 neurons, the application of XE991 did not increase the frequency of mEPSCs (0.23 ± 0.08 Hz *vs.* 0.20 ± 0.06 Hz, $P = 0.46$, Fig. 5*A* and *C*). In the other four CA1 pyramidal neurons, XE991 still significantly increased the frequency of mEPSCs (0.16 ± 0.03 Hz *vs.* 0.31 ± 0.07 Hz, $P < 0.05$, Fig. 5*B* and *D*). Blocking N-type channels with ω-conotoxin GVIA also prevented the effect of XE991 on the frequency of mEPSCs in half of the CA1 pyramidal neurons from which recordings were made. In 4 of 8 neurons, the effect of XE991 was eliminated (0.33 ± 0.05 Hz *vs.* 0.34 ± 0.04 Hz, $P = 0.47$, Fig. 6*A* and *C*). In the other four neurons, XE991 significantly increased the frequency of mEPSCs (0.24 ± 0.04 Hz *vs.* 0.43 ± 0.07 Hz, $P < 0.05$, Fig. 6*B* and *D*).

Next, we applied the blockers of two channels simultaneously. Slices were incubated in ω-agatoxin TK and ω-conotoxin GVIA for 25–40 min, and after 5 min baseline recording, XE991 was applied. The mean frequency was not significantly increased (baseline, 0.78 ± 0.08 Hz, XE991, 0.82 ± 0.09 Hz; $n = 8$, $P = 0.08$, Fig. 7*A*), and there was no significant shift of cumulative distribution of inter-event intervals for each cell and pooled data (Fig. 7*B*). This result suggested the enhancement of the frequency of mEPSCs by XE991 was mediated by calcium influx though P/Q- and N-type calcium channels.

McN-A-343 and XE991 depolarize and increase action potential firing in CA3 neurons

The aforementioned data suggested that inhibition of M-channels resulted in the depolarization of presynaptic terminals of the CA3 pyramidal neuron, which then activated P/Q- or N-type calcium channels, thereby causing calcium influx and ultimately leading to increased glutamate release. We tested the effect of M-channels on

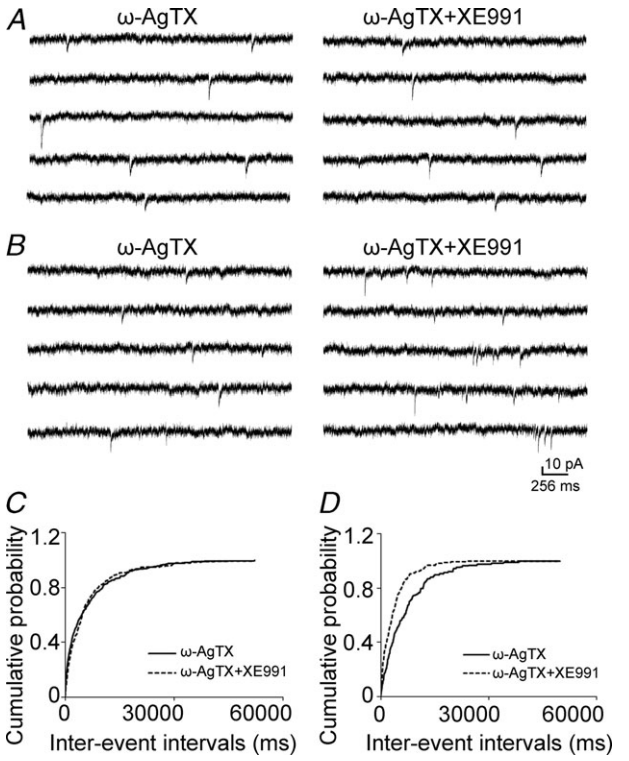

Figure 5. P/Q-type calcium channel blocker on the effect of XE991 on mEPSC frequency
A and *B*, representative mEPSC recordings obtained from a CA1 pyramidal neuron in which the blocking of P/Q-type of calcium channels by 200 nM ω-agatoxin TK did (*A*) or did not (*B*) prevent the effect of 10 μM XE991. The left panels include data from recordings in the presence of ω-agatoxin TK before the application of XE991, and the right panels include data from recordings after the application of XE991. *C* and *D*, cumulative probability plots of mEPSC frequency obtained by pooling data from CA1 pyramidal neurons before (continuous lines) and after (dashed lines) the application of XE991 in the presence of ω-agatoxin TK that did (*C*) or did not (*D*) prevent the effect of XE991.

© 2012 The Authors. The Journal of Physiology © 2012 The Physiological Society

Downloaded from J Physiol (jp.physoc.org) at UNIV OF VIRGINIA on July 30, 2012

the membrane properties of CA3 pyramidal neurons. To study the effects of McN-A-343 and XE991 on CA3 pyramidal neurons, current-clamp recordings of the membrane potentials were obtained from neurons in slices from juvenile rats (24–28 days old). McN-A-343 significantly depolarized CA3 neurons and increased the frequency of action potential firing (0.17 ± 0.08 Hz *vs.* 2.16 ± 0.72 Hz, $n = 6$, $P < 0.01$) of CA3 pyramidal neurons (Fig. 8*A* and *C*). To measure the membrane potential more accurately, action potentials were blocked by TTX (1 μM). Application of McN-A-343 depolarized CA3 pyramidal neuron membrane potentials from -61.39 ± 1.49 mV to -49.00 ± 1.78 mV ($n = 7$, $P < 0.01$, Fig. 8*B* and *D*).

XE991 had similar effect to that of McN-A-343. It increased the action potential firing frequency (0.42 ± 0.17 Hz *vs.* 0.79 ± 0.20 Hz, $n = 9$, $P < 0.01$, Fig. 9*A* and *D*) and depolarized CA3 pyramidal neurons (-61.32 ± 2.45 mV *vs.* -52.62 ± 2.43 mV, $n = 10$, $P < 0.05$, Fig. 9*B* and *E*). Furthermore, and consistent with these findings, the M-channel opener flupirtine (20 μM) hyperpolarized CA3 neurons (-58.02 ± 1.61 mV, *vs.* -62.97 ± 1.36 mV, $n = 7$, $P < 0.01$) (Fig. 9*C* and *F*).

To test whether the inhibition of M-channels increases membrane input resistance in CA3 pyramidal neurons, current–voltage (*I–V*) relationships were studied. Current was injected from −40 pA to15 pA in 5 pA steps. Exposure

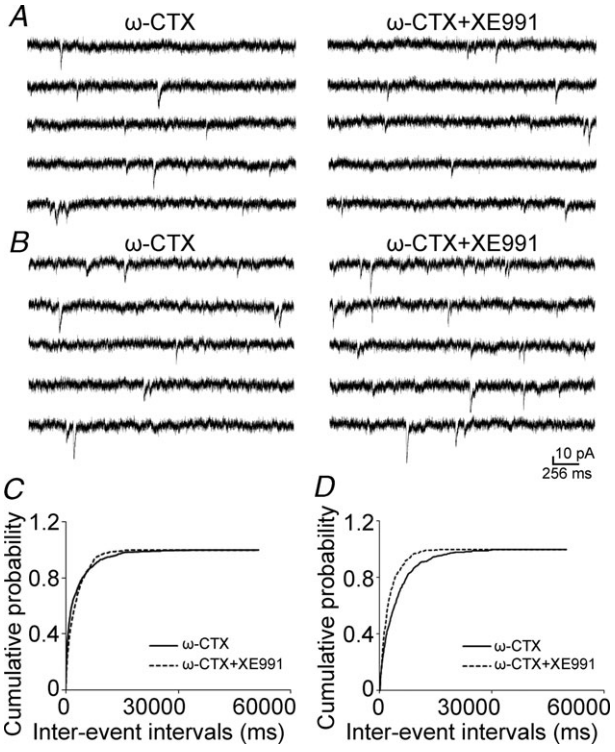

Figure 6. N-type calcium channel blocker on the effect of XE991 on mEPSC frequency
A and *B*, representative mEPSC recordings obtained from a CA1 pyramidal neuron in which the blocking of N-type calcium channels by ω-conotoxin GVIA (1 μM) did (*A*) or did not (*B*) prevent the effects of 10 μM XE991. Data in the left panels are from recordings in the presence of ω-conotoxin GVIA before the application of XE991, and data in the right panels are from recordings after the application of XE991. *C* and *D*, cumulative probability plots of mEPSC frequency obtained by pooling data from CA1 pyramidal neurons before (continuous lines) and after (dashed lines) the application of XE991 in the presence of ω-conotoxin GVIA that did (*C*) or did not (*D*) prevent the effect of XE991.

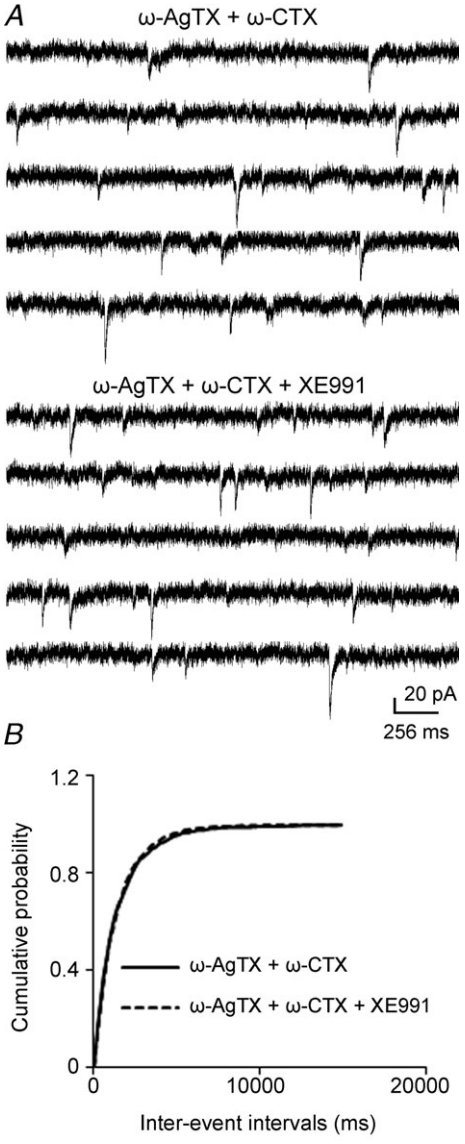

Figure 7. Combination of P/Q- and N-type calcium channel blockers on the effect of XE991 on mEPSC frequency
A, representative mEPSC recordings obtained from a CA1 pyramidal neuron in the presence of both ω-agatoxin TK and ω-conotoxin GVIA before the application of XE991 (top), and after the application of XE991 (bottom). *B*, cumulative probability plots of mEPSC frequency obtained by pooling data from CA1 pyramidal neurons before (continuous lines) and after (dashed lines) the application of XE991 in the presence of ω-agatoxin TK and ω-conotoxin GVIA.

© 2012 The Authors. The Journal of Physiology © 2012 The Physiological Society

Downloaded from J Physiol (jp.physoc.org) at UNIV OF VIRGINIA on July 30, 2012

to McN-A-343 shifted the *I–V* curve to a more negative membrane potentials with negative current injections. The slope of the *I–V* curve increased from 140 MΩ to 197 MΩ (Fig. 10*A*, $n = 6$). McN-A-343 increased the input resistance from 156.43 ± 17.51 MΩ to 228.07 ± 17.16 MΩ ($n = 6$, $P < 0.01$) analysed by Clampfit. Exposure to XE991 had an effect on membrane input resistance that was similar to that of exposure to McN-A-343 in CA3 pyramidal neurons. The slope of the *I–V* curve increased from 122 MΩ to 175 MΩ (Fig. 10*B*, $n = 7$). XE991 increased the input resistance from 129.75 ± 8.63 MΩ to 194.53 ± 17.92 MΩ ($n = 7$, $P < 0.01$) analysed by Clampfit. These results suggested that the M1 agonist McN-A-343 and the M-channel blocker XE991 close M-type potassium channels in CA3 pyramidal neurons.

Discussion

The present study found that M1 muscarinic activation potentiated glutamate release and that inhibiting M-channels had a similar effect. The application of M-channel blockers increased the frequency of sEPSCs and mEPSCs but had no effect on their amplitudes; the application of an M1 muscarinic receptor agonist had a similar effect to that of the M-channel blockers. The effect of XE991 was dependent on Ca^{2+} influx through P/Q- and N-type calcium channels. Both the blocking of M-channels and the activation of M1 receptors depolarized CA3 pyramidal neurons. These results suggest that M1 receptor activation inhibits M-type potassium channels and depolarizes CA3 neurons. This causes an influx of Ca^{2+} through presynaptic voltage-dependent calcium channels and increase spontaneous glutamate release to CA1 neurons. This study demonstrates that M-channels modulate action-potential-independent neurotransmitter release from presynaptic terminals in Schaffer collateral–CA1 pyramidal neuron synapses. These actions occur in addition to the effects on cell soma and axon initial segment, resulting from increased membrane resistance.

M1 receptor agonists and M-channel blockers increase presynaptic glutamate release

In the present study, McN-A-343, a selective agonist for M1receptors, significantly increased the frequency of mEPSCs but had no effect on their amplitudes, which

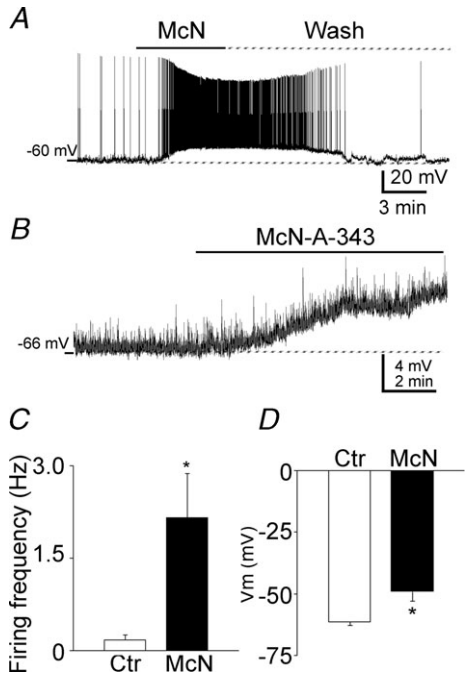

Figure 8. M1 agonist McN-A-343 depolarized and increased action potential firing in CA3 pyramidal neurons
A, representative traces of the membrane potential of a CA3 pyramidal neuron before, during, and after a wash of McN-A-343. Note the profound depolarization and the repetitive action potentials. *B*, a representative trace of the depolarizing effect of McN-A-343 on the membrane potential of a CA3 pyramidal neuron with action potentials blocked by TTX (1 μM). *C* and *D*, quantification of the effect of McN-A-343 on the firing frequency (*C*) and membrane potential (*D*) of CA3 pyramidal neurons (means ± SEM).

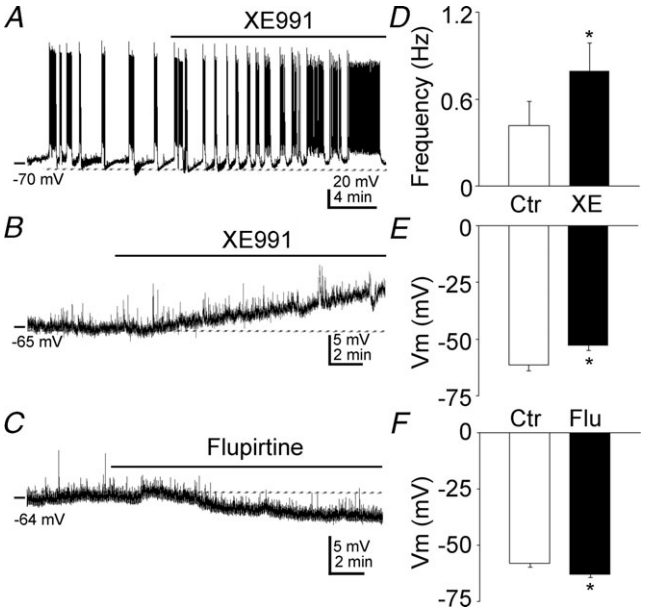

Figure 9. M-channel blocker and opener on membrane potential and action potential firing in CA3 pyramidal neurons
A, representative effect of XE991 on the membrane potential of CA3 pyramidal neurons. *B* and *C*, representative recordings of the effects of XE991 (*B*) and flupirtine (*C*) on the membrane potential of CA3 pyramidal neurons in the presence of TTX (1 μM). *D*, quantification of the effect of XE991 on the firing frequency of CA3 pyramidal neurons (means ± SEM). *E* and *F*, quantification of the effect of XE991 (*E*) and flupirtine (*F*) on the membrane potential of CA3 pyramidal neurons (means ± SEM).

© 2012 The Authors. The Journal of Physiology © 2012 The Physiological Society

Downloaded from J Physiol (jp.physoc.org) at UNIV OF VIRGINIA on July 30, 2012

suggests that M1 receptor activation increases presynaptic action potential-independent glutamate release from the Schaffer collaterals. These results are consistent with results from other studies about muscarinic potentiation of glutamatergic transmission in the hippocampus. M1 is the predominant muscarinic receptor in the hippocampus (accounting for approximately 60% of all muscarinic receptors in the hippocampus), whereas M2 and M4 are less abundant (approximately 20%) (Volpicelli & Levey, 2004). The muscarinic agonist carbachol has been associated with increases in presynaptic glutamate release in cultured rat hippocampal neurons and dentate granule cells in slices (Bouron & Reuter, 1997; Kozhemyakin *et al.* 2010). An M1 agonist has been shown to cause the potentiation of *N*-methyl-D-aspartate (NMDA) receptor currents in CA1 hippocampal pyramidal neurons (Marino *et al.* 1998). The activation of muscarinic receptors induces a long-lasting synaptic enhancement at Schaffer collaterals both *in vivo* and *in vitro* via an increase in the post-synaptic release of calcium stored in the endoplasmic reticulum (Fernández de Sevilla *et al.* 2008). A recent study that combined calcium imaging with two-photon laser glutamate uncaging suggests that M1 receptor activation increases glutamate synaptic potentials and Ca^{2+} transients in CA1 pyramidal neurons (Giessel & Sabatini, 2010). Muscarinic M1 (or at some sites M3 or possibly M5) receptor activation inhibits the M-channel (Brown & Passmore, 2009), which was first named in the 1980s (Brown & Adams, 1980; Constanti & Brown, 1981). Immunochemical studies suggest that M-channels are highly expressed in the axon initial segments of neurons (Chung *et al.* 2006; Pan *et al.* 2006; Rasmussen *et al.* 2007). Thus, M-channels are very important for tuning the firing rates and excitability of various neurons (Yue & Yaari, 2004; Shen *et al.* 2005; Gu *et al.* 2005; Shah *et al.* 2008). Interestingly, M-channel activity also affects the release of neurotransmitters from superior cervical ganglion (SCG) neurons and hippocampal synaptosomes (Martire *et al.* 2004; Hernandez *et al.* 2008). Our findings in the current study suggest that M-channels modulate action potential-independent neurotransmitter release from the presynaptic terminals of the Schaffer collaterals. M-channels are active at the resting membrane potential (Constanti & Brown, 1981) and are expressed in pre-synaptic terminals (Cooper *et al.* 2001; Chung *et al.* 2006; Garcia-Pino *et al.* 2010). The presynaptic potentiation effect of the M-channel blocker XE991 was reversed over a long period of time. This might be due to its binding kinetics. The dissociation of linopirdine, an analogue of XE991, is slow and begins after 60 min (Wolff *et al.* 2005).

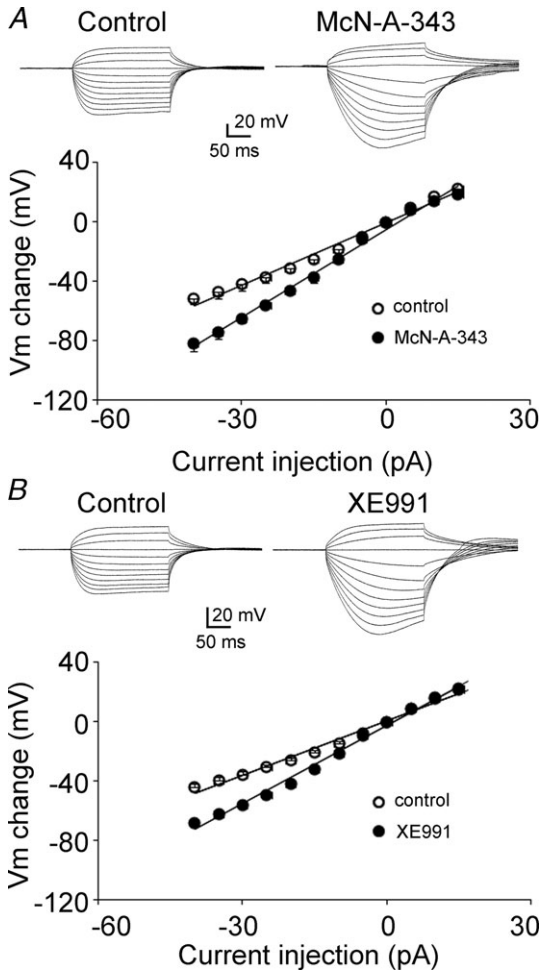

Figure 10. McN-A-343 and XE991 increased input resistance in CA3 neurons
A, top, representative recordings of current injections from −40 pA (in 5 pA steps) before (left) and after (right) the application McN-A-343. Bottom, *I–V* relationship before (open circles) and after (filled circle) the application of McN-A-343 in CA3 neurons ($n = 6$). *B*, top, representative recordings of current injections from −40 pA (in 5 pA steps) before (left) and after (right) the application of XE991. Bottom, *I–V* relationship before (open circles) and after (filled circles) the application of XE991 in CA3 neurons ($n = 7$).

M1 receptor agonist and M-channel blocker depolarize CA3 neurons

An M1 agonist and an M-channel blocker depolarized CA3 pyramidal neurons. This finding is consistent with the location and function of the receptor in these neurons. The M1 receptor is the most commonly expressed muscarinic receptor in the hippocampus in both the pyramidal neuron layer and the stratum radiatum of the CA3 and CA1 regions (Tayebati *et al.* 2002). A comparable slow, muscarinic receptor-dependent depolarization can be evoked in pyramidal neurons by the direct electrical stimulation of cholinergic afferents in the hippocampus (Cole & Nicoll, 1983; Madison *et al.* 1987; Segal, 1988; Pitler & Alger, 1990; Morton & Davies, 1997) or medial septal nucleus in a septo-hippocampal slice (Cobb

© 2012 The Authors. The Journal of Physiology © 2012 The Physiological Society

Downloaded from J Physiol (jp.physoc.org) at UNIV OF VIRGINIA on July 30, 2012

& Davies, 2005). The medial septal nucleus provides the major source of cholinergic innervations to the hippocampus (Dutar *et al.* 1995) and presents a direct synaptic input to both principal neurons and interneurons (Frotscher & Léránth, 1985; Léránth & Frotscher, 1987). Muscarinic acetylcholine receptors modulate several ionic conductances in addition to the M-current, including I_{AHP} (the Ca^{2+}-activated K^+ current that is responsible for slowing action potential discharges) and I_{leak} (the background leak current) (Halliwell, 1990). Activation of mAChRs also potentiates two mixed cation currents (I_h, the hyperpolarization-activated cation current; and I_{cat}, the Ca^{2+}-dependent non-specific cation current) (Halliwell, 1990; Colino & Halliwell, 1993) and the *N*-methyl-D-aspartate (NMDA) receptor (Markram & Segal, 1990). This may explain why, in our study, the M1 agonist McN-A-343 had a stronger depolarization effect than the M-channel blocker XE991 in CA3 pyramidal neurons.

Muscarinic receptor and intracellular calcium level

Current study suggested that M1 receptor activation depolarizes presynaptic membrane and activates voltage-gated calcium channel to increase intracellular calcium level and neurotransmitter release by inhibition of M-channels. Previous studies suggested that muscarinic stimulation inhibits voltage-gated calcium channels (Toselli *et al.* 1989; Qian & Saggau, 1997). However these studies did not classify the subtype of muscarnic receptor that mediates this effect. It was reported that the inhibitory effect of muscarinic receptor activation on calcium channels was mediated by M4 subtype in rat sympathetic neurons (Bernheim *et al.* 1992) and by M2 subtype in rat magocellular cholinergic basal forebrain neurons (Allen & Brown, 1993). There is no report to suggest that M1 subtype muscarinic receptor inhibits calcium channels.

Muscarinic receptors activate inositol 1,4,5-trisphosphate (IP_3) receptor to trigger calcium release from endoplasmic reticulum (ER) stores in CA1 pyramidal neurons, and appears to be action potential independent (Power & Sah, 2002). Another study suggested this effect is mediated by M1 receptor (Fernández de Sevilla *et al.* 2008). The role of these stores in enhancing synaptic release remains uncertain. Although spontaneous transmitter release (in the absence of action potentials) is largely mediated by calcium release from internal stores (Emptage *et al.* 2001), our study suggests the modulation of spontaneous transmitter release could be mediated by calcium influx though voltage-gated calcium channels.

Overall, this study demonstrated that M1 muscarinic receptor activation inhibits M-type potassium channels, thereby increasing excitatory glutamate neurotransmitter release from the presynaptic terminals of CA3 neurons by increasing the rate of calcium influx through voltage-dependent calcium channels. This effect of M1 receptor activation could contribute to the generation of seizures.

References

Allen TG & Brown DA (1993). M2 muscarinic receptor-mediated inhibition of the Ca^{2+} current in rat magnocellular cholinergic basal forebrain neurones. *J Physiol* **466**, 173–189.

Bernheim L, Mathie A & Hille B (1992). Characterization of muscarinic receptor subtypes inhibiting Ca^{2+} current and M-current in rat sympathetic neurons. *Proc Natl Acad Sci U S A* **89**, 9544–9548.

Biervert C, Schroeder BC, Kubisch C, Berkovic SF, Propping P, Jentsch TJ & Steinlein OK (1998). A potassium channel mutation in neonatal human epilepsy. *Science* **279**, 403–406.

Bouron A & Reuter H (1997). Muscarinic stimulation of synaptic activity by protein kinase C is inhibited by adenosine in cultured hippocampal neurons. *Proc Natl Acad Sci U S A* **94**, 12224–12229.

Brown DA & Adams PR (1980). Muscarinic suppression of a novel voltage-sensitive K^+ current in a vertebrate neurone. *Nature* **283**, 673–676.

Brown DA & Passmore GM (2009). Neural KCNQ (Kv7) channels. *Br J Pharmacol* **156**, 1185–1195.

Brown JT & Randall AD (2009). Activity-dependent depression of the spike after-depolarization generates long-lasting intrinsic plasticity in hippocampal CA3 pyramidal neurons. *The Journal of Physiology* **587**, 1265–1281.

Chung HJ, Jan YN & Jan LY (2006). Polarized axonal surface expression of neuronal KCNQ channels is mediated by multiple signals in the KCNQ2 and KCNQ3 C-terminal domains. *Proc Natl Acad Sci U S A* **103**, 8870–8875.

Cobb SR & Davies CH (2005). Cholinergic modulation of hippocampal cells and circuits. *J Physiol* **562**, 81–88.

Cole AE & Nicoll RA (1983). Acetylcholine mediates a slow synaptic potential in hippocampal pyramidal cells. *Science* **221**, 1299–1301.

Colino A & Halliwell JV (1993). Carbachol potentiates Q current and activates a calcium-dependent non-specific conductance in rat hippocampus in vitro. *Eur J Neurosci* **5**, 1198–1209.

Constanti A & Brown DA (1981). M-currents in voltage-clamped mammalian sympathetic neurones. *Neurosci Lett* **24**, 289–294.

Cooper EC, Harrington E, Jan YN & Jan LY (2001). M-channel KCNQ2 subunits are localized to key sites for control of neuronal network oscillations and synchronization in mouse brain. *J Neurosci* **21**, 9529–9540.

Delmas P & Brown DA (2005). Pathways modulating neural KCNQ/M (Kv7) potassium channels. *Nat Rev Neurosci* **6**, 850–862.

Devaux JJ, Kleopa KA, Cooper EC & Scherer SS (2004). KCNQ2 is a nodal K^+ channel. *J Neurosci* **24**, 1236–1244.

© 2012 The Authors. The Journal of Physiology © 2012 The Physiological Society

Downloaded from J Physiol (jp.physoc.org) at UNIV OF VIRGINIA on July 30, 2012

Dutar P, Bassant MH, Senut MC & Lamour Y (1995). The septohippocampal pathway: structure and function of a central cholinergic system. *Physiol Rev* **75**, 393–427.

Emptage NJ, Reid CA & Fine A (2001). Calcium stores in hippocampal synaptic boutons mediate short-term plasticity, store-operated Ca^{2+} entry, and spontaneous transmitter release. *Neuron* **29**, 197–208.

Fernandez de Sevilla D, Núñez A, Borde M, Malinow R & Buño W. (2008). Cholinergic-mediated IP3-receptor activation induces long-lasting synaptic enhancement in CA1 pyramidal neurons. *J Neurosci* **28**, 1469–1478.

Frotscher M & Léránth C (1985). Cholinergic innervation of the rat hippocampus as revealed by choline acetyltransferase immunocytochemistry: a combined light and electron microscopic study. *J Comp Neurol* **239**, 237–246.

Garcia-Pino E, Caminos E & Juiz JM (2010). KCNQ5 reaches synaptic endings in the auditory brainstem at hearing onset and targeting maintenance is activity-dependent. *J Comp Neurol* **518**, 1301–1314.

Geiger J, Weber YG, Landwehrmeyer B, Sommer C & Lerche H (2006). Immunohistochemical analysis of KCNQ3 potassium channels in mouse brain. *Neurosci Lett* **400**, 101–104.

Giessel AJ & Sabatini BL (2010). M1 muscarinic receptors boost synaptic potentials and calcium influx in dendritic spines by inhibiting postsynaptic SK channels. *Neuron* **68**, 936–947.

Gu N, Vervaeke K, Hu H & Storm JF (2005). Kv7/KCNQ/M and HCN/h, but not KCa2/SK channels, contribute to the somatic medium after-hyperpolarization and excitability control in CA1 hippocampal pyramidal cells. *J Physiol* **566**, 689–715.

Halliwell JV (1990). Physiological mechanisms of cholinergic action in the hippocampus. *Prog Brain Res* **84**, 255–272.

Hernandez CC, Zaika O, Tolstykh GP & Shapiro MS (2008). Regulation of neural KCNQ channels: signalling pathways, structural motifs and functional implications. *J Physiol* **586**, 1811–1821.

Higley MJ, Soler-Llavina GJ & Sabatini BL (2009). Cholinergic modulation of multivesicular release regulates striatal synaptic potency and integration. *Nat Neurosci* **12**, 1121–1128.

Jentsch TJ (2000). Neuronal KCNQ potassium channels:physislogy and role in disease. *Nat Rev Neurosci* **1**, 21–30.

Kanaumi T, Takashima S, Iwasaki H, Itoh M, Mitsudome A & Hirose S (2008). Developmental changes in KCNQ2 and KCNQ3 expression in human brain: possible contribution to the age-dependent etiology of benign familial neonatal convulsions. *Brain Dev* **30**, 362–369.

Kozhemyakin M, Rajasekaran K & Kapur J (2010). Central cholinesterase inhibition enhances glutamatergic synaptic transmission. *J Neurophysiol* **103**, 1748–1757.

Langmead CJ, Watson J & Reavill C (2008). Muscarinic acetylcholine receptors as CNS drug targets. *Pharmacol Ther* **117**, 232–243.

Léránth C & Frotscher M (1987). Cholinergic innervation of hippocampal GAD- and somatostatin-immunoreactive commissural neurons. *J Comp Neurol* **261**, 33–47.

Madison DV, Lancaster B & Nicoll RA (1987). Voltage clamp analysis of cholinergic action in the hippocampus. *J Neurosci* **7**, 733–741.

Marino MJ, Rouse ST, Levey AI, Potter LT & Conn PJ (1998). Activation of the genetically defined M1 muscarinic receptor potentiates N-methyl-D-aspartate (NMDA) receptor currents in hippocampal pyramidal cells. *Proc Natl Acad Sci U S A* **95**, 11465–11470.

Markram H & Segal M (1990). Acetylcholine potentiates responses to N-methyl-D-aspartate in the rat hippocampus. *Neurosci Lett* **113**, 62–65.

Marrion NV, Smart TG, Marsh SJ & Brown DA (1989). Muscarinic suppression of the M-current in the rat sympathetic-ganglion is mediated by receptors of the M1-subtype. *Br J Pharmacol* **98**, 557–573.

Martire M, Castaldo P, D'Amico M, Preziosi P, Annunziato L & Taglialatela M (2004). M-channels containing KCNQ2 subunits modulate norepinephrine, aspartate, and GABA release from hippocampal nerve terminals. *J Neurosci* **24**, 592–597.

Morton RA & Davies CH (1997). Regulation of muscarinic acetylcholine receptor-mediated synaptic responses by adenosine receptors in the rat hippocampus. *J Physiol* **502**, 75–90.

Pan Z, Kao T, Horvath Z, Lemos J, Sul JY, Cranstoun SD, Bennett V, Scherer SS & Cooper EC (2006). A common ankyrin-G-based mechanism retains KCNQ and NaV channels at electrically active domains of the axon. *J Neurosci* **26**, 2599–2613.

Peretz A, Sheinin A, Yue C, Degani-Katzav N, Gibor G, Nachman R, Gopin A, Tam E, Shabat D, Yaari Y & Attali B (2007). Pre- and postsynaptic activation of M-channels by a novel opener dampens neuronal firing and transmitter release. *J Neurophysiol* **97**, 283–295.

Pitler TA & Alger BE (1990). Activation of the pharmacologically defined M3 muscarinic receptor depolarizes hippocampal pyramidal cells. *Brain Res* **534**, 257–262.

Power JM & Sah P (2002). Nuclear calcium signaling evoked by cholinergic stimulation in hippocampal CA1 pyramidal neurons. *J Neurosci* **22**, 3454–3462.

Qian J & Noebels JL (2000). Presynaptic Ca^{2+} influx at a mouse central synapse with Ca^{2+} channel subunit mutations. *J Neurosci* **20**, 163–170.

Qian J & Saggau P (1997). Presynaptic inhibition of synaptic transmission in the rat hippocampus by activation of muscarinic receptors: involvement of presynaptic calcium influx. *Br J Pharmacol* **122**, 511–519.

Rasmussen HB, Frøkjær-Jensen C, Jensen CS, Jensen HS, Jørgensen NK, Misonou H, Trimmer JS, Olesen SP & Schmitt N (2007). Requirement of subunit co-assembly and ankyrin-G for M-channel localization at the axon initial segment. *J Cell Sci* **120**, 953–963.

Safiulina VF, Zacchi P, Taglialatela M, Yaari Y & Cherubini E (2008). Low expression of Kv7/M channels facilitates intrinsic and network bursting in the developing rat hippocampus. *J Physiol* **586**, 5437–5453.

Segal M (1988). Synaptic activation of a cholinergic receptor in rat hippocampus. *Brain Res* **452**, 79–86.

Selyanko AA, Delmas P, Hadley JK, Tatulian L, Wood IC, Mistry M, London B & Brown DA (2002). Dominant-negative subunits reveal potassium channel families that contribute to M-like potassium currents. *J Neurosci* **22**, RC212.

© 2012 The Authors. The Journal of Physiology © 2012 The Physiological Society

Downloaded from J Physiol (jp.physoc.org) at UNIV OF VIRGINIA on July 30, 2012

Shah MM, Migliore M, Valencia I, Cooper EC & Brown DA (2008). Functional significance of axonal Kv7 channels in hippocampal pyramidal neurons. *Proc Natl Acad Sci U S A* **105**, 7869–7874.

Shah MM, Mistry M, Marsh SJ, Brown DA & Delmas P (2002). Molecular correlates of the M-current in cultured rat hippocampal neurons. *J Physiol* **544**, 29–37.

Shen W, Hamilton SE, Nathanson NM & Surmeier DJ (2005). Cholinergic suppression of KCNQ channel currents enhances excitability of striatal medium spiny neurons. *J Neurosci* **25**, 7449–7458.

Sim JA & Griffith WH (1996). Muscarinic Inhibition of glutamatergic transmission onto rat magnocellular basal forebrain neurons in a thin-slice preparation. *Eur J Neurosci* **8**, 880–891.

Tayebati SK, Amenta F, El-Assouad D & Zaccheo D (2002). Muscarinic cholinergic receptor subtypes in the hippocampus of aged rats. *Mech of Ageing Dev* **123**, 521–528.

Toselli M, Lang J, Costa T & Lux HD (1989). Direct modulation of voltage-dependent calcium channels by muscarinic activation of a pertussis toxin-sensitive G-protein in hippocampal neurons. *Pflugers Arch* **415**, 255–261.

Vervaeke K, Gu N, Agdestein C, Hu H & Storm JF (2006). Kv7/KCNQ/M-channels in rat glutamatergic hippocampal axons and their role in regulation of excitability and transmitter release. *J Physiol* **576**, 235–256.

Vogt KE & Regehr WG (2001). Cholinergic modulation of excitatory synaptic transmission in the CA3 area of the hippocampus. *J Neurosci* **21**, 75–83.

Volpicelli LA & Levey AI (2004). Muscarinic acetylcholine receptor subtypes in cerebral cortex and hippocampus. *Prog Brain Res* **145**, 59–66.

Wang HS, Pan Z, Shi W, Brown BS, Wymore RS, Cohen IS, Dixon JE & McKinnon D (1998). KCNQ2 and KCNQ3 potassium channel subunits: molecular correlates of the M-channel. *Science* **282**, 1890–1893.

Weber YG, Geiger J, Kämpchen K, Landwehrmeyer B, Sommer C & Lerche H (2006). Immunohistochemical analysis of KCNQ2 potassium channels in adult and developing mouse brain. *Brain Res* **1077**, 1–6.

Wheeler DB, Randall A & Tsien RW (1994). Roles of N-type and Q-type Ca^{2+} channels in supporting hippocampal synaptic transmission. *Science* **264**, 107–111.

Wolff C, Gillard M, Fuks B & Chatelain P (2005). [^{3}H]Linopirdine binding to rat brain membranes is not relevant for M-channel interaction. *Eur J Pharmacol* **518**, 10–17.

Yajeya J, De La Fuente A, Criado JM, Bajo V, Sánchez-Riolobos A & Heredia M (2000). Muscarinic agonist carbachol depresses excitatory synaptic transmission in the rat basolateral amygdala in vitro. *Synapse* **38**, 151–160.

Yue C & Yaari Y (2004). KCNQ/M Channels control spike afterdepolarization and burst generation in hippocampal neurons. *J Neurosci* **24**, 4614–4624.

Zhang HM, Chen SR & Pan HL (2007). Regulation of glutamate release from primary afferents and interneurons in the spinal cord by muscarinic receptor subtypes. *J Neurophysiol* **97**, 102–109.

Author contributions

J.S. and J.K. designed the study. J.S. performed the experiments and analysed the data. J.S. and J.K. interpreted the data, drafted and revised the article.

Acknowledgements

This study was supported by peer reviewed Medical Research Program of the Department of Defense PR 093963 and NINDS (NIH) RO1 NS 40337.

© 2012 The Authors. The Journal of Physiology © 2012 The Physiological Society

Downloaded from J Physiol (jp.physoc.org) at UNIV OF VIRGINIA on July 30, 2012

Epilepsy Research (2012) xxx, xxx—xxx

journal homepage: www.elsevier.com/locate/epilepsyres

Characterization of status epilepticus induced by two organophosphates in rats

Marko S. Todorovic, Morgan L. Cowan, Corrinee A. Balint, Chengsan Sun, Jaideep Kapur*

Department of Neurology, University of Virginia Health Sciences Center, Charlottesville, VA 22908, USA

Received 10 August 2011; received in revised form 8 April 2012; accepted 17 April 2012

KEYWORDS
Organophosphate;
Status epilepticus;
EEG;
Seizures;
Benzodiazepine;
Diazepam

Summary Organophosphates (OPs) inhibit the enzyme cholinesterase and cause accumulation of acetylcholine, and are known to cause seizures and status epilepticus (SE) in humans. The animal models of SE caused by organophosphate analogs of insecticides are not well characterized. SE caused by OPs paraoxon and diisopropyl fluorophosphate (DFP) in rats was characterized by electroencephalogram (EEG), behavioral observations and response to treatment with the benzodiazepine diazepam administered at various stages of SE. A method for SE induction using intrahippocampal infusion of paraoxon was also tested. Infusion of 200 nmol paraoxon into the hippocampus caused electrographic seizures in 43/52 (82.7%) animals tested; and of these animals, 14/43 (30%) had self-sustaining seizures that lasted 4—18 h after the end of paraoxon infusion. SE was also induced by peripheral subcutaneous injection of diisopropyl fluorophosphate (DFP, 1.25 mg/kg) or paraoxon (1.00 mg/kg) to rats pretreated with atropine (2 mg/kg) and 2-pralidoxime (2-PAM, 50 mg/kg) 30 min prior to OP injection. SE occurred in 78% paraoxon-treated animals and in 79% of DFP-treated animals. Diazepam (10 mg/kg) was administered 10 min and 30 min after the onset of continuous EEG seizures induced by paraoxon and it terminated SE in a majority of animals at both time points. DFP-induced SE was terminated in 60% animals when diazepam was administered 10 min after the onset of continuous EEG seizure activity but diazepam did not terminate SE in any animal when it was administered 30 min after the onset of continuous seizures. These studies demonstrate that both paraoxon and DFP can induce SE in rats but refractoriness to diazepam is a feature of DFP induced SE.
© 2012 Elsevier B.V. All rights reserved.

Introduction

Status epilepticus (SE) is a neurological emergency characterized by recurrent or continuous self-sustaining seizures. SE can contribute to morbidity, sustained neuronal injury and contribute to mortality (Fujikawa et al., 2000; Fujikawa, 2005). Understanding mechanisms of SE in humans is a

* Corresponding author at: Department of Neurology, Box 800394, University of Virginia HSC, Charlottesville, VA 22908-800394, USA. Tel.: +1 434 924 5312; fax: +1 434 982 1726.
E-mail address: jk8t@virginia.edu (J. Kapur).

0920-1211/$ — see front matter © 2012 Elsevier B.V. All rights reserved.
http://dx.doi.org/10.1016/j.eplepsyres.2012.04.014

Please cite this article in press as: Todorovic, M.S., et al., Characterization of status epilepticus induced by two organophosphates in rats. Epilepsy Res. (2012), http://dx.doi.org/10.1016/j.eplepsyres.2012.04.014

particular challenge because patients have to be treated promptly and underlying neurological insult contributes to the pathology. Animal models have been used to understand the pathophysiology of SE and test novel therapies (Chen et al., 2007; Wasterlain et al., 1993). Current animals models of SE are based on chemical stimulation of cholinergic system by muscarinic agonists such as pilocarpine, agonists of glutamate receptors such as kainate and electrical stimulation of limbic structures (Turski et al., 1983; Honchar et al., 1983; Lothman et al., 1981, 1989; Mazarati et al., 1998b). However, there are few instances of these toxins causing human SE.

Organophosphates (OPs) are potent inhibitors of the enzyme cholinesterase, and several of these cause SE in humans and experimental animals. OPs such as parathion and malathion are used as insecticides and there are numerous reports of SE in humans induced by these insecticides (Garcia et al., 2003; Hoffmann and Papendorf, 2006). Extremely potent OPs, such as soman, sarin and VX are also used as nerve agents for chemical warfare and in civilian terrorist attacks, and they cause SE (McDonough and Shih, 1997; Morita et al., 1995; Nozaki et al., 1995). However, OP nerve agents sarin, soman, VX, etc. are restricted use chemicals and SE induced by these agents has been studied in defense labs. Therefore, acceptable surrogate OP agents must be used for civilian research to understand the mechanisms, pathophysiology and treatment of OP induced SE.

Several organophosphates are available for civilian use including diisopropyl fluorophosphate (DFP), paraoxon, chlorfenvinphos or dichlorvos. Chlorfenvinphos does not appear to cause seizures, and dichlorvos primarily causes fatalities by central respiratory depression (Bird et al., 2003; Gralewicz et al., 1989). On the other hand DFP and paraoxon models have been have been used to study neuropathology, drug response and calcium homeostasis neuropathology associated with OPs (Deshpande et al., 2010; Harrison et al., 2004; Kadriu et al., 2011; Li et al., 2011; Zaja-Milatovic et al., 2009; Zhu et al., 2010). However, these studies did not characterize the evolution SE with EEG. Thus the time to initiation of seizures, duration of seizures and their EEG characteristics remain unknown. Furthermore, they did not test responsiveness to benzodiazepines, such as diazepam. Benzodiazepines are the mainstay of treatment of seizures and OP induced seizures (Alldredge et al., 2001; Treiman et al., 1998; Treiman, 2007). These drugs fail in 35—45% of cases and better treatments are needed.

We characterized SE induced by paraoxon and DFP by means of EEG and behavior. We also characterized the response to treatment with benzodiazepine diazepam at various stages of SE.

Materials and methods

Surgery

All procedures on animals were performed according to a protocol approved by the institutional Animal Care and Use Committee. Adult male Sprague-Dawley rats (Taconic) weighing 175—300 g were housed with food and water ad libitum. The animals were anesthetized with ketamine (50 mg/kg) and xylazine (10 mg/kg) for implantation. For animals undergoing intrahippocampal infusion, a bipolar electrode was implanted in the left ventral hippocampus (AP −5.3, ML −4.9, DV −5.0 to dura; incisor bar −3.3). A guide cannula (Plastics One, Roanoke, VA) was implanted into the right ventral hippocampus (AP −5.8, ML +4.6, DV −2.5 from dura; incisor bar −3.3), alongside a second bipolar electrode. A teflon coated 0.01 inch diameter stainless-steel wire positioned near the frontal sinus served as a ground electrode. For animals undergoing peripheral injection studies, three supra-dural cortical electrodes were placed over the cortex. In both procedures, the electrodes were inserted into a strip connector and then secured to the skull with dental acrylic as previously described (Lothman et al., 1988).

Intrahippocampal infusion

Following a 1 week recovery, animals were connected via a cable to a data acquisition system (Stellate Systems). Paraoxon was suspended in 4% hydroxypropyl-B-cyclodextrin (Sigma, St. Louis, MO). An injection needle connected to a 0.1 mL Hamilton syringe and driven by an infusion pump (KD Scientific, Portland, OR) was back filled with paraoxon and inserted such that it extended 3 mm below the end of the cannula guide. Paraoxon was then infused at a rate of either 0.5 μL/min or 1 μL/min for a total volume of 20 μL. EEG and video monitoring began 10 min prior to paraoxon infusion and continued for 24 h after infusion completion.

EEG recordings were subsequently reviewed for the presence of seizures as well as SE. Seizures were characterized by the appearance of high frequency (>2 Hz), rhythmic spike wave discharges with amplitudes at least three times that of the baseline EEG. Animals were considered to have SE if there was continuous epileptiform activity for 30 min, during which spike frequencies were more than 2 Hz, and spike amplitude was at least 3 times the background. Behavioral seizures were scored according to the Racine scale (Racine, 1972).

Peripheral injection

EEG recording was initiated prior to administration of 2 mg/kg atropine (Sigma, St. Louis, MO) and 50 mg/kg 2 pralidoxime (2-PAM) iodide (Sigma, St. Louis, MO) intraperitoneally. After 30 min, DFP (Sigma, St. Louis, MO) or paraoxon (Chem Service, West Chester, PA) was injected subcutaneously (SC). In some experiments animals were given 10 mg/kg diazepam 10 min or 30 min after onset of continuous SE activity. A non-diazepam injected group served as controls. 2-PAM and atropine were both dissolved in solution within 1 h of injection. DFP and paraoxon were both mixed into cold saline immediately prior to injection. Animals were monitored via EEG and video for 24 h following organophosphate injection.

Epileptiform activity was monitored and defined as follows. Seizures were defined as the appearance of high frequency (>2 Hz), rhythmic spike wave discharges with amplitudes at least 3 times that of the baseline EEG. The criterion for the onset of SE was the occurrence of continuous seizure activity for 10 min, during which spike frequencies do not drop below 2 Hz. The end of SE was characterized by non-uniform spike frequencies that remained lower than

Please cite this article in press as: Todorovic, M.S., et al., Characterization of status epilepticus induced by two organophosphates in rats. Epilepsy Res. (2012), http://dx.doi.org/10.1016/j.eplepsyres.2012.04.014

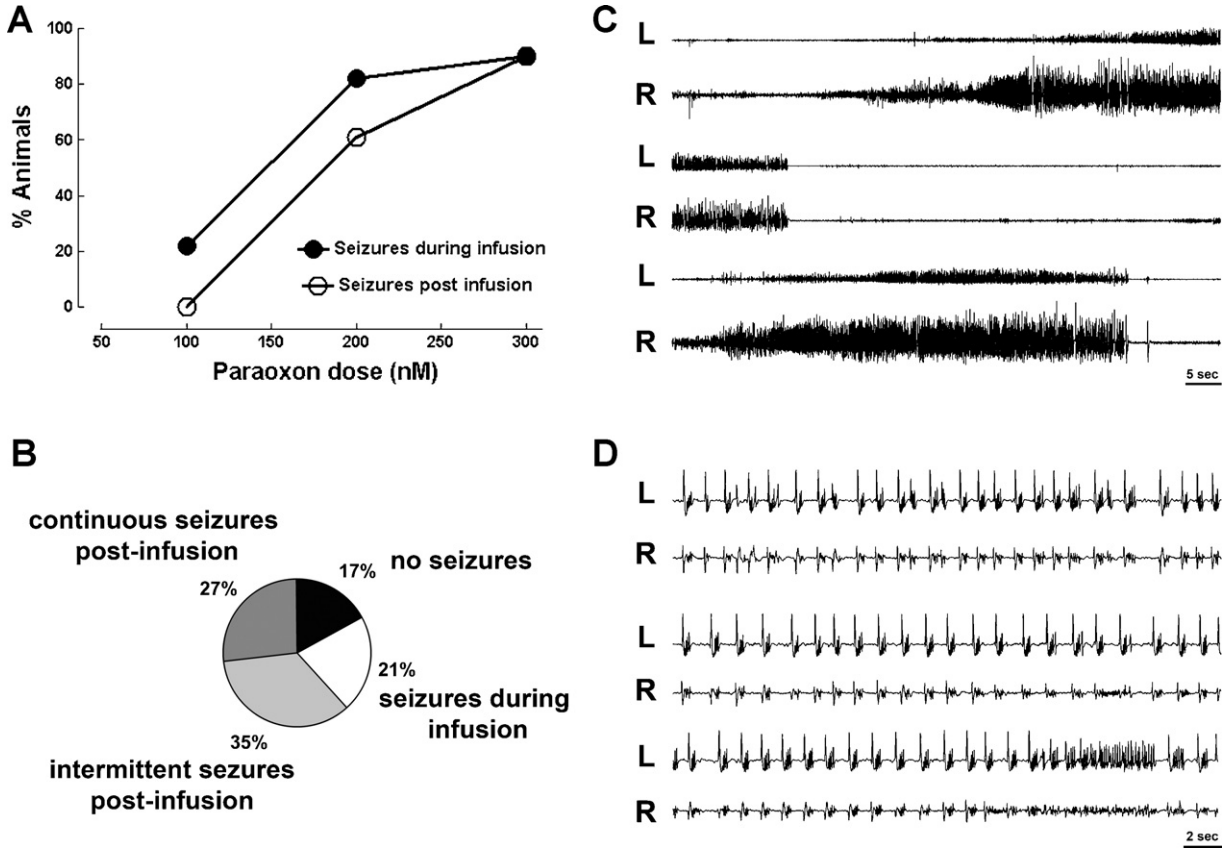

Figure 1 Seizures caused by intra-hippocampal infusion of the organophosphate paraoxon. (A) Displays % fraction of animals having seizures in response to 100 nmol ($n = 9$), 200 nmol ($n = 52$) and 300 nmol ($n = 11$) of intra-hippocampal paraoxon. (B) A pie chart of four responses to 200 nmol paraoxon infused in the hippocampus: no seizures, seizures during infusion, intermittent post infusion seizures and continuous post infusion seizures. (C) Displays EEG recordings from right (R) and left (L) hippocampus showing intermittent seizures following infusion of 200 nmol paraoxon solution into the right hippocampus. A seizure begins in the right hippocampus, spreads to the left hippocampus and ends several second later (middle two traces), and soon thereafter another seizure begins and spreads to the left hippocampus. (D) Displays a continuous electrographic seizures occurring in right and left hippocampi, note faster time base. The seizure consists of continuous spike-wave discharges.

1 Hz. EEG data was polled every 10 min after the onset of SE to determine SE termination during a 5 h interval after SE began.

Immunohistochemistry for Fluorojade and NeuN

The procedures of tissue preparation were described in detail previously (Sun et al., 2004, 2007). Briefly, animals were anesthetized with an overdose of pentobarbitone sodium and perfused through the ascending aorta with 50—100 mL 0.9% NaCl followed by 350—450 mL 4% paraformaldehyde in 0.1 M phosphate buffer (PB, pH 7.4). Brains were removed and post-fixed in the same fixative for 2 h at 4 °C. Brains were frozen by immersion in −70 °C isopentane. Coronal sections from the anterior block were cut at 40 μm to collect dorsal sections.

In order to stain for NeuN and Fluoro-Jade B, immunohistochemical technique was modified as described previously (Jakab and Bowyer, 2002; Sun et al., 2007). Sections were incubated for 48 h at 4 °C in the anti-NeuN primary antibody mouse anti-NeuN (diluted at 1:200,Millipore), followed by incubation with a secondary antibody conjugated to Alexa Fluor 594 (5 μg/mL; molecular probes) for 60 min at room temperature. Sections were wet-mounted on glass slides, air-dried at 50 °C for 15 min, and stained with Fluoro-Jade B. The slides were immersed in distilled water for 1 min and oxidized in a 0.006% solution of $KMnO_4$ for 5 min. After rinsing in distilled water twice for 30 s, sections were stained for 10 min in a 0.0003% solution of Fluoro-Jade B in 0.1% acetic acid. Finally, sections were rinsed in distilled water, air-dried, and cleared with xylene.

Results

Seizures and SE caused by paraoxon infusion

Infusion of 100 nmol paraoxon into the hippocampus caused electrographic seizures in 2/9 (22.2%) animals tested. None of the animals had seizures lasting beyond the end of infusion and 2 animals displayed intermittent seizures during paraoxon infusion which were not self-sustaining. No change in baseline EEG, and no behavioral seizures occurred in the remaining 7 animals (Fig. 1A).

Please cite this article in press as: Todorovic, M.S., et al., Characterization of status epilepticus induced by two organophosphates in rats. Epilepsy Res. (2012), http://dx.doi.org/10.1016/j.eplepsyres.2012.04.014

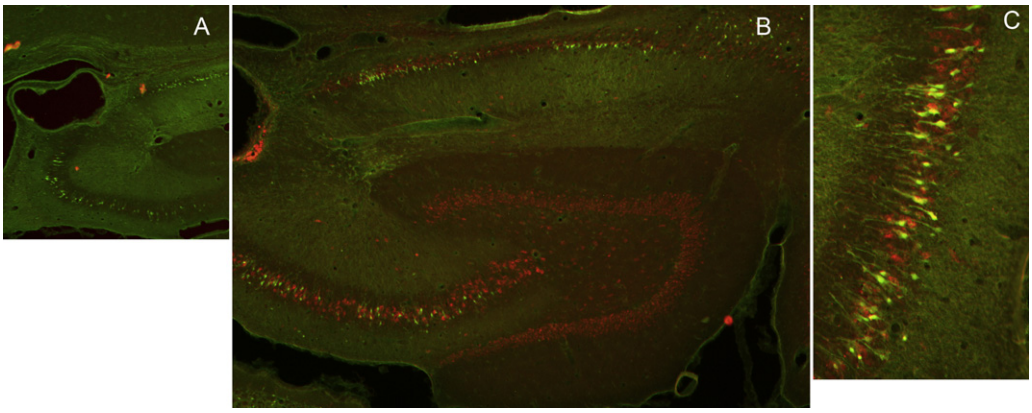

Figure 2 Images of hippocampal sections from animals that had prolonged seizures following intra-hippocampal paraoxon administration, which were stained for neuronal injury stain Fluoro-Jade B (green) and neuronal marker NeuN (red). (A) A low magnification image of the hippocampus showing drug infusion site close to the CA3 region of the hippocampus. (B) A section of the hippocampus displaying green Fluorojade positive CA3, CA1 pyramidal neurons and neurons in the subiculum. (C) A higher magnification image of Fluorojade positive neurons in the CA3 region of the hippocampus.

Infusion of 200 nmol paraoxon into the hippocampus caused electrographic seizures in 43/52 (82.7%) animals tested. In 32 animals seizures lasted beyond the end of infusion (61.5%) and 11 animals displayed intermittent seizures during paraoxon infusion which were not self-sustaining, and did not continue through the end of infusion (Fig. 1B). There was no change in baseline EEG in remaining 9 animals. These animals did not display behavioral characteristics indicative of seizure activity.

Among animals with seizures lasting beyond paraoxon infusion, two distinct types of electrographic seizure activity occurred: intermittent and continuous seizures. Intermittent seizures, which occurred in 18 animals, frequently appeared first in the paraoxon infusion site in the right hippocampus, and then spread to the contra-lateral (left) hippocampus (Fig. 1C). Seizures consisted of rhythmic high frequency spike wave discharges that evolved in frequency and amplitude. There were brief periods of suppression of activity between seizures.

Continuous seizures occurred in 14 animals following paraoxon infusion, and these consisted of sustained bilateral discharges of repetitive spike patterns evolving over time (Fig. 1D). Continuous electrographic seizures started at approximately 15 min post infusion, and persisted for 4—18 h. These prolonged self-sustaining seizures constituted SE. Paraoxon-induced SE was further confirmed upon observation of behavioral seizures. Animals experiencing SE exhibited freezing, staring, blinking, and hyper-exploratory movement, as well as wet-dog shaking movements for 4—18 h.

Infusion of 300 nmol paraoxon into the hippocampus caused electrographic seizures in 10/11 (90.9%) of animals tested. The seizures in all of these animals continued beyond the end of infusion in form of SE with behavioral seizures ranging from 2 to 5 on the Racine scale. The majority of animals in SE (7) died of respiratory arrest, several of these exhibited symptoms of peripheral cholinergic stimulation, including muscle contractions and fasciculations. The remaining 3 animals survived, exhibiting seizures that lasted long beyond the end of infusion. Only 1 animal receiving paraoxon 300 nM infusion displayed neither behavioral characteristics indicative of seizure activity, nor EEG seizure activity (9.0%).

The location of the cannula was confirmed by sectioning the hippocampus. In many animals, the cannula and electrode tracts were localized by sectioning the brain in the plane of the electrode. In other animals, immunohistochemistry for neuronal stain Neun and staining for neuro-degeneration dye Fluorojade J, was performed 3 days after SE caused by infusion of paraoxon. The site of infusion was at the ventricular border the CA3 layer of the hippocampus (Fig. 2A). Fluorojade positive neurons were present in CA1and CA3 regions and of the hippocampus and the subiculum (Fig. 2B and C). Occasional Fluorojade positive cells were present in the hilus.

Peripheral injection of paraoxon

Preliminary experiments were performed to optimize the model. Paraoxon (0.35 mg/kg) administered by the intraperitoneal route caused widespread muscle contractions, fasciculations, rare tonic convulsions, respiratory arrest and death in all four animals tested. Pretreatment of animals with scopolamine (4 mg/kg) protected against peripheral and systemic effects of paraoxon ($n = 4$ animals). Subsequently, based on the work of Deshpande et al. (2010) oxime reactivator 2-PAM and muscarinic antagonist atropine was combined with peripheral paraoxon administration. In preliminary experiments we tested other doses of these agents and confirmed that most optimal doses were used.

Paraoxon (1 mg/kg) was administered SC to 23 animals 30 min after pre-treatment with 2 mg/kg atropine and 50 mg/kg 2-PAM and prolonged seizures were observed. SE occurred in 17 of the 23 animals (74%) with animals displaying a combination of chewing, head-bobbing, single and bilateral limb clonus and rearing, leading to constant full body tremors. In 3 animals there was no effect from the OP injection and 3 animals died from respiratory arrest without any seizures.

Please cite this article in press as: Todorovic, M.S., et al., Characterization of status epilepticus induced by two organophosphates in rats. Epilepsy Res. (2012), http://dx.doi.org/10.1016/j.eplepsyres.2012.04.014

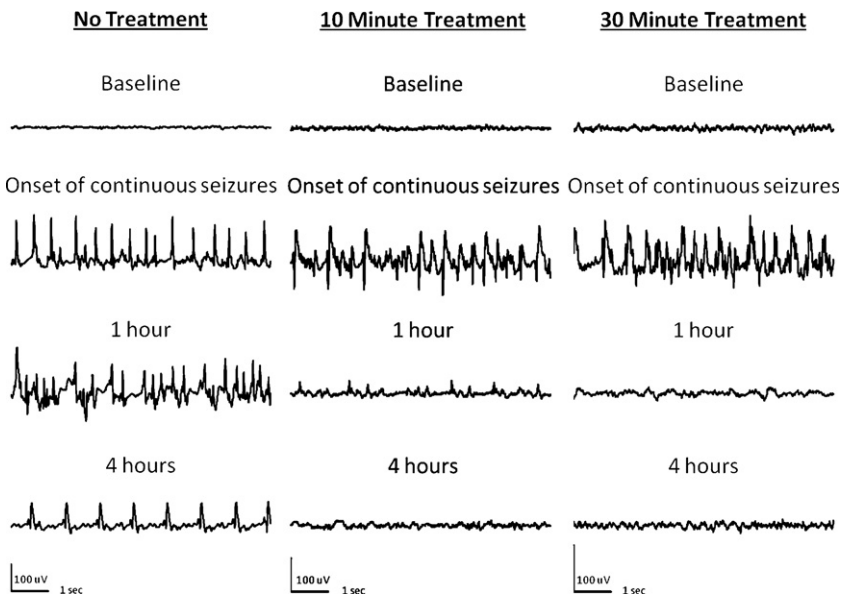

Figure 3 EEG recordings from hippocampi of animals given paraoxon subcutaneously after injection of atropine and 2-PAM. Left panel shows samples of recording from an animal in SE. Note continuous electrographic seizures for 4 h with evolving morphology and frequency. Middle panel (10 min treatment) shows EEG from an animal treated with diazepam 10 min after the onset of continuous electrographic seizures. Seizures were terminated promptly and animals stayed seizure free. Right panel (30 min treatment) shows onset of continuous seizures and their termination when diazepam was administered 30 min after the onset of continuous electrographic seizures.

In these animals electrographic seizures either started as continuous long lasting seizures or evolved from discrete seizures to continuous seizures (Fig. 3, panel control). The mean time for the onset of first electrographic seizure in animals treated with paraoxon was 6 min 4 s ± 42 s. The first seizure was also the onset or continuous EEG activity in 29% (5/17) of the animals studied. In 7 of the 18 animals, a discrete electrographic seizure lasting 30—60 s was the first electrographic seizure, followed by a prolonged period of suppression. This was followed by the onset of continuous electrographic seizure activity. The remaining 35% (6/17) progressed from discrete seizure continuous EEG with a period of brief suppression (10—30 s) between 30 and 60 s seizure bursts. The mean time for onset of continuous electrographic seizure activity after paraoxon injection was 10 min 3 s ± 1 min. At the onset of continuous EEG seizure activity, electrographic spiking occurred at a rate of 2—4 Hz, and frequency increased to 4—8 Hz within 10 min of onset.

One group of animals ($n = 6$) was left untreated after the onset of continuous seizures. One animal died 2 h 45 min

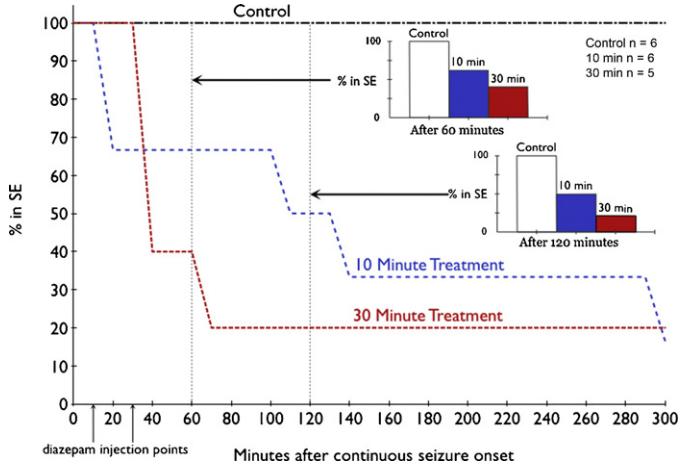

Figure 4 Time-course of SE induced by peripheral paraoxon injection in three groups: no further treatment, diazepam given 10 min after the onset of continuous seizures (blue line) or 30 min after the onset of continuous seizures (red line). In this study, 23 animals were studied, 17 developed continuous seizures, 6 were left untreated (control), 6 received diazepam 10 min after the onset of continuous seizures, and 5 received diazepam 30 min after the onset of continuous electrographic seizures. Diazepam effectively terminated SE in similar proportion of animals regardless of time of treatment (inset bar charts).

Please cite this article in press as: Todorovic, M.S., et al., Characterization of status epilepticus induced by two organophosphates in rats. Epilepsy Res. (2012), http://dx.doi.org/10.1016/j.eplepsyres.2012.04.014

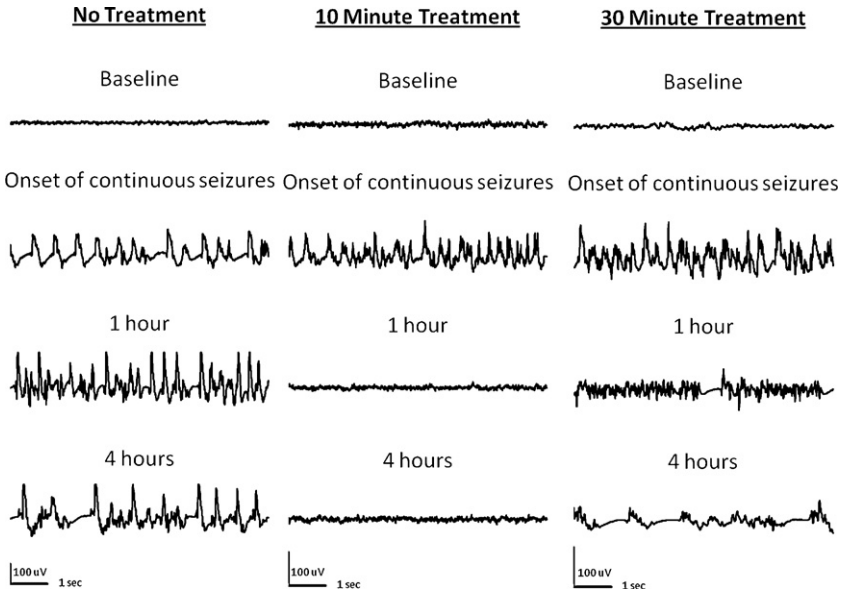

Figure 5 SE induced by peripheral injection of DFP and response to diazepam treatment. Samples of recording from an animal in SE show continuous electrographic seizures for 4 h. Recordings an animal treated with diazepam 10 min after the onset of continuous electrographic seizures (middle panel, 10 min treatment) demonstrate prompt termination of SE. When diazepam was administered 30 min after the onset of continuous electrographic seizures (right panel 30 min treatment) SE continued with only a mild suppression of amplitude of spikes but continued high frequency spike-wave discharges (1 h) and complex poly-spike-wave rhythmic discharges (4 h).

after the onset of continuous seizures. The mean SE duration was 10 h 15 min ± 1 h 42 min in the remaining five animals, ranging from 7 to 17 h. The SE ended with the frequency of epileptiform activity falling below 1 Hz in all 5 of the animals within 18 h of onset.

A group of animals ($n = 6$) in paraoxon induced SE was treated with 10 mg/kg diazepam 10 min after the onset of continuous seizure activity (Fig. 3, middle panel). Diazepam terminated continuous seizures at this time point (Fig. 4, middle panel). In two of these animals, SE was terminated within the first 10 min of treatment (Fig. 4). In these animals, spike frequency dropped from 4—6 Hz to 0 and baseline EEG was restored. Seizures did not recur. In two animals SE ended 90—150 min after onset (Fig. 4). The spike frequency gradually dropped from 4 to 6 Hz with poly-spikes to single spikes with a frequency of less than 1 Hz (Fig. 3). All animals were seizure free by 7 h. There was no mortality within 24 h.

Animals ($n = 5$) treated with 10 mg/kg of diazepam 30 min after continuous EEG activity also responded to treatment, with (60%) becoming seizure free within 10 min of treatment (Fig. 3, right panel). Only one of the five animals was still having seizures 70 min after continuous seizures began, and continuous seizures lasted for 12 h (Fig. 4). No animal in this group died during the 24 h period.

DFP

Preliminary experiments were performed to optimize DFP model of SE. Rats that were pretreated with 1 mg/kg atropine 30 min and then given 1.25 mg/kg DFP SC ($n = 4$) all died from respiratory arrest, whereas 50% of rats pretreated with 1 mg/kg atropine and 25 mg/kg 2-PAM ($n = 4$) survived and exhibited prolonged seizure activity. Higher DFP dose of 1.5 mg/kg combined with a pretreatment of larger doses of atropine (2 mg/kg) and 2-PAM (50 mg/kg) caused death in 2 animals. These observations and previously published data suggested that 1.25 mg/kg DFP SC in cold saline with a pretreatment of 2 mg/kg atropine and 50 mg/kg 2-PAM were likely to produce SE in animals.

This combination was used to study DFP induced SE, and it caused continuous seizure activity and SE in 15 out of 19 (79%) of the animals studied, with the remainder dying of respiratory arrest. Animals in SE group exhibited a combination of chewing, head-bobbing, single and bi-limb clonus and rearing, leading to constant full body tremors and SE. The mean time to first EEG seizure in this group was 21 min 43 s ± 3 min 25 s. In 7 of 15 animals, the first electrographic seizure was also the onset of continuous seizure activity. In 7 other animals, seizure progression went from periods of discrete seizures, separated by normal EEG followed by seizures lasting 10—30 s with periods of suppression, after which seizures merged into continuous epileptiform activity. In one animal, a brief discrete seizure was followed by continuous seizure activity. Continuous epileptiform activity started at a frequency of 2 Hz and accelerated to 4—6 Hz within 10 min. The latency to the development of continuous electrographic activity was 24 min 41 s ± 3 min 48 s after DFP injection.

In 5 animals left untreated after the DFP induced SE, 3 survived to 5 h after continuous seizure onset and the remaining died. Seizures stopped in one animal 4.5 h after the onset of continuous seizure activity, while the other two displayed electrographic seizures which lasted for more than 8 h.

DFP induced seizures were much more resistant to diazepam treatment when given at 30 min than when

Please cite this article in press as: Todorovic, M.S., et al., Characterization of status epilepticus induced by two organophosphates in rats. Epilepsy Res. (2012), http://dx.doi.org/10.1016/j.eplepsyres.2012.04.014

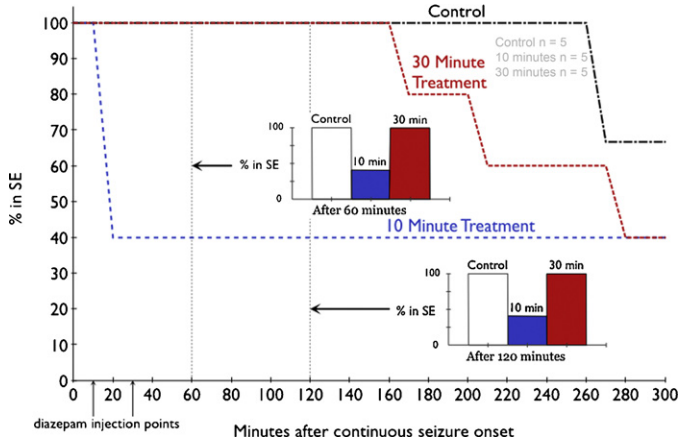

Figure 6 Time-course of SE induced by peripheral DFP injection in three groups: no further treatment, diazepam given 10 min after the onset of continuous seizures (blue line) or 30 min after the onset of continuous seizures (red line). Continuous seizures developed in 15 of 19 animals treated with DFP, and 5 were left untreated (control), 5 each were treated diazepam 10 or 30 min after the onset of continuous electrographic seizures. Diazepam effectively terminated SE in animals treated 10 min after the onset of continuous electrographic seizure but not in animals treated 30 min (inset bar charts).

treated at 10 min (Figs. 5 and 6). Three out of the five rats (60%) given diazepam after 10 min after continuous EEG activity demonstrated rapid drop in spike wave discharge frequency and amplitude with return of baseline EEG; the remaining two out of five animals (40%) continued to have seizures for more than 5 h. No animal in this group died within the 24 h after SE onset.

Diazepam given 30 min after the start of continuous EEG activity did not stop SE within 60 and 120 min after onset of SE in any of the 5 animals tested (Figs. 5 and 6). First termination of SE in these animals first occurred 2.5 h after treatment injection, with 60% (3/5) of rats coming out of SE within the first 5 h of diazepam injection (Fig. 6). In addition, while treatment at 30 min did eventually terminate SE, this termination was marked by appearance arrhythmic spikes and the baseline EEG was not restored in any animal.

Discussion

We have characterized SE induced by two different organophosphates, intrahippocampal infusion of paraoxon and peripheral injection of DFP or paraoxon following treatment of 2-PAM and atropine. Peripheral injection of OP agents has a higher incidence of producing self-sustaining seizures, while intrahippocampal infusion has the benefit of not requiring pretreatment with 2-PAM and atropine.

Direct injection of 200 nmol paraoxon into the hippocampus caused self-sustaining seizures without killing animals due to peripheral poisoning, but animals given 300 nmol paraoxon began to display peripheral OP poisoning effects and the majority of these animals did not survive. The mechanism of these peripheral effects is unknown, but they closely resembled those seen in preliminary trials when paraoxon was given IP without any pretreatment. Compared to peripheral dosing of paraoxon, intrahippocampal injections produced seizures less likely to become self-sustaining SE. Furthermore this model is cumbersome requiring cannula implantation and slow drug infusion. DFP was not tested using this method because of inconsistent development SE using intra-hippocampal infusion of paraoxon.

The volume of paraoxon infusion into the hippocampus was somewhat large (20 μL). However there are previous reports where 20 μL drug volume was infused into the hippocampus (Modol et al., 2011). Another study found that intracranial pressure was not increased by 10 μL infusion into the hippocampus (Drabek et al., 2011). Finally, in a previously published study we have infused up to 40 μL of saline into the hippocampus, and this did not cause seizures (Williamson et al., 2004).

In the case of both DFP and paraoxon given peripherally, both 2-PAM and atropine were required to prevent mortality due to respiratory arrest. A 30 min pretreatment was decided on instead of treatment immediately after OP injection in order to minimize the effects on seizure activity of these agents. This allowed us to better understand the effects of diazepam given at various time points during SE. 2-PAM reactivates the enzyme cholinesterase, which does not penetrate the blood brain barrier. OPs inhibit the enzyme choline acetyl-transferase by acting as substrates for the enzyme and causing its phosphorylation rather than acetylation caused by natural substrate acetylcholine. The phosphorylated enzyme is stable and can no longer deacetylate acetylcholine. Oximes such as 2 PAM dephosphorylate the enzyme and reactivate it (Jokanovic and Stojiljkovic, 2006).

The methods for peripheral OP poisoning described above more accurately mimic those used for high dose pilocarpine experiments, allowing comparison with these models. The onset of continuous EEG seizure activity, which corresponds to EEG stage III as described by Treiman et al. (1990), was found to be a better marker of treatment refractoriness than behavioral seizures in the lithium-pilocarpine model of SE (Wang et al., 2009). The time of treatment was based on the onset of continuous seizure activity, because this most closely correlates with the time at which SE becomes refractory to diazepam.

Please cite this article in press as: Todorovic, M.S., et al., Characterization of status epilepticus induced by two organophosphates in rats. Epilepsy Res. (2012), http://dx.doi.org/10.1016/j.eplepsyres.2012.04.014

Both DFP and paraoxon are OPs, which increase concentration of acetylcholine levels in the brain rapidly by inhibiting its breakdown by the enzyme cholinesterase (Shih and McDonough, 1997). This elevation in acetylcholine levels is likely to activate muscarinic and nicotinic receptors in the hippocampus (Harrison et al., 2004; Kozhemyakin et al., 2010). It was recently suggested that muscarinic receptor activation by paraoxon causes increased release of glutamate from presynaptic terminals (Kozhemyakin et al., 2010). In vitro models of recurrent bursting suggest that increased presynaptic release (frequency of EPSC) can contribute to the development of neuronal synchrony and seizures (Mangan and Kapur, 2004; Traub and Dingledine, 1990).

DFP-induced SE became resistant to treatment with diazepam as SE progressed. This phenomenon has been described previously in SE induced by electrical stimulation, pilocarpine, lithium-pilocarpine and soman (Jones et al., 2002; Kapur and Macdonald, 1997; Mazarati et al., 1998a; Shih et al., 1999). However, the paraoxon model for SE does not exhibit the same phenomenon, making it less suitable as a surrogate for military OP poisoning studies. The current recommendation of 2-PAM, atropine and diazepam as a treatment for OP poisoning is incomplete because of the time dependent nature of its treatment. These studies demonstrate the importance of finding novel methods for dealing with and treating victims of OP poisoning.

Previous studies of seizures caused by organophosphate cholinesterase inhibitors have largely been carried out in defense labs using agents such as sarin VX and other nerve agents (McDonough and Shih, 1997). However, organophosphate poisoning needs to be studied in civilian research laborites because organophosphate pesticide poisoning afflicts civilians and civilian populations can be targets of nerve agent attacks. A World Health Organization report suggested that there were more than 2 million cases of accidental or intentional organophosphate poisoning in the world each year (Jeyaratnam, 1990). Development of DFP and paraoxon models can lead to better treatments for OP poisoning.

Acknowledgments

The research is supported by the CounterACT Program, National Institutes of Health Office of the Director, and the National Institute Neurological Disorders and Stroke, Grant Numbers NIH-NINDS UO1 NS58204 and RO1 NS040337 and also by the Department of Defense grant PR093963.

References

Alldredge, B.K., Gelb, A.M., Isaacs, S.M., Corry, M.D., Allen, F., Ulrich, S., Gottwald, M.D., O'Neil, N., Neuhaus, J.M., Segal, M.R., Lowenstein, D.H., 2001. A comparison of lorazepam, diazepam, and placebo for the treatment of out-of-hospital status epilepticus. N. Engl. J. Med. 345, 631–637.

Bird, S.B., Gaspari, R.J., Dickson, E.W., 2003. Early death due to severe organophosphate poisoning is a centrally mediated process. Acad. Emerg. Med. 10, 295–298.

Chen, J.W., Naylor, D.E., Wasterlain, C.G., 2007. Advances in the pathophysiology of status epilepticus. Acta Neurol. Scand. Suppl. 186, 7–15.

Deshpande, L.S., Carter, D.S., Blair, R.E., DeLorenzo, R.J., 2010. Development of a prolonged calcium plateau in hippocampal neurons in rats surviving status epilepticus induced by the organophosphate diisopropylfluorophosphate. Toxicol. Sci. 116, 623–631.

Drabek, T., Janata, A., Jackson, E.K., End, B., Stezoski, J., Vagni, V.A., Janesko-Feldman, K., Wilson, C.D., van, R.N., Tisherman, S.A., Kochanek, P.M., 2011. Microglial depletion using intrahippocampal injection of liposome-encapsulated clodronate in prolonged hypothermic cardiac arrest in rats. Resuscitation, http://dx.doi.org/10.1016/j.resuscitation.2011.09.016(Epub ahead of print).

Fujikawa, D.G., 2005. Prolonged seizures and cellular injury: understanding the connection. Epilepsy Behav. 7 (Suppl. 3), S3–S11.

Fujikawa, D.G., Itabashi, H.H., Wu, A., Shinmei, S.S., 2000. Status epilepticus-induced neuronal loss in humans without systemic complications or epilepsy. Epilepsia 41, 981–991.

Garcia, S.J., Abu-Qare, A.W., Meeker-O'Connell, W.A., Borton, A.J., Abou-Donia, M.B., 2003. Methyl parathion: a review of health effects. J. Toxicol. Environ. Health B: Crit. Rev. 6, 185–210.

Gralewicz, S., Tomas, T., Socko, R., 1989. Effects of single exposure to chlorphenvinphos, an organophosphate insecticide, on electrical activity (EEG) of the rat brain. Pol. J. Occup. Med. 2, 309–320.

Harrison, P.K., Sheridan, R.D., Green, A.C., Scott, I.R., Tattersall, J.E., 2004. A guinea pig hippocampal slice model of organophosphate-induced seizure activity. J. Pharmacol. Exp. Ther. 310, 678–686.

Hoffmann, U., Papendorf, T., 2006. Organophosphate poisonings with parathion and dimethoate. Intensive Care Med. 32, 464–468.

Honchar, M.P., Olney, J.W., Sherman, W.R., 1983. Systemic cholinergic agents induce seizures and brain damage in lithium-treated rats. Science 220, 323–325.

Jakab, R.L., Bowyer, J.F., 2002. Parvalbumin neuron circuits and microglia in three dopamine-poor cortical regions remain sensitive to amphetamine exposure in the absence of hyperthermia, seizure and stroke. Brain Res. 958, 52–69.

Jeyaratnam, J., 1990. Acute pesticide poisoning: a major global health problem. World Health Stat. Q 43, 139–144.

Jokanovic, M., Stojiljkovic, M.P., 2006. Current understanding of the application of pyridinium oximes as cholinesterase reactivators in treatment of organophosphate poisoning. Eur. J. Pharmacol. 553, 10–17.

Jones, D.M., Esmaeil, N., Maren, S., Macdonald, R.L., 2002. Characterization of pharmacoresistance to benzodiazepines in the rat Li-Pilocarpine model of status epilepticus. Epilepsy Res. 50, 301–312.

Kadriu, B., Guidotti, A., Costa, E., Davis, J.M., Auta, J., 2011. Acute imidazenil treatment after the onset of DFP-induced seizure is more effective and longer lasting than midazolam at preventing seizure activity and brain neuropathology. Toxicol. Sci. 120, 136–145.

Kapur, J., Macdonald, R.L., 1997. Rapid seizure-induced reduction of benzodiazepine and Zn^{2+} sensitivity of hippocampal dentate granule cell GABAA receptors. J. Neurosci. 17, 7532–7540.

Kozhemyakin, M., Rajasekaran, K., Kapur, J., 2010. Central cholinesterase inhibition enhances glutamatergic synaptic transmission. J. Neurophysiol. 103, 1748–1757.

Li, Y., Lein, P.J., Liu, C., Bruun, D.A., Tewolde, T., Ford, G., Ford, B.D., 2011. Spatiotemporal pattern of neuronal injury induced by DFP in rats: a model for delayed neuronal cell death following acute OP intoxication. Toxicol. Appl. Pharmacol. 253, 261–269.

Lothman, E.W., Bertram, E.H., Bekenstein, J.W., Perlin, J.B., 1989. Self-sustaining limbic status epilepticus induced by 'continuous' hippocampal stimulation: electrographic and behavioral characteristics. Epilepsy Res. 3, 107–119.

Please cite this article in press as: Todorovic, M.S., et al., Characterization of status epilepticus induced by two organophosphates in rats. Epilepsy Res. (2012), http://dx.doi.org/10.1016/j.eplepsyres.2012.04.014

Lothman, E.W., Salerno, R.A., Perlin, J.B., et al., 1988. Screening and characterization of antiepileptic drugs with rapidly recurring hippocampal seizures in rats. Epilepsy Res. 2, 367—379.

Lothman, E.W., Collins, R.C., Ferrendelli, J.A., 1981. Kainic acid-induced limbic seizures: electrophysiologic studies. Neurology 31, 806—812.

Mangan, P.S., Kapur, J., 2004. Factors underlying bursting behavior in a network of cultured hippocampal neurons exposed to zero magnesium. J. Neurophysiol. 91, 946—957.

Mazarati, A.M., Baldwin, R.A., Sankar, R., Wasterlain, C.G., 1998a. Time-dependent decrease in the effectiveness of antiepileptic drugs during the course of self-sustaining status epilepticus. Brain Res. 814, 179—185.

Mazarati, A.M., Wasterlain, C.G., Sankar, R., Shin, D., 1998b. Self sustaining status epilepticus after brief electrical stimulation of the perforant path. Brain Res. 801, 251—253.

McDonough Jr., J.H., Shih, T.M., 1997. Neuropharmacological mechanisms of nerve agent-induced seizure and neuropathology. Neurosci. Biobehav. Rev. 21, 559—579.

Modol, L., Darbra, S., Pallares, M., 2011. Neurosteroids infusion into the CA1 hippocampal region on exploration, anxiety-like behaviour and aversive learning. Behav. Brain Res. 222, 223—229.

Morita, H., Yanagisawa, N., Nakajima, T., Shimizu, M., Hirabayashi, H., Okudera, H., Nohara, M., Midorikawa, Y., Mimura, S., 1995. Sarin poisoning in Matsumoto, Japan. Lancet 346, 290—293.

Nozaki, H., Aikawa, N., Shinozawa, Y., Hori, S., Fujishima, S., Takuma, K., Sagoh, M., 1995. Sarin poisoning in Tokyo subway. Lancet 345, 980—981.

Racine, R.J., 1972. Modification of seizure activity by electrical stimulation. II. Motor seizure. Electroencephalogr. Clin. Neurophysiol. 32, 281—294.

Shih, T.M., McDonough Jr., J.H., 1997. Neurochemical mechanisms in soman-induced seizures. J. Appl. Toxicol. 17, 255—264.

Shih, T., McDonough Jr., J.H., Koplovitz, I., 1999. Anticonvulsants for soman-induced seizure activity. J. Biomed. Sci. 6, 86—96.

Sun, C., Sieghart, W., Kapur, J., 2004. Distribution of alpha1, alpha4, gamma2, and delta subunits of GABAA receptors in hippocampal granule cells. Brain Res. 1029, 207—216.

Sun, C., Mtchedlishvili, Z., Bertram, E.H., Erisir, A., Kapur, J., 2007. Selective loss of dentate hilar interneurons contributes to reduced synaptic inhibition of granule cells in an electrical stimulation-based animal model of temporal lobe epilepsy. J. Comp. Neurol. 500, 876—893.

Traub, R.D., Dingledine, R., 1990. Model of synchronized epileptiform bursts induced by high potassium in CA3 region of rat hippocampal slice. Role of spontaneous EPSPs in initiation. J. Neurophysiol. 64, 1009—1018.

Treiman, D.M., 2007. Treatment of convulsive status epilepticus. Int. Rev. Neurobiol. 81, 273—285.

Treiman, D.M., Meyers, P.D., Walton, N.Y., Collins, J.F., Colling, C., Rowan, A.J., Handforth, A., Faught, E., Calabrese, V.P., Uthman, B.M., Ramsay, R.E., Mamdani, M.B., 1998. A comparison of four treatments for generalized convulsive status epilepticus. N. Engl. J. Med. 339, 792—798.

Treiman, D.M., Walton, N.Y., Kendrick, C., 1990. A progressive sequence of electroencephalographic changes during generalized convulsive status epilepticus. Epilepsy Res. 5, 49—60.

Turski, W.A., Cavalheiro, E.A., Schwarz, M., Czuczwar, S.J., Kleinrok, Z., Turski, L., 1983. Limbic seizures produced by pilocarpine in rats: behavioural, electroencephalographic and neuropathological study. Behav. Brain Res. 9, 315—335.

Wang, N.C., Good, L.B., Marsh, S.T., Treiman, D.M., 2009. EEG stages predict treatment response in experimental status epilepticus. Epilepsia 50, 949—952.

Wasterlain, C.G., Fujikawa, D.G., Penix, L., Sankar, R., 1993. Pathophysiological mechanisms of brain damage from status epilepticus. Epilepsia 34 (Suppl. 1), S37—S53.

Williamson, J., Mtchedlishvili, Z., Kapur, J., 2004. Characterization of the convulsant action of pregnenolone sulfate. Neuropharmacology 46, 856—864.

Zaja-Milatovic, S., Gupta, R.C., Aschner, M., Milatovic, D., 2009. Protection of DFP-induced oxidative damage and neurodegeneration by antioxidants and NMDA receptor antagonist. Toxicol. Appl. Pharmacol. 240, 124—131.

Zhu, H., O'Brien, J.J., O'Callaghan, J.P., Miller, D.B., Zhang, Q., Rana, M., Tsui, T., Peng, Y., Tomesch, J., Hendrick, J.P., Wennogle, L.P., Snyder, G.L., 2010. Nerve agent exposure elicits site-specific changes in protein phosphorylation in mouse brain. Brain Res. 1342, 11—23.

Please cite this article in press as: Todorovic, M.S., et al., Characterization of status epilepticus induced by two organophosphates in rats. Epilepsy Res. (2012), http://dx.doi.org/10.1016/j.eplepsyres.2012.04.014